FAST MICROWAVE-ASSISTED THERMOCHEMICAL CONVERSION OF BIOMASS FOR BIOFUEL PRODUCTION

A DISSERTATION
SUBMITTED TO THE FACULTY OF
UNIVERSITY OF MINNESOTA
BY

QINGLONG XIE

IN PARTIAL FULFILLMENT OF THE REQUIREMENTS
FOR THE DEGREE OF
DOCTOR OF PHILOSOPHY

Roger Ruan

December, 2015

ACKNOWLEDGEMENTS

First and foremost, I would like to cordially thank my advisor, Dr. Roger Ruan, for his great efforts in guiding me all these years in both my research and life. It is Dr. Ruan's profound knowledge and deep insight into related fields that helped me complete my PhD program and this dissertation smoothly. I have learnt a lot from Dr. Ruan, and the most important is how to do the research which will have significant influence on my future life and career.

I am also greatly indebted to my co-advisor, Dr. Paul Chen, for his helpful guidance and suggestions on my research approach, thesis scheme, and academic writing. I would also like to acknowledge my committee members, Drs. Thomas Halbach and Bo Hu, for carefully reviewing my dossier and giving constructive comments that significantly improved the quality of my thesis.

I am also grateful to my friends, Min Min, Wenguang Zhou, Yun Li, Shaobo Deng, Pu Peng, Yong Nie, Zhenyi Du, Bing Hu, Fernanda Borges, Michael Mohr, Richard Griffith, Mi Yan, Hongjian Lin, Xiaochen Ma, Zhen Wang, Zongqiang Fu, Qian Lu, Shiyu Liu, Bo Zhang, Guiwei Tan, Peng Peng, Xin Zhang, Juntao Ye, Kim Faber, etc., for their encouragement, assistance and guidance during the period of pursuing my PhD degree. I feel very happy and lucky to know all of them.

Finally, I would like to express my deepest gratitude towards my parents for their constant love, understanding and encouragement, which helped me in completion of my PhD program.

ABSTRACT

Concerns about diminishing fossil fuels and increasing greenhouse gas emissions are driving many countries to develop renewable energy sources. In this respect, biomass provides a carbon-neutral and sustainable solution. Pyrolysis and gasification belong to thermochemical processes which are currently the most appropriate and widely used among all the biomass utilization technologies. Microwave irradiation can provide heating for biomass pyrolysis and gasification, and has many advantages over conventional heating methods. In this dissertation, microwave heating was used in biomass pyrolysis and gasification for the production of bio-oil and syngas, respectively. In addition, in order to utilize the syngas produced, a single-step process was investigated for converting syngas to dimethyl ether (DME) on various bifunctional catalysts.

In Chapter 2, the microwave heating characteristics of various biomass feedstocks and microwave absorbents were examined and compared. Experimental results show that microwave absorbents absorbed the microwave irradiation more effectively than biomass. The addition of these microwave absorbents to biomass feedstock during microwave-assisted thermochemical conversion significantly improved the heating characteristics. Among the three microwave absorbents studied, silicon carbide (SiC) exhibited higher microwave absorbing ability than activated carbon (AC) and graphite (GE), which was mainly attributed to a higher dielectric loss tangent (tan δ) value of silicon carbide. In addition, higher microwave absorbing ability and heating rates were achieved when more microwave absorbents were used. Finally, a fast microwave-assisted biomass conversion system was developed.

In Chapter 3, fast microwave-assisted catalytic co-pyrolysis of microalgae and scum on HZSM-5 catalyst for bio-oil production was investigated. The effects of co-pyrolysis temperature, catalyst to feed ratio, and microalgae to scum ratio on bio-oil yield and composition were examined. Experimental results show that temperature had great influence on the co-pyrolysis process. The optimal temperature was 550 ºC since the maximum bio-oil yield and highest proportion of aromatic hydrocarbons in the bio-oil were obtained at this temperature. The bio-oil yield decreased when catalyst was used, but the production of aromatic hydrocarbons was significantly promoted when the catalyst to feed ratio increased from 1:1 to 2:1. Co-feeding of scum improved the bio-oil and aromatics production, with the optimal microalgae to scum ratio being 1:2 from the perspective of bio-oil quality. The synergistic effect between microalgae and scum during the co-pyrolysis process became significant only when the effective hydrogen index (EHI) of feedstock was larger than about 0.7. In addition, to better understand the fMAP of microalgae, the different roles of three major components, i.e., carbohydrates, proteins, and lipids, were investigated. Cellulose, egg whites, and canola oil were employed as the model compounds of the three components, respectively. Non-catalytic and catalytic fMAP were carried out to identify and quantify some major products, and several reaction pathways were proposed for the pyrolysis of each model compound based on the data obtained. Moreover, a two-step process of microalgae pyrolysis and downstream catalytic reforming was conducted and compared with the one-step process for bio-oil production. The results show that a lower bio-oil yield and higher bio-oil quality were achieved for the two-step process than the one-step process at the same catalyst to feed ratio. The main advantages of the two-step process lie in catalyst saving and reuse.

Furthermore, fast microwave-assisted catalytic pyrolysis of sewage sludge was investigated for bio-oil production, with HZSM-5 as the catalyst. Pyrolysis temperature and catalyst to feed ratio were examined for their effects on bio-oil yield and composition. Experimental results show that microwave is an effective heating method for sewage sludge pyrolysis. Temperature has great influence on the pyrolysis process. The maximum bio-oil yield and the lowest proportions of oxygen- and nitrogen-containing compounds in the bio-oil were obtained at 550 ^{o}C. The oil yield decreased when catalyst was used, but the proportions of oxygen- and nitrogen-containing compounds were significantly reduced when the catalyst to feed ratio increased from 1:1 to 2:1. Essential mineral elements were concentrated in the biochar after pyrolysis, which could be used as a soil amendment in place of fertilizer. Results of XRD analyses demonstrated that HZSM-5 catalyst exhibited good stability during the microwave-assisted pyrolysis of sewage sludge.

In Chapter 4, the microwave-assisted biomass conversion system developed in Chapter 2 was used in corn stover gasification for syngas production. Three catalysts including Fe, Co and Ni with Al_2O_3 support were examined and compared for their effects on syngas production and tar removal. Experimental results show that microwave is an effective heating method for biomass gasification. Ni/Al_2O_3 was found to be the most effective catalyst for syngas production and tar removal. The gas yield reached above 80% and the composition of tar was the simplest when Ni/Al_2O_3 catalyst was used. The optimal catalyst to biomass ratio was determined to be 1:5–1:3. The addition of steam was found to be able to improve the gas production and syngas quality. Results of XRD analyses demonstrate that Ni/Al_2O_3 catalyst had good stability during gasification

process. Finally, a new concept of microwave-assisted dual fluidized bed gasifier was put forward for the first time in all studies in the literature.

To further utilize the syngas produced from biomass gasification, single-step synthesis of DME from syngas on bifunctional catalysts containing Cu-ZnO-Al_2O_3 and seven different zeolites was investigated in Chapter 5. Various characterization techniques were used to determine the structure, reducibility, and surface acidity of the catalysts. Experimental results show that the zeolite type had great influence on the activity, selectivity and stability of the bifunctional catalyst during the syngas-to-DME process. Zeolite properties including density of weak and strong acid sites, pore structure, and Si/Al distribution were found to affect the CO conversion and DME selectivity of the bifunctional catalyst. In addition, the deactivation of the bifunctional catalyst could be attributed to the sintering of metallic Cu and a loss of the zeolite dehydration activity.

In summary, microwave irradiation is an effective heating method for biomass thermochemical conversion for biofuel production. Fast microwave-assisted biomass pyrolysis and gasification, using silicon carbide as the microwave absorbent, were carried out for the production of bio-oil and syngas, respectively. In addition, single-step synthesis of DME from syngas on various bifunctional catalysts was conducted with the aim of fully utilizing the syngas produced from biomass gasification. Although there are still many challenges associated with the production of biofuels via fast microwave-assisted thermochemical conversion, this dissertation offers a valuable insight into the potential of and some basic mechanisms of the technology.

TABLE OF CONTENTS

LIST OF TABLES ix
LIST OF FIGURES x
INTRODUCTION 1
1.1 Background and significance of the research 1
1.2 Biomass conversion technologies 1
1.3 Advantages of microwave-assisted conversion technology 2
1.4 Objectives or hypothesis to be tested 3
CHAPTER 1 LITERATURE REVIEW 5
2.1 Biomass pyrolysis 5
2.1.1 Comparison between slow and fast pyrolysis 5
2.1.2 Different feedstocks for biomass pyrolysis 7
2.1.3 Improvement of bio-oil quality 9
2.1.4 Coke formation during catalytic biomass pyrolysis 10
2.2 Biomass gasification 11
2.3 DME synthesis from syngas 14
2.4 Microwave-assisted conversion technologies 16
2.3.1 Heating mechanism of microwaves 17
2.3.2 Microwave-assisted conversion processes 20
2.3.3 Development of fast microwave-assisted conversion processes 21
CHAPTER 2 MICROWAVE HEATING CHARACTERISTICS OF BIOMASS AND MICROWAVE ABSORBENTS 22
3.1 Materials and methods 22
3.1.1 Materials 22
3.1.2 Determination of microwave heating characteristics 23
3.2 Results and discussion 24
3.2.1 Effect of microwave absorbents on microwave heating characteristics of biomass 24
3.2.2 Microwave heating characteristics of different microwave absorbents 25
3.3 Development of fast microwave-assisted biomass conversion system 26
3.4 Conclusions 28
CHAPTER 3 FAST MICROWAVE-ASSISTED BIOMASS PYROLYSIS FOR BIO-OIL PRODUCTION 30

4.1 Introduction 31
4.2 Materials and methods 35
4.2.1 Materials 35
4.2.2 Apparatus 38
4.2.3 Bio-oil analysis 39
4.2.4 Biochar analysis 39
4.2.5 Catalyst characterization 40
4.3 Catalytic co-pyrolysis of microalgae and scum 40
4.3.1 Effect of pyrolysis temperature on bio-oil production 40
4.3.2 Effect of catalyst to feed ratio on bio-oil production 42
4.3.3 Effect of microalgae to scum ratio on bio-oil production 45
4.4 Pyrolysis pathways for fMAP of microalgae 48
4.4.1 FMAP of microalgae and model compounds 48
4.4.2 Catalytic pyrolysis of microalgae and model compounds 52
4.5 Two-step process of microalgae pyrolysis and downstream catalytic reforming 55
4.6 Catalytic pyrolysis of sewage sludge 58
4.6.1 Effect of pyrolysis temperature on bio-oil production 58
4.6.2 Effect of catalyst to feed ratio on bio-oil production 61
4.6.3 Analysis of biochar 64
4.6.4 Catalyst characterization 65
4.7 Conclusions 66
CHAPTER 4 FAST MICROWAVE-ASSISTED CATALYTIC BIOMASS GASIFICATION FOR SYNGAS PRODUCTION 68
5.1 Introduction 68
5.2 Materials and methods 70
5.2.1 Materials 70
5.2.2 Apparatus 71
5.2.3 Gas and tar analyses 71
5.2.4 Catalyst characterization 72
5.3 Results and discussion 72
5.3.1 Effects of different catalysts on syngas production 72
5.3.2 Effects of different catalysts on tar conversion 75
5.3.3 Effect of catalyst to biomass ratio on gasification process 77
5.3.4 Effect of steam on syngas production and tar removal 78

5.3.5 Catalyst characterization 79
5.3.6 A new concept of microwave-assisted dual fluidized bed gasifier 81
5.4 Conclusions 83
CHAPTER 5 SINGLE-STEP SYNTHESIS OF DME FROM SYNGAS 84
6.1 Introduction 84
6.2 Materials and methods 86
6.2.1 Catalyst preparation 86
6.2.2 Catalyst characterization 87
6.2.3 Catalytic synthesis experiments 88
6.3 Results and discussion 89
6.3.1 Characterization of catalysts 89
6.3.2 Catalytic synthesis experiments 92
6.4 Conclusions 98
CHAPTER 6 SUMMARY AND FUTURE WORK 100
7.1 Summary 100
7.2 Future work 102
7.2.1 Development of a continuous microwave-based biomass conversion system for biofuel production 102
7.2.2 FMAP of microalgae cultivated in different metabolic pathways 102
7.2.3 Fast microwave-assisted co-gasification for syngas production 103
7.2.4 Modification of zeolite for single-step DME synthesis from syngas 103
BIBLIOGRAPHY 105
APPENDIX A EXPERIMENTAL MATERIALS, EQUIPMENT AND SAMPLES 116

LIST OF TABLES

Table 2.1 Range of the main operating parameters for pyrolysis processes. 5

Table 2.2 Dielectric loss tangents for different carbon materials at a frequency of 2.45 GHz and room temperature, ca., 298 K (Menéndez et al., 2010). 19

Table 3.1 Characteristics of corn stover. 23

Table 4.1 Characteristics of dried algal biomass powder. 35

Table 4.2 Characteristics of model compounds. 36

Table 4.3 Characteristics of sewage sludge. 37

Table 4.4 Comparison between the theoretical values and the actual values of bio-oil yield and proportion of aromatics in the bio-oil under different microalgae to scum ratios. 48

Table 4.5 Contents of main compounds in the bio-oils produced from fMAP of microalgae and model compounds at 550 ºC (GC/MS peak area percentage, %). 49

Table 4.6 Contents of main compounds in the bio-oils produced from fast microwave-assisted catalytic pyrolysis of microalgae and model compounds at 550 ºC (GC/MS peak area percentage, %). 53

Table 4.7 Contents of mineral elements in biochar from microwave-assisted pyrolysis of sewage sludge at 550 ^{o}C. 64

Table 4.8 Comparison of peak areas and crystallite sizes at characteristic diffraction angles of HZSM-5 XRD patterns before and after pyrolysis reactions under different temperatures. 66

Table 5.1 Comparison of effects of different catalysts in microwave-assisted biomass gasification for syngas production. 75

Table 5.2 Main compounds in tars obtained over different catalysts. 76

Table 5.3 Comparison of NiO and Ni^0 phases on catalysts before and after reaction. 81

Table 6.1 Physicochemical properties of the zeolites. 89

Table 6.2 Surface acidity of the bifunctional catalysts as determined by NH_3-TPD. 92

Table 6.3 The influence of different zeolites on single-step synthesis of DME from syngas. 92

Table 6.4 Pore structures of different types of zeolites. 94

LIST OF FIGURES

Fig. 2.1 The microwave-assisted thermochemical conversion concept..... 17

Fig. 2.2 Schematic illustration of temperature gradient and heat and mass flows in cross-section of a wood cylinder subjected to conventional and microwave heating..... 18

Fig. 3.1 The temperature profiles for corn stover with and without SiC under microwave heating..... 25

Fig. 3.2 The temperature profiles for different microwave absorbents under microwave heating..... 26

Fig. 3.3 Schematic diagram of fast microwave-assisted biomass conversion system..... 27

Fig. 4.1 Effect of temperature on fast microwave-assisted catalytic co-pyrolysis of microalgae and scum. (a) Product distribution. (b) Bio-oil composition. 42

Fig. 4.2 Effect of catalyst to feed ratio on fast microwave-assisted catalytic co-pyrolysis of microalgae and scum. (a) Product distribution. (b) Bio-oil composition. 44

Fig. 4.3 EHI values of feedstock under different microalgae to scum ratios..... 45

Fig. 4.4 Effect of microalgae to scum ratio on fast microwave-assisted catalytic co-pyrolysis of microalgae and scum. (a) Product distribution. (b) Bio-oil composition. 46

Fig. 4.5 Postulated pathways for fMAP of carbohydrates..... 50

Fig. 4.6 Postulated pathways for fMAP of proteins..... 51

Fig. 4.7 Postulated pathways for fMAP of lipids..... 52

Fig. 4.8 Postulated pathways for fast microwave-assisted catalytic pyrolysis of carbohydrates (Scheme 1), lipids (Scheme 2), and proteins (Scheme 3)..... 55

Fig. 4.9 Comparison between two-step and one-step processes of fast microwave-assisted catalytic pyrolysis of microalgae. (a) Product distribution. (b) Bio-oil composition..... 57

Fig. 4.10 Effect of temperature on product distribution from microwave-assisted pyrolysis of sewage sludge. Catalyst: HZSM-5, catalyst to feed ratio: 2:1..... 59

Fig. 4.11 Effect of temperature on bio-oil composition from microwave-assisted pyrolysis of sewage sludge. Catalyst: HZSM-5, catalyst to feed ratio: 2:1..... 61

Fig. 4.12 Effect of catalyst to feed ratio on product distribution from microwave-assisted pyrolysis of sewage sludge. Catalyst: HZSM-5, pyrolysis temperature: 550 ºC..... 62

Fig. 4.13 Effect of catalyst to feed ratio on bio-oil composition from microwave-assisted pyrolysis of sewage sludge. Catalyst: HZSM-5, pyrolysis temperature: 550 ºC..... 63

Fig. 5.1 Effect of catalyst on product distribution in microwave-assisted gasification of corn storver. Gasification temperature: 900 ºC..... 73

Fig. 5.2 Effect of catalyst on major gases contents in microwave-assisted gasification of corn storver. Gasification temperature: 900 ºC..... 74

Fig. 5.3 Effect of catalyst to biomass ratio on (a) product distribution, and (b) major gases contents. Catalyst: Ni/Al_2O_3, gasification temperature: 900 ºC..... 78

Fig. 5.4 XRD patterns for Ni/Al_2O_3 catalyst (a) before reaction, (b) after reaction without steam, and (c) after reaction with steam, with phases labeled as: Ni (cubic Ni^0), NiO (NiO), and A (Al_2O_3). 80

Fig. 5.5 Schematic of the microwave-assisted dual fluidized bed gasifier. 82

Fig. 6.1 TPR profiles for the bifunctional catalysts. 91

Fig. 6.2 NH_3-TPD profiles for the bifunctional catalysts. 91

Fig. 6.3 CO conversion as a function of time on stream (TOS) in syngas-to-DME experiments using different bifunctional catalysts. 96

Fig. 6.4 XRD patterns of bifunctional catalysts after reaction. 97

Fig. 6.5 Selectivity to the main reaction products as a function of TOS in syngas-to-DME experiments on bifunctional catalysts (a) CZA/Y(5.1) and (b) CZA/Y(80)..... 98

Fig. A.1 Fast microwave-assisted biomass conversion system. 116

Fig. A.2 *Nannochloropsis* sp. powder used in the fMAP experiments..... 117

Fig. A.3 Scum used in the co-pyrolysis experiments..... 117

Fig. A.4 System for the single-step synthesis of DME from syngas. 118

Fig. A.5 Catalysts used in the single-step synthesis of DME from syngas. 118

INTRODUCTION

1.1 Background and significance of the research

Recently, increasing studies have been conducted on renewable energy, as a solution to current energy and environmental issues caused by traditional fossil fuels. Since the carbon emission of biomass during its conversion roughly equals to the carbon absorbed during the plant growth, the use of biomass does not contribute to the buildup of CO_2 in the atmosphere (McKendry, 2002a). In addition, biomass can improve national energy security by reducing the reliance on foreign sources. The Vision for Bioenergy and Biobased Products in the United States developed by the Biomass Technical Advisory Committee established long-term goals that 20 percent of transportation fuels and 25 percent of chemicals and materials would be produced from biomass by 2030 (U.S. Department of Energy and Department of Agriculture, 2002). Therefore, the efficient uses of biomass are considered very promising in the future energy portfolio (Richardson et al., 2012).

1.2 Biomass conversion technologies

Biomass can be converted through a wide range of technologies to different forms of energy, chemicals, and materials that are conventionally derived from fossil resources (Goyal et al., 2008). Biomass conversion technologies include first generation technologies such as fermentation and transesterification, and second generation or advanced technologies such as enzymatic and thermochemical conversion of biomass to produce biofuels.

Among all the biomass utilization technologies, thermochemical methods including pyrolysis and gasification are currently the most appropriate and widely used (Encinar et al., 2000). Pyrolysis and gasification are conversion processes during which organic materials decompose to small volatiles or inorganic gases at high temperature. The main product from biomass pyrolysis is bio-oil which can be upgraded to high quality liquid fuels or liquid fuel intermediates. The production of syngas from biomass gasification is also considered as an attractive route to produce chemicals, biofuels, hydrogen and electricity (Damartzis and Zabaniotou, 2011; Kirkels and Verbong, 2011; Lin and Huber, 2009). Therefore, the successful development of cost-effective processes for high-quality bio-oil or syngas production will greatly promote biomass utilization.

1.3 Advantages of microwave-assisted conversion technology

Microwave irradiation is an alternative heating method and has already been successfully used in some waste conversion (Bu et al., 2012; Du et al., 2011; Wang et al., 2012). Microwave assisted heating has many advantages over conventional processes, which include: (1) Microwave can provide uniform internal heating for material particles since the electromagnetic energy is directly converted into heat at the molecular level (Sobhy and Chaouki, 2010). (2) Microwave heating is easier to control due to its instantaneous response for rapid start-up and shut-down. (3) The set-up of microwave system is simple, which facilitates its adaption to currently available large-scale industrial technologies. (4) It does not require high degree of feedstock grinding and can be used to handle large chuck of feedstock. (5) Microwave heating is a mature technology and the development of microwave heating system is of low cost. Despite many advantages of

microwave heating over traditional heating methods and some progress made in waste conversion, research in biomass pyrolysis and gasification using microwave technology is limited.

1.4 Objectives or hypothesis to be tested

The overall goal of this research is to develop a fast microwave-assisted system and use it in biomass pyrolysis and gasification for biofuels production. The specific objectives consist of four major parts as follows:

(1) To investigate and compare the microwave heating characteristics of various biomass materials and microwave absorbents. The optimum microwave absorbent will be determined in terms of the heating rate under the microwave irradiation. Based on the results, a fast microwave-assisted biomass conversion system will be developed for biofuel production.

(2) To study fast microwave-assisted pyrolysis (fMAP) of biomass for bio-oil production. Co-pyrolysis of microalgae and scum will be studied to improve the bio-oil yield and quality. The effects of co-pyrolysis temperature, catalyst to feed ratio, and microalgae to scum ratio on bio-oil production will be investigated. In addition, the pyrolysis mechanism of microalgae will be studied through fMAP of three major components of microalgae, i.e., carbohydrates, proteins, and lipids. Moreover, a two-step process of microalgae pyrolysis and downstream catalytic reforming will be conducted and compared with the one-step process for bio-oil production. Furthermore, catalytic pyrolysis of sewage sludge will be carried out for bio-oil production.

(3) To study fast microwave-assisted gasification (fMAG) of corn stover and compare the effects of Fe-, Co-, and Ni-based catalysts on syngas production and tar removal. The influence of steam addition on syngas yield and quality will be examined. In addition, XRD technique will be used to examine the catalyst stability during the gasification process.

(4) To test the single-step synthesis of dimethyl ether (DME) from the syngas produced through fMAG using bifunctional catalyst consisting of Cu-ZnO-Al_2O_3 (CZA) and zeolite. The influence of zeolite type will be investigated on the overall activity, selectivity, and stability of the bifunctional catalyst during the syngas-to-DME process.

CHAPTER 1 LITERATURE REVIEW

This chapter will review previous research in biomass pyrolysis and gasification, DME synthesis from syngas, as well as microwave-assisted conversion technologies.

2.1 Biomass pyrolysis

Pyrolysis is the conversion of biomass into bio-oil, biochar and syngas at elevated temperature (300–700 °C) in the absence of oxygen (Bridgwater and Peacocke, 2000). The yield and properties of each fraction vary with biomass feedstock composition, i.e., carbohydrates (cellulose, hemicellulose, lignin, and starch), protein, lipids, and ash contents (Balat, 2008a; Du et al., 2013; Goyal et al., 2008).

2.1.1 Comparison between slow and fast pyrolysis

Depending on the variables including temperature, heating rate, and residence time of vapors in the reactor, the pyrolysis process can be generally divided into three subclasses, i.e., slow, fast and flash pyrolysis (Luque et al., 2012), as shown in Table 2.1.

Table 2.1 Range of the main operating parameters for pyrolysis processes.

Pyrolysis process	Heating rate ($^{o}C\ s^{-1}$)	Temperature (^{o}C)	Residence time (s)
Slow	0.1–1	300–700	450–550
Fast	10–200	550–1000	0.5–10
Flash	>1000	800–1100	<0.5

Conventional slow pyrolysis has been applied for thousands of years and has been mainly used for the production of charcoal. The heating rate in slow pyrolysis is typically much slower than that used in fast pyrolysis. In slow pyrolysis, vapors do not escape as rapidly as they do in fast pyrolysis. Thus, components in the vapor phase continue to

react with each other, which favors the formation of solid char. Gercel (2011) conducted slow pyrolysis with low heating rate of about 7 ^{o}C/min and obtained up to 24–43% of bio-oil. However, most studies on slow pyrolysis reported high production of char at the expense of bio-oil (Grierson et al., 2011; Karaosmanoglu et al., 1999; Ucar and Karagoz, 2009). Ucar and Karagoz (2009) carried out slow pyrolysis of pomegranate seeds and observed the maximum bio-oil yield of 21.98% at the temperature of 500 ^{o}C and heating rate of 30 ^{o}C/min. Karaosmanoglu et al. (1999) investigated slow pyrolysis of the straw and stalk of the rapeseed plant in a tubular reactor at the temperature range of 350–650 ^{o}C. The maximum bio-oil yield was only about 17% while the maximum char yield reached up to 47% at the heating rate of 10 ^{o}C/min.

Fast pyrolysis is a novel and effective method for biomass conversion, in which rapid thermal decomposition of organic compounds occurs in the absence of oxygen to produce liquid, char, and gas (Bridgwater and Peacocke, 2000). If the target product is liquid with low water content, a high heating rate, a moderately high temperature, and a short residence time should be used while an elevated temperature favors gas production. The most commonly used reactors for biomass fast pyrolysis include fixed bed and fluidized bed. Ateş et al. (2004) studied fast pyrolysis of sesame stalk in a fixed-bed reactor and obtained the maximum bio-oil yield of 37.2 wt% at the temperature of 550 ^{o}C and heating rate of 500 ^{o}C/min. Lee et al. (2005) investigated the production of bio-oil from rice straw by fast pyrolysis using a fluidized bed reactor. It was found that the optimum reaction temperature range for bio-oil production was 410–510 ^{o}C, at which the bio-oil yield was about 50 wt%. Duman et al. (2011) conducted and compared slow and

fast pyrolysis of cherry seeds, observing bio-oil yields of 21 wt% and 44 wt% from the two processes, respectively.

In summary, fast pyrolysis technology is a more promising alternative approach than slow pyrolysis to convert a wide range of biomass feedstocks for bio-oil production (Bridgwater and Peacocke, 2000; Mohan et al., 2006).

2.1.2 Different feedstocks for biomass pyrolysis

Various feedstocks such as corn stover, wood sawdust, rice husk, cassava stalk and microalgae have been used for biomass pyrolysis. The bio-oil production can be greatly influenced by the feedstock type because of the different composition of various biomass feedstocks. Since microalgae usually have faster growth rates, shorter growing cycles, higher photosynthetic efficiencies and oil contents than terrestrial lignocellulosic biomass (Gouveia and Oliveira, 2009; Pirt, 1986; Schenk et al., 2008), they have received growing interest these days (Chisti, 2008; Luque et al., 2010). The bio-oils obtained from microalgae have better quality in many aspects than those from lignocellulosic biomass such as wood (Du et al., 2012; Li et al., 2012; Maddi et al., 2011; Thangalazhy-Gopakumar et al., 2012). Algal bio-oils usually have lower density and oxygen content, higher carbon, hydrogen content and heating value, and desirable pH. In addition, microalgae can be cultivated on marginal lands and waterbodies. Therefore, they do not compete with traditional agricultural resources and have much less impact on current land-use for food production (Chen et al., 2009; Yu et al., 2011). Miao et al. (2004) performed fast pyrolysis of *Chllorella protothecoides* and *Microcystis areuginosa* at 500

°C, and bio-oil yields of 18% and 24% were obtained, respectively. The bio-oil exhibited a higher carbon and nitrogen content, lower oxygen content than wood bio-oil.

Many recent studies about microalgae pyrolysis have been focused on the optimization of liquid bio-oil, as it is easily storable and transportable with the potential of being upgraded to high quality drop-in fuels. The bio-oil can replace heavy and light fuel oils in industrial boiler for heat production (Mohan et al., 2006). However, the high level of oxygen (30–40%) makes bio-oil unstable and unable to be used as transportation fuels directly. Thus, upgrading of bio-oil, such as catalytic cracking, becomes necessary (Zhang et al., 2007). In catalytic cracking, oxygenated compounds are decomposed to hydrocarbons with oxygen removed as H_2O, CO and CO_2. Recently, researchers became interested in catalytic pyrolysis, also known as *in-situ* upgrading, which incorporates catalysts directly into the pyrolysis reactions by mixing biomass with catalysts or setting up an upgrading fixed bed right at the outlet of pyrolysis vapors. The evolved volatiles from thermal decomposition of organics can react directly or immediately on catalysts. Thangalazhy-Gopakumar et al. (2012) found that a type of zeolite, namely HZSM-5, increased the carbon yield of aromatic hydrocarbons from 0.9% to 25.8% in the bio-oil from pyrolysis of *Chlorella vulgaris*. Du et al. (2013) evaluated the performance of different zeolites for the production of aromatic hydrocarbons from catalytic pyrolysis of *Chlorella vulgaris* and reported the maximum aromatic yield of 18.13% when HZSM-5 with a moderate Si/Al ratio of 80 was used as the catalyst. The catalytic pyrolysis could eventually eliminate the costly condensation and re-evaporation procedures used in traditional upgrading of pyrolytic oil (Zhang, et al., 2010).

Sewage sludge as the feedstock for biomass pyrolysis has also attracted more and more interest nowadays. Fonts et al. (2008) conducted pyrolysis of sewage sludge in a fluidized bed and obtained the maximum liquid yield of about 33 wt% at the temperature of 540 ^{o}C with a solid feed rate of 3.0 g/min and nitrogen flow rate of 4.5 L/min. By using a quartz reactor, Sánchez et al. (2009) examined the effect of temperature increase from 350 ^{o}C to 950 ^{o}C on the composition of the oils obtained from sewage sludge pyrolysis and observed an increase in the concentration of mono-aromatic hydrocarbons and a strong decrease in the concentration of phenol and its alkyl derivatives. In order to improve the yield and quality of the bio-oil, many researchers used different catalysts in the pyrolysis of sewage sludge. Kim and Parker (2008) investigated the effect of zeolite on the product distribution from pyrolysis of different types of sewage sludges and concluded that zeolite did not improve oil and char yields due to the increased conversion of volatile matter to gas. However, Park et al. (2010) found that metal oxide catalysts (CaO and La_2O_3) contributed to a slight decrease in bio-oil yield but were significantly effective in removal of chlorine from the bio-oil.

2.1.3 Improvement of bio-oil quality

Most solid biomass feedstocks are hydrogen deficient, which has adverse impacts on hydrocarbon production from the pyrolysis process. Chen et al. (1988) defined the effective hydrogen index (EHI) to reflex the relative hydrogen content of various biomass feedstocks. EHI is an indicator of hydrogen/carbon ratio after debiting the compound's hydrogen content for complete conversion of heteroatoms to NH_3, H_2S and H_2O, which is expressed as the following equation,

$$EHI = (H - 2O - 3N - 2S)/C \quad (2.1)$$

where H, C, O, N and S are the number of moles of hydrogen, carbon, oxygen, nitrogen and sulfur in the feedstock, respectively. The EHI of biomass and biomass-derived feedstocks is only 0–0.3, which exhibits an extreme lack of hydrogen. Du et al. (2013) found that the EHI value for *Chlorella* microalgae is 0.23. Zhang et al. (2011) conducted the zeolite conversion of ten biomass-derived feedstocks with different EHI values and found a strong positive correlation between the EHI and the hydrocarbon content in the product. Co-pyrolysis of biomass with an additional feedstock with a high EHI value is an attractive route to increase the hydrogen content of feedstock, and hence the hydrocarbon yield in the pyrolysis bio-oil will be increased. Grease (EHI = ~1.5), polyethylene (PE) (EHI = 2), and saturated monohydric alcohols (EHI = 2) can be used as the hydrogen source and co-fed with biomass to increase the overall EHI of the feedstocks. Zhang et al. (2012) investigated the catalytic co-pyrolysis of biomass and methanol, and a high yield of premium products were obtained over HZSM-5 catalyst.

2.1.4 Coke formation during catalytic biomass pyrolysis

The major competing reaction occurring during the catalytic biomass pyrolysis process is the formation of coke, which is the main cause for catalyst deactivation. It is likely that during biomass pyrolysis some intermediates polymerize to form resins, which further decompose to form unsaturated coke on the catalyst. Carlson et al. (2010) studied catalytic fast pyrolysis of glucose with HZSM-5 as the catalyst and found that the coked catalyst pore volume is decreased significantly compared to fresh catalyst. However, there is no additional change in the pore volume with increasing coke levels. The initial

decrease in pore volume is likely due to the formation of the hydrocarbon pool within the zeolite framework. Once the hydrocarbon pool is formed, additional carbon is deposited on the surface not within the pores. Bjorgen et al. (2007) investigated the conversion of methanol to hydrocarbons (MTH) over HZSM-5 and reported that catalyst deactivation occurs from highly unsaturated coke on the external surface of the catalyst and not from large species within the pores. In contrast, larger caged zeolites such as HY and β-zeolite are mainly deactivated by the formation of polyaromatic species within the pore systems (Bjorgen et al., 2003; Haw et al., 2003).

2.2 Biomass gasification

Gasification typically involves the partial oxidation of biomass into fuel gases at high temperatures (> 800 °C). It is usually carried with air or steam as the gasification agent to generate a mixture of CO, H_2, CO_2, and some light hydrocarbons (Demirbas, 2001).

The gas produced from biomass gasification is mainly composed of H_2, CO, CO_2, CH_4 and some light hydrocarbons and also contains contaminants such as H_2S, HCl, tar, and solid particles. Among all the contaminants, tar is the most common and troublesome compound and has been extensively discussed in previous studies (Anis and Zainal, 2011; Li and Suzuki, 2009; Torres et al., 2007). Tar is a complex mixture of organic chemicals largely composed of aromatic hydrocarbons and can cause serious problems including fouling of engines and deactivation of catalysts, due to its condensation and polymerization (Devi et al., 2003; Devi et al., 2005; Han and Kim, 2008). Therefore,

some strategies such as catalytic gasification have been considered to reduce tar content in syngas.

Traditional types of biomass gasification reactors include fixed bed and fluidized bed (Dong et al., 2010; Van der Meijden et al., 2009; Xie et al., 2012). Dong et al. (2010) studied gasification of coffee grounds using a two-stage dual fluidized bed gasifier (DFBG), obtaining syngas with H_2 and CO contents of 31.23% and 29.20%, respectively. The tar content was reduced from about 40 g/m^3 to 10 g/m^3 raw gas with Ca impregnation onto fuel. Employing a circulating fluidized bed (CFB) as the gasifier and a bubbling fluidized bed (BFB) as the combustor, Van der Meijden et al. (2009) examined steam gasification of wood pellets and obtained syngas containing around 38% of H_2, 19% of CO and 40 g/m^3 of tar at the temperature of 925 ºC. Xie et al (2012) investigated two-stage catalytic pyrolysis and gasification of pine sawdust in a fixed bed reactor and observed a maximum syngas yield of 3.29 m^3/kg biomass. However, the yield of liquid fraction was around 15–20 wt% of dry biomass.

Based on the tar removal technologies used, biomass gasification process can be broadly divided into two approaches: primary methods and secondary methods (Devi et al., 2003). In primary methods, gasification process and tar elimination are carried out simultaneously in gasifier; while in secondary methods, gas cleanup is conducted in a separate reformer in the downstream of gasifier.

The primary methods have gained much attention (Ahmed et al., 2009; Göransson et al., 2011; Karmakar et al., 2011; Moghtaderi, 2007; Ueki et al., 2011). Ahmed et al. (2009) examined steam gasification of cardboard using a batch reactor, obtaining most

syngas of about 1.2 m^3/kg biomass at 600 ºC. Karmakar et al. (2011) studied steam gasification of rice husk in a fluidized bed reactor and generated syngas with maximum yield of 1.21 m^3/kg biomass and lower heating value (LHV) of 11.18 MJ/m^3 at 750 ºC. Moghtaderi (2007) investigated steam gasification of pine sawdust catalyzed by Ni/Al_2O_3 and observed a maximum H_2 yield of 1.6 m^3/kg biomass at 600 ºC. Although primary methods eliminate the need for downstream cleanup, they cannot effectively solve the purpose of tar reduction without affecting the useful gas composition and heating value (Devi et al., 2003). As a result, the syngas yields of primary methods will be relatively low compared with secondary methods.

Extensive studies on secondary methods of biomass gasification have also been conducted (Gao et al., 2009; Lv et al., 2007; Wang et al., 2006; Xiao et al., 2011; Yang et al., 2010). By steam gasification of pine sawdust using an updraft gasifier combined with a porous ceramic reformer, Gao et al. (2009) obtained syngas with maximum yield of 1.72 m^3/kg biomass and lower heating value (LHV) of 11.73 MJ/m^3 at 950 ºC. Employing a fluidized bed gasifier and a downstream fixed bed as the reactors, Lv et al. (2007) studied catalytic gasification of pine sawdust and the maximum gas yield reached 2.41 m^3/kg biomass at 850 ºC. Similarly, Xiao et al. (2011) utilized primary fluidized bed and secondary reforming fixed bed to investigate steam gasification of waste biomass with Ni/BCC as catalyst and obtained syngas with yield of 2 m^3/kg biomass and LHV of 14 MJ/m^3 around 600 ºC. Secondary methods are effective in reducing tar content and improving syngas yield, but additional equipment will increase the investment.

2.3 DME synthesis from syngas

Dimethyl ether (DME) as an alternative to diesel fuel attracts increasing interest due to its high cetane number (55–60), low auto-ignition temperature, and reduced emissions of pollutants such as CO, NO_x, SO_x, and particulate matter on its combustion (Arcoumanis et al., 2008; Hu et al., 2005; Semelsberger et al., 2006). DME is an important feedstock in the production of chemicals such as dimethyl sulfate and methyl acetate, as well as ethers and oxygenates. Moreover, DME can be utilized as a residential fuel replacing liquefied petroleum gas (LPG) or propane since they have similar physical properties, or as a feedstock for hydrogen production due to its high H/C ratio and energy density (Semelsberger et al., 2006). In addition, the boiling point of DME is very low (–24 ºC), thus it can be used as a low-temperature solvent and extraction agent, which is applicable to certain laboratory procedures.

Traditionally, DME is produced using fossil fuels as the raw materials such as natural gas, coal, and oil. These sources need to be firstly converted to syngas using various gasifying agents like air, oxygen, and steam. After purification and conditioning, the syngas is then converted to methanol followed by its dehydration to DME on certain catalysts. Recently, the utilization of biomass as the feedstock for syngas production has attracted considerable interest (Lv et al., 2009), since biomass is a CO_2 neutral and extensively distributed resource in the world (Lv et al., 2007). However, the composition of biomass-derived syngas varies with different raw materials, reactor types, temperatures, and other process parameters (Karmakar and Datta, 2011; Xiao et al., 2011; Xie et al., 2012).

DME is conventionally produced using a two-step process comprising synthesis of methanol from syngas on a Cu-ZnO-based catalyst and methanol dehydration to DME on a solid acid catalyst (Spivey, 1991). However, the step of syngas to methanol is limited by the thermodynamic equilibrium, making the overall conversion rate very low (García-Trenco and Martínez, 2012). A new single-step synthesis of DME directly from syngas has gained much attention due to its thermodynamic and economic advantages (García-Trenco and Martínez, 2012; Hayer et al., 2011; Li et al., 2011). The main reactions involved in the single-step process are represented by equations (2.2)–(2.5), assuming that syngas simply consists of H_2 and CO.

Methanol synthesis reaction:

$$2H_2 + CO \leftrightarrow CH_3OH \quad (2.2)$$

$$3H_2 + CO_2 \leftrightarrow CH_3OH + H_2O \quad (2.3)$$

Methanol dehydration reaction:

$$2CH_3OH \leftrightarrow CH_3OCH_3 + H_2O \quad (2.4)$$

Water-gas shift (WGS) reaction:

$$CO + H_2O \leftrightarrow H_2 + CO_2 \quad (2.5)$$

The equilibrium limitation existing in syngas to methanol process can be overcome through reaction (2.4) which consumes methanol and shifts the chemical equilibrium of reactions (2.2) and (2.3) to the right-hand side. Therefore, more syngas can be utilized and the overall conversion rate is improved. Moreover, the water formed in reactions (2.3) and (2.4) reacts with CO through the WGS reaction (equation (2.5)) and produce H_2 and

CO_2, which are reactants of the reaction (2.3) for methanol synthesis. It can be seen from the above reactions that a bifunctional catalyst is required for the single-step of synthesis of DME from syngas. The catalyst should be able to simultaneously catalyze both the methanol synthesis and the methanol dehydration reactions. The bifunctional catalyst typically consists of a Cu-ZnO-based component for the conversion of syngas to methanol and a solid acid component for the methanol dehydration to DME.

2.4 Microwave-assisted conversion technologies

Despite the progresses and advancements made in the past decades, current pyrolysis and gasification technologies are still faced significant technical challenges in terms of product yield and quality and process energy efficiency. One of the solutions is to develop methods for efficient heating, precise control of the heating parameters, and reducing less adverse impacts on the product quality. Microwave irradiation is an efficient way to provide heating to thermochemical conversion of biomass. The integration of microwaves and thermochemical processing is a novel conceptual design which can potentially be a very suitable alternative to efficiently convert waste and/or biomass feedstocks to biofuels (Budarin et al., 2009), as shown in Fig. 2.1.

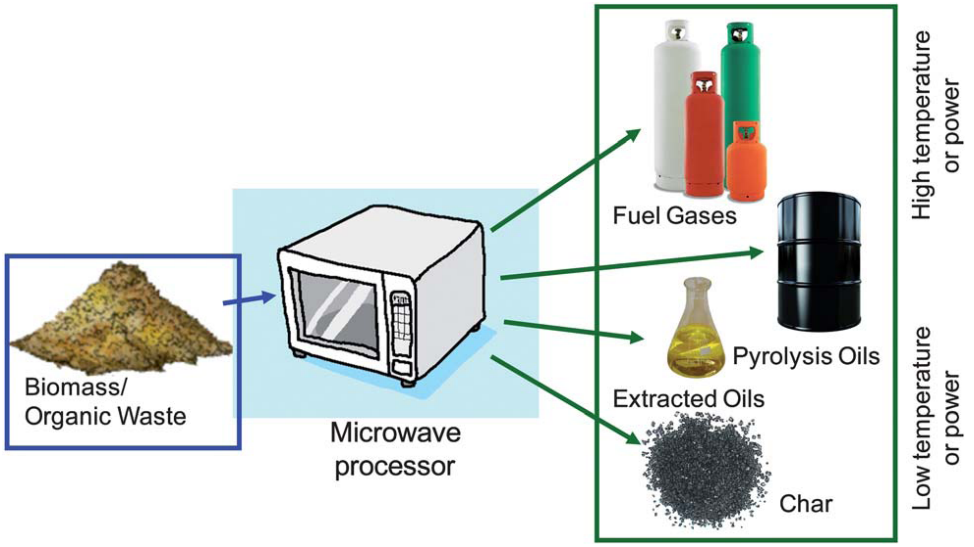

Fig. 2.1 The microwave-assisted thermochemical conversion concept.

2.3.1 Heating mechanism of microwaves

The heating mechanism is different between conventional heating and microwave heating. The heat flow and mass flow directions in the two heating methods are shown in Fig. 2.2. In the case of conventional heating, heat is transferred from the surface to the core of the material through conduction driven by temperature gradients. Mass flow, which is always outward, is the movement of gaseous compounds generated by thermochemical reactions. Thus, heat flow and mass flow are countercurrent for conventional heating. In the case of microwave heating, microwaves induce heat at the molecular level by direct conversion of the electromagnetic energy into heat. Therefore, microwave irradiation can provide uniform internal heating for material particles, making the heat flow and mass flow concurrent. In addition, the surrounding of the biomass particle in conventional heating is very hot while that in microwave heating is relatively cool. The faster movement of emitted gaseous compounds and cooler surrounding in

microwave heating is likely to cause less secondary reactions and may hence resulted in higher yields of desirable products compared with conventional heating.

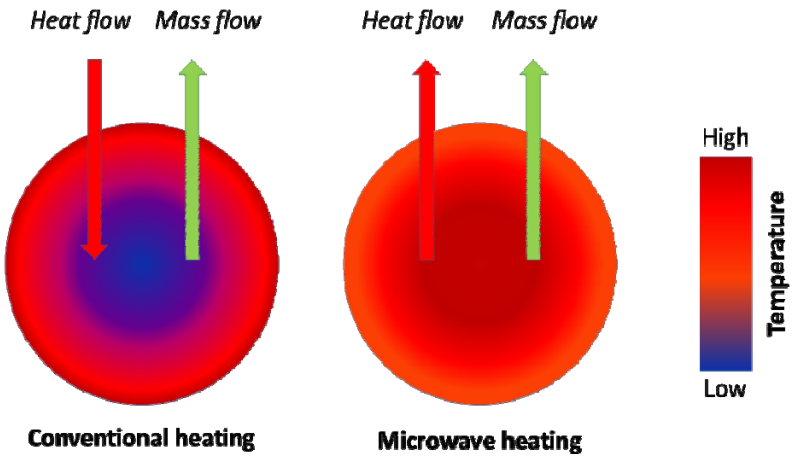

Fig. 2.2 Schematic illustration of temperature gradient and heat and mass flows in cross-section of a wood cylinder subjected to conventional and microwave heating.

Heating of material using microwave is a result of interactions between microwave irradiation and molecules in the material. Irradiation of a material at microwave frequencies results in the dipoles or ions aligning in the applied electric field, giving rise to the main mechanisms of microwave heating: (a) dipole rotation; (b) ionic migration. As the applied field oscillates, the dipole or ion field attempts to realign itself with the alternating electric field. In this process, energy is dissipated as heat from internal resistance to the rotation.

Microwave heating relies on the ability of a specific material to absorb microwave energy and convert it into heat, which in turn depends on the dielectric properties of the material, i.e., dielectric constant (ε′) and dielectric loss (ε″) (Thostenson and Chou, 1999). Materials with a high conductance and low capacitance (such as metals) have high dielectric loss factors. As the dielectric loss factor gets very large, the penetration depth

approaches zero. Materials with this dielectric behavior are considered conductors or reflectors. Materials with low dielectric loss factors have a very large penetration depth. As a result, very little of the energy is absorbed in the material, and the material is transparent to microwave energy and considered insulator. Therefore, microwaves transfer energy most effectively to materials that have dielectric loss factors in the middle of the conductivity range. These materials are considered microwave absorbers.

The ratio of the dielectric loss to dielectric constant is referred to as the loss tangent, $\tan \delta = \varepsilon''/\varepsilon'$, which is used to describe the overall efficiency of a material to absorb microwave radiation. In general, materials can be classified as high ($\tan \delta > 0.5$), medium (0.1–0.5), and low microwave absorbing (<0.1). Table 2.2 shows the $\tan \delta$ values of some carbon rich materials relevant to biomass conversion. Most of these carbon materials except coal and carbon foam are good microwave absorbers, especially activated carbon and silicon carbide (SiC). These materials can be added to low loss biomass feedstocks during microwave assisted pyrolysis in order to improve heating, and such strategy has been proposed and tested by a number of researchers.

Table 2.2 Dielectric loss tangents for different carbon materials at a frequency of 2.45 GHz and room temperature, ca., 298 K (Menéndez et al., 2010).

Carbon material	$\tan \delta = \varepsilon''/\varepsilon'$	Carbon material	$\tan \delta = \varepsilon''/\varepsilon'$
Coal	0.02–0.08	Activated carbon	0.57–0.80
Carbon foam	0.05–0.20	Activated carbon[a]	0.22–2.95
Charcoal	0.11–0.29	Carbon nanotube	0.25–1.14
Carbon black	0.35–0.83	SiC nanofibres	0.58–1.00

[a] Activated carbon at a mean temperature of 398 K.

2.3.2 Microwave-assisted conversion processes

The novel microwave-assisted biomass conversion technology has recently attracted more attention compared to previous years and has been proved to be suitable for the processing of feedstocks including a variety of raw materials such as seaweed and coffee hulls (Luque et al., 2012). Most of previous studies about microwave-assisted thermochemical conversion of biomass focused on biomass pyrolysis.

In terms of product distributions, yields, and quality, microwave-assisted pyrolysis (MAP) is reported to be superior to conventional pyrolysis (CP). The bio-oils were obtained in larger quantities from MAP and were found to contain virtually no polycyclic aromatic hydrocarbons (PAH) (Domínguez et al., 2003), which are undesirable due to their carcinogenic and/or mutagenic effects. In addition, significantly higher proportions of syngas and less CO_2 (almost double in some cases and less than half, respectively) were obtained in the gases from MAP compared to those from CP under strictly comparable conditions (Fernández and Menéndez, 2011). Furthermore, the biochar generated during CP processes is usually fragile due to the convective heating profiles and differences in temperatures of the outer and inner surface. Comparatively, the homogeneous and selective heating of MAP leads to a higher quality biochar at lower temperatures (Salema and Ani, 2011). Since on oxygen is present during the MAP process, the formation of oxides and other toxic compounds such as dioxins is minimized under usual working conditions. Du et al. (2011) investigated microwave-assisted pyrolysis of *Chlorella sp.* with char as microwave reception enhancer and obtained the maximum bio-oil yield of 28.6% under the microwave power of 750 W. However, most previous studies on microwave-assisted biomass conversion processes focused on direct

microwave heating of biomass and the heating rate could not meet the criteria for fast pyrolysis or gasification.

2.3.3 Development of fast microwave-assisted conversion processes

In ceramic processing using microwave, SiC is often used as "susceptor" to surround low loss ceramic materials such as zirconia (ZrO_2) and alumina (Al_2O_3) to increase the temperature of ceramic materials to their critical temperatures at which they become highly absorptive and heat up directly (Lasri et al., 2000). The combination of indirect and direct heating methods can be considered "hybrid heating". This concept can be employed to develop fast microwave-assisted thermochemical conversion processes. A bed of microwave susceptors/adsorbents is initially placed in a microwave reactor and heated up to a desired temperature. Biomass material is then put in contact with the hot adsorbents and heated rapidly. The biomass, once heated, becomes highly microwave absorbing, further increasing the heating rate. As a result, the conversion process can proceed at a very high heating rate, meeting the criteria for fast pyrolysis and gasification. The outcome of such fast process is expected to be different from that of direct microwave heating of biomass (Lam and Chase, 2012). Borges et al. (2014) performed fast microwave-assisted pyrolysis (fMAP) of *Chllorella sp.* and *Nannochloropsis* strains in the presence of SiC as the microwave adsorbent and HZSM-5 as the catalyst, and the maximum bio-oil yields of 57 wt.% and 59 wt.% were obtained, respectively. The results show that the use of microwave adsorbent in fMAP increased bio-oil yields and quality, and it is a promising technology to improve the commercial application and economic outlook of the microwave-assisted pyrolysis technology.

CHAPTER 2 MICROWAVE HEATING CHARACTERISTICS OF BIOMASS AND MICROWAVE ABSORBENTS

Abstract

In this chapter, the microwave heating characteristics of various biomass feedstocks and microwave absorbents were examined and compared. Experimental results show that microwave absorbents absorbed the microwave irradiation more effectively than biomass. The addition of these microwave absorbents to biomass feedstock during microwave-assisted thermochemical conversion significantly improved the heating characteristics. Among the three microwave absorbents studied, silicon carbide (SiC) exhibited higher microwave absorbing ability than activated carbon (AC) and graphite (GE), which was mainly attributed to a higher dielectric loss tangent (tan δ) value of silicon carbide. In addition, higher microwave absorbing ability and heating rates were achieved when more microwave absorbents were used. Finally, a fast microwave-assisted biomass conversion system was developed.

3.1 Materials and methods

3.1.1 Materials

In this study, corn stover as the biomass feedstock, and three microwave absorbents, i.e., silicon carbide (SiC), activated carbon (AC), and graphite (GE) were used.

The corn stover was obtained from a farm field located in Saint Paul Campus, University of Minnesota (Twin Cities). The basic physico-chemical characteristics of the corn stover including proximate analysis and element analysis are shown in Table 3.1.

The elemental analysis was performed with an elemental analyzer (CE-440, Exerter Analytical Inc., MA). According to the elemental analysis, the simplified chemical formula of the raw material that derives is $CH_{1.53}O_{0.97}$. Prior to its use, the corn stover samples were ground using a rotary cutting mill and then screened to limit the particle size smaller than 0.5 mm. Afterwards, these ground samples were dried at 80±1 ºC for more than 24 h.

Table 3.1 Characteristics of corn stover.

Proximate analysis (wet basis, wt.%)			Elemental analysis (dry basis, wt.%)				HHV[b] (MJ/kg)	NHV[c] (MJ/kg)
Moisture	Volatile	Ash	C	H	N	O[a]		
5.27	81.89	2.06	40.38	5.16	0.38	52.01	15.06	13.07

[a] Calculated by difference, O (%) = 100 – C – H – N – Ash;
[b] Higher heating value, calculated using the equation (Vallios et al., 2009) HHV (MJ/kg) = 34.1 C + 123.9 H – 9.85 O + 6.3 N + 19.1 S;
[c] Net heating value, calculated using the equation (Vallios et al., 2009) NHV (MJ/kg) = (HHV – 21.92 H) (1 – MCWB/100) – 0.02452 MCWB, where MCWB is the moisture content on a wet basis of biomass.

Silicon carbide with the particle size of 36 grit (0.5 mm) was purchased from Arrowhead Lapidary and Supply (Wellington, OH). Activated carbon (50 mesh, 0.297 mm) and graphite (80 mesh, 0.177 mm) were obtained from Alfa Aesar (Ward Hill, MA).

3.1.2 Determination of microwave heating characteristics

The microwave heating characteristics of biomass feedstocks with and without the microwave absorbents were studied and compared. The optimum microwave absorbent was determined in terms of the heating rate under the microwaves.

3.2 Results and discussion

3.2.1 Effect of microwave absorbents on microwave heating characteristics of biomass

The microwave heating characteristics of corn stover with and without microwave absorbent (SiC) were determined and compared. As shown in Fig. 3.1, for 150 grams of corn stover, the temperature continuously increased with time under the microwave heating. A sharp increase in temperature was noticed at about 320 ºC which indicated the beginning of exothermic pyrolysis reaction. The temperature decreased slightly after it reached the maximum value of 844 ºC. This was because that corn stover was pyrolyzed to produce biochar which was good microwave absorbent and effectively absorbed the microwave irradiation to keep the temperature stable. Similar trend of temperature change was found for 150 grams of corn stover mixed with the same amount of SiC, but the heating rate was much higher which resulted in much shorter time to complete the pyrolysis reaction. It demonstrated that microwave absorbents such as SiC can absorb microwave more effectively than biomass. The addition of these microwave absorbents to biomass feedstock can significantly improve the microwave heating characteristics.

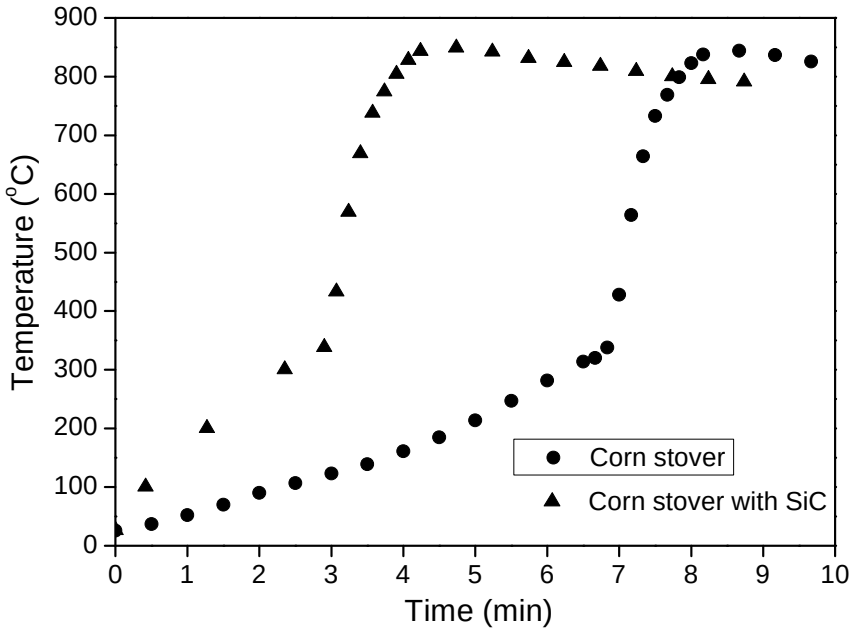

Fig. 3.1 The temperature profiles for corn stover with and without SiC under microwave heating.

3.2.2 Microwave heating characteristics of different microwave absorbents

The microwave heating behaviors of different microwave absorbents including silicon carbide, activated carbon, and graphite were investigated and compared. As shown in Fig. 3.2, the heating rate of silicon carbide was higher than that of the same amount of activated carbon or graphite under the microwave heating. It means that silicon carbide is a better microwave absorber than activated carbon and graphite. The ability of a specific material to absorb microwave energy and convert it into heat mainly depends on the dielectric properties of the material. The dielectric loss tangent (tan δ) is used to describe the overall efficiency of a material to absorb microwave radiation. Materials with higher tan δ values have higher microwave absorbing ability and can be considered better microwave absorbers. The tan δ value of SiC (0.58–1.00) is usually higher than that of AC (0.57–0.80) or GE (0.35–0.83). Therefore, SiC was selected as the microwave

absorbent for the following experiments. In addition, it can be seen from Fig. 3.2 that the heating rate of 800 grams of SiC was higher than that of 500 grams of SiC. It indicates that larger amounts of microwave absorbents result in higher microwave absorbing ability, and more microwave absorbents are needed if higher heating rates and temperatures are required.

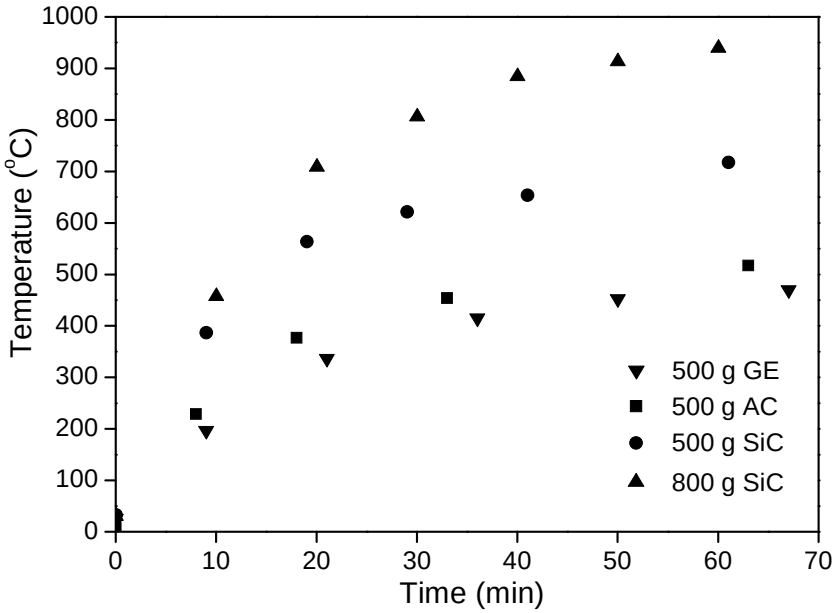

Fig. 3.2 The temperature profiles for different microwave absorbents under microwave heating.

3.3 Development of fast microwave-assisted biomass conversion system

Based on the above results, a fast microwave-assisted biomass conversion system has been developed. The tests of fast microwave-assisted pyrolysis (fMAP) and gasification (fMAG) will be performed in a microwave oven (MAX, CEM Corporation), with the power of 750 W at a frequency of 2,450 MHz. The schematic diagram of experimental apparatus is shown in Fig. 3.3. The system is composed of: (1) biomass feeder; (2) inlet quartz connector; (3) microwave oven; (4) quartz reactor; (5) microwave

absorbent bed; (6) thermocouple (K-type) to measure the temperature of cavity; (7) thermocouple (K-type) to measure the temperature of bed particles; (8) outlet quartz connectors; (9) liquid fraction collectors; (10) condensers; (11) connection for vacuum pump. For safety purpose, a microwave detector (MD-2000, Digital Readout) will be used to monitor microwave leakage.

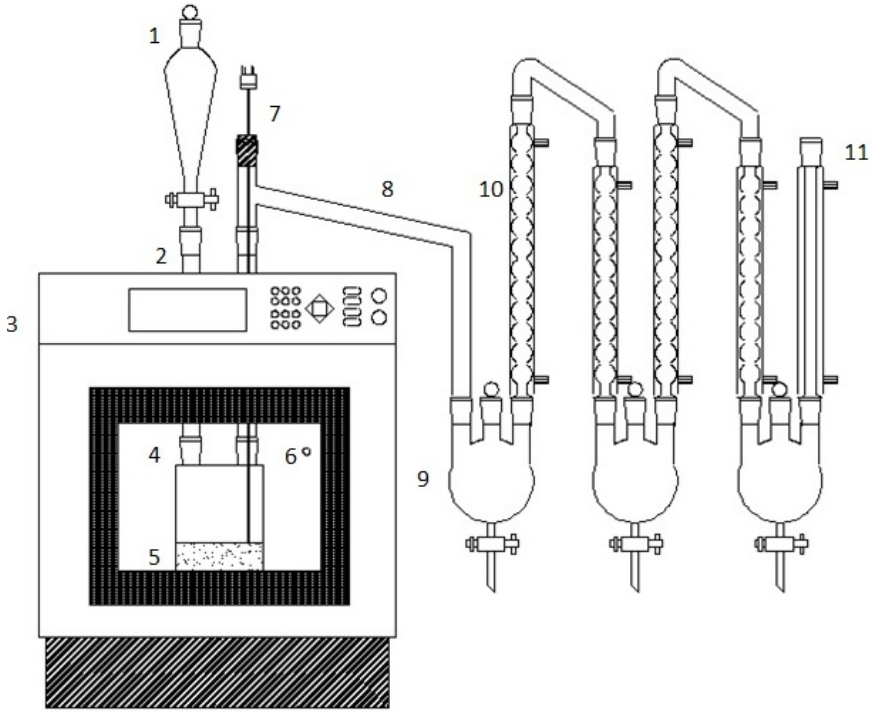

Fig. 3.3 Schematic diagram of fast microwave-assisted biomass conversion system.

In this study, SiC particles with particle size of 36 grit will be used as the microwave absorbent bed, whose temperature will be increased very quickly when they absorb the microwave. A prescribed amount of SiC particles will be first put in the quartz reactor, which will then be placed in the cavity of the microwave oven. For biomass pyrolysis, in order to maintain an inert atmosphere within the reactor, the system will be vacuumed at 80 mmHg for 10 min prior to the commencement of the microwave heating, with the

vacuum being maintained during the entire heating process. The microwave oven is then turned on for heating process. When the temperature of the SiC bed reached the set temperature, the prepared sample will be introduced into the reactor through the feeder and the pyrolysis/gasification reaction occurs once the sample is dropped onto the hot bed. At the same time, the microwave oven is set to be on or off in order to maintain a stable temperature of the absorbent bed, with the deviation of temperature measured by the thermocouple within ±5 ºC. For each run, the pyrolysis/gasification temperature will be kept for about 30 minutes after the feeding to ensure that the pyrolysis/gasification process is complete. Flowing through the condensers, the condensable components in the product will be condensed and collected into the liquid collectors as bio-oil for subsequent analysis, and the non-condensable gas product will be collected at the outlet of the condensers into sampling bags for offline analysis. The residue in the reactor after reaction is collected as biochar for pyrolysis or ash for gasification. The yields of bio-oil and biochar/ash are calculated on the basis of their actual weight, while the gas yield is calculated by difference based on the mass balance.

3.4 Conclusions

In this chapter, the microwave heating characteristics of various biomass feedstocks and microwave absorbents were investigated and compared. Microwave absorbents absorbed microwave more effectively than biomass and the addition of these microwave absorbents to biomass feedstock significantly improved the microwave heating characteristics. Silicon carbide proved to be a better microwave absorber than activated carbon and graphite, and hence was selected as the microwave absorbent for the

following research. Based on these results, a fast microwave-assisted biomass conversion system was developed.

CHAPTER 3 FAST MICROWAVE-ASSISTED BIOMASS PYROLYSIS FOR BIO-OIL PRODUCTION

Abstract

In this chapter, fast microwave-assisted catalytic co-pyrolysis of microalgae and scum on HZSM-5 catalyst for bio-oil production was investigated. The effects of co-pyrolysis temperature, catalyst to feed ratio, and microalgae to scum ratio on bio-oil yield and composition were examined. Experimental results show that temperature had great influence on the co-pyrolysis process. The optimal temperature was 550 ºC since the maximum bio-oil yield and highest proportion of aromatic hydrocarbons in the bio-oil were obtained at this temperature. The bio-oil yield decreased when catalyst was used, but the production of aromatic hydrocarbons was significantly promoted when the catalyst to feed ratio increased from 1:1 to 2:1. Co-feeding of scum improved the bio-oil and aromatics production, with the optimal microalgae to scum ratio being 1:2 from the perspective of bio-oil quality. The synergistic effect between microalgae and scum during the co-pyrolysis process became significant only when the effective hydrogen index (EHI) of feedstock was larger than about 0.7. In addition, to better understand the fMAP of microalgae, the different roles of three major components, i.e., carbohydrates, proteins, and lipids, were investigated. Cellulose, egg whites, and canola oil were employed as the model compounds of the three components, respectively. Non-catalytic and catalytic fMAP were carried out to identify and quantify some major products, and several reaction pathways were proposed for the pyrolysis of each model compound based on the data obtained. Moreover, a two-step process of microalgae pyrolysis and downstream

catalytic reforming was conducted and compared with the one-step process for bio-oil production. The results show that a lower bio-oil yield and higher bio-oil quality were achieved for the two-step process than the one-step process at the same catalyst to feed ratio. The main advantages of the two-step process lie in catalyst saving and reuse. Furthermore, fast microwave-assisted catalytic pyrolysis of sewage sludge was investigated for bio-oil production, with HZSM-5 as the catalyst. Pyrolysis temperature and catalyst to feed ratio were examined for their effects on bio-oil yield and composition. Experimental results show that microwave is an effective heating method for sewage sludge pyrolysis. Temperature has great influence on the pyrolysis process. The maximum bio-oil yield and the lowest proportions of oxygen- and nitrogen-containing compounds in the bio-oil were obtained at 550 ^{o}C. The oil yield decreased when catalyst was used, but the proportions of oxygen- and nitrogen-containing compounds were significantly reduced when the catalyst to feed ratio increased from 1:1 to 2:1. Essential mineral elements were concentrated in the biochar after pyrolysis, which could be used as a soil amendment in place of fertilizer. Results of XRD analyses demonstrated that HZSM-5 catalyst exhibited good stability during the microwave-assisted pyrolysis of sewage sludge.

4.1 Introduction

Recently, increasing studies have been conducted on renewable energy, as a solution to current energy and environmental issues caused by traditional fossil fuels use. Since the carbon emission of biomass during its conversion roughly equals to the carbon absorbed during the plant growth, the use of biomass does not contribute to the buildup of

CO_2 in the atmosphere (McKendry, 2002a). The biomass utilization technologies including biological conversion such as ethanol fermentation and anaerobic digestion and physicochemical conversion such as pyrolysis are considered very promising in the future energy portfolio (Richardson et al., 2012). However, the growth of lignocellulosic biomass on arable land would compete for land-use with food production and lead to undesirable land clearing (Fargione et al., 2008). Since microalgae usually have faster growth rates, shorter growing cycles, higher photosynthetic efficiencies and oil contents than terrestrial crops (Gouveia and Oliveira, 2009; Pirt, 1986; Schenk et al., 2008), they have received growing interest these days (Chisti, 2008; Luque et al., 2010). The bio-oils obtained from microalgae have better quality in many aspects than those from lignocellulosic biomass such as wood (Du et al., 2012; Li et al., 2012; Maddi et al., 2011; Thangalazhy-Gopakumar et al., 2012). In addition, microalgae can be cultivated on marginal lands and waterbodies. Therefore, they do not compete with traditional agricultural resources and have much less impact on current land-use for food production (Chen et al., 2009; Yu et al., 2011).

Traditional conversion of microalgae to biofuels is usually realized through oil extraction by organic solvents, hydrothermal liquefaction or pyrolysis process. However, there are many issues with these methods including low conversion rate, long conversion time, high energy consumption, etc. (Ehimen et al., 2010; Paik et al., 2009; Wang et al., 2013). Recently, a new conversion route, microwave-assisted pyrolysis (MAP) process has been developed and gained much attention (Bu et al., 2012; Huang et al., 2010; Wan et al., 2009; Wang et al., 2012). The new method offers many advantages over traditional processes, including uniform internal heating of large particles, rapid start-up and shut-

down, and low cost. In addition, the process operation involves a simple set-up and can be easily adapted to currently available large-scale industrial technologies. Du et al. (2011) investigated microwave-assisted pyrolysis of *Chlorella* sp. and obtained the maximum bio-oil yield of 28.6% under the microwave power of 750 W. In order to improve the quality of algal bio-oil, catalysts were always used in the microalgae pyrolysis process (Babich et al., 2011; Thangalazhy-Gopakumar et al., 2012) to reduce the contents of oxygenates and nitrogenates (Jena and Das, 2011; Maddi et al., 2011; Pan et al., 2010) in the bio-oil.

However, microalgae are hydrogen deficient, which has adverse impacts on hydrocarbon production from the pyrolysis process. Co-pyrolysis of biomass with an additional feedstock with a high EHI value (see equation (2.1)) is an attractive route to increase the hydrogen content of feedstock, and hence the hydrocarbon yield in the pyrolysis bio-oil will be increased. Scum is the floating debris skimmed from the surface of the primary and secondary settling tanks in wastewater treatment plants. It is a complex mixture containing animal fat, vegetable oil, food wastes, plastic materials, soaps, waxes, and many other wastes discharged from restaurants, households, and other facilities (Bi et al., 2015). Scum is usually disposed in landfills, which not only increases the treatment cost, but also causes many environmental problems. However, scum has the potential to be a better hydrogen supplier than conventional hydrogen sources due to its large generation, low price, and high EHI value. In addition, despite a few previous studies conducted on microwave-assisted pyrolysis of microalgae, no research has been reported on the pyrolysis mechanism.

Sewage sludge from municipal and industrial wastewater treatment plants is a great issue risking the environment and human health, and has raised growing concern recently (Fytili and Zabaniotou, 2008; Laturnus et al., 2007). Nowadays, the most common methods for treatment and disposal of sewage sludge include landfill, agricultural application and incineration (Fonts et al., 2012). However, they all have drawbacks and have become less acceptable (Houillon and Jolliet, 2005; Rio et al., 2006; Werther and Ogada, 1999). An alternative management technique is pyrolysis which could achieve 50% reduction in waste volume (Inguanzo et al., 2002), the stabilization of organic matter, as well as the production of fuels. Elements such as Na and Mg will be concentrated in the pyrolysis char, which can then be used as the soil amendment or be upgraded to become an adsorbent (Bridle and Pritchard, 2004; Smith et al., 2009). The produced gas and oil can be either directly burned as a fuel to provide heat and electricity, or further converted to other chemicals through subsequent processes (Domínguez et al., 2006; Park et al., 2008). Despite some reports on pyrolysis of sewage sludge, only a few studies have been conducted on sewage sludge pyrolysis using microwave technology and the effects of catalyst on the pyrolysis process were not examined in their research (Domínguez et al., 2006; Menéndez et al., 2002).

In this chapter, fast microwave-assisted catalytic co-pyrolysis of microalgae and scum was carried out with HZSM-5 as the catalyst for bio-oil production under different conditions. The effects of pyrolysis temperature, catalyst to feed ratio, and microalgae to scum ratio on product distribution and bio-oil composition were investigated. In addition, microcrystalline cellulose, dried egg whites, and canola oil were used as the model compounds of the three major components of microalgae, i.e., carbohydrates, proteins,

and lipids, respectively. The reaction pathways during the fMAP of microalgae were investigated through pyrolysis of the model compounds. Catalytic pyrolysis of the three model compounds for the production of aromatic compounds was also studied, using HZSM-5 as the catalyst. Furthermore, a two-step process of microalgae pyrolysis and downstream catalytic reforming was carried out and compared with the one-step process for bio-oil production. Moreover, microwave-assisted catalytic pyrolysis of sewage sludge was carried out with HZSM-5 as the catalyst for bio-oil production under different conditions. The effects of pyrolysis temperature and catalyst to feed ratio were investigated on product distribution and bio-oil composition. X-ray Diffraction (XRD) analyses of catalyst before and after reaction were conducted to examine its stability during pyrolysis process. In addition, characterization of biochar was conducted using elemental analysis and ICP-OES multi-element determination.

4.2 Materials and methods

4.2.1 Materials

Nannochloropsis sp., a commercial microalgae strain, was purchased from Reed Mariculture Inc. (Campbell, CA). Prior to use, the algal slurry (80% moisture content) was dried in a vacuum freeze drier (Freezemobile, VirTis) at –85 ºC for 72 h, and then mechanically pulverized and sifted through a 40-mesh sieve. The basic physico-chemical characteristics of the dried algal biomass powder including proximate analysis and elemental analysis are shown in Table 4.1. The EHI value of microalgae calculated using equation (2.1) was –0.095.

Table 4.1 Characteristics of dried algal biomass powder.

Proximate analysis[a] (wt%)		Elemental analysis[a] (wt%)	
Protein	58.6[c]	C	40.5
Lipid (Total)	14.5[c]	H	5.7
Carbohydrate	20.0[c]	N	5.7
Ash	5.9[c]	O[b]	38.2

[a] Dry basis;
[b] Calculated by difference, O (%) = 100 – C – H – N – Ash.
[c] Data provided by the supplier.

Scum was collected from the Metropolitan Wastewater Treatment Plant, Saint Paul, Minnesota. Prior to use, the solid scum was dried at 105 ºC for 24 h, and at the same time melted so the oily materials in scum can be in a liquid state, and then filtered through a 100-micron polyester mesh filter bag to remove large solid particles. The elemental composition of the solid scum (on dry basis) was 73.2 wt% carbon, 11.6 wt% hydrogen, 0.06 wt% nitrogen, and 15.1 wt% oxygen (by difference). The EHI value of scum was 1.59.

Laboratory grade microcrystalline cellulose was bought from Sigma Aldrich (St Louis, MO). Egg white powder was obtained from Rose Acres Farms, Inc. (Seymour, IN). Food grade canola oil was purchased from a local grocery store. The basic physico-chemical characteristics of the three model compounds are listed in Table 4.2. The cellulose and canola oil samples were considered as pure carbohydrates and lipids, respectively. The protein content of egg whites was obtained by multiplying nitrogen content by a factor of 6.25 (Rao and Labuza, 2012). The ash content of egg whites was determined according to ASTM E1755.

Table 4.2 Characteristics of model compounds.

Compound	Elemental analysis[a] (wt%)				Proximate analysis[a] (wt%)			
	C	H	N	O[b]	Proteins	Lipids	Ash	Others[c]
Cellulose	43.7	6.1	0.0	50.2	0.0	0.0	0.0	100.0
Egg whites	47.7	6.4	13.3	26.7	83.1	0.0	5.9	11.0

Canola oil	77.9	10.9	0.1	11.1	0.0	100.0	0.0	0.0

[a] Dry basis;
[b] Calculated by difference, O (%) = 100 – C – H – N – Ash;
[c] Calculated by difference, Others (%) = 100 – Proteins – Lipids – Ash.

The sewage sludge used as the raw material for this study was obtained from the Metropolitan Wastewater Treatment Plant, Saint Paul, Minnesota. The sewage sludge was a mixture of primary and secondary sludge. The basic physico-chemical characteristics of the sewage sludge including proximate analysis, elemental analysis and mineral elements determination are shown in Table 4.3. According to the elemental analysis, the simplified chemical formula of the raw material that derives is $CH_{1.67}N_{0.10}O_{0.47}$. The higher heating value (HHV) observed for sewage sludge is similar to that of other conventional and non-conventional fuels such as paper, wood, black liquor or low rank coal (Perry, 1984). It is reported that the presence of inorganic matter can influence the thermal decomposition process (Mohan et al., 2006; Oasmaa et al., 2010; Richards and Zheng, 1991). It can be seen from Table 4.3 that there are considerable amounts of P, Ca and K in the sewage sludge, whereas other metals such as Co, Ni, Cu and Zn are in lower proportions. Prior to use, the sewage sludge samples were ground using a rotary cutting mill and then screened to limit the particle size smaller than 2 mm. These ground samples were then dried at 80±1 ºC for 72 h.

Table 4.3 Characteristics of sewage sludge.

Proximate analysis (wt.%)				Elemental analysis[a, b] (wt.%)				HHV[d]	NHV[e]
M	A[a]	V[a]	FC[a, c]	C	H	N	O[c]	(MJ/kg)	(MJ/kg)
4.53	15.01	68.57	16.42	53.24	7.39	6.12	33.25	24.42	21.77

Mineral elements[a] (mg/L)										
Al	As	B	Be	Ca	Cd	Co	Cr	Cu	Fe	K
4188.5	6.2	22.4	0.36	20737.2	0.96	3.8	44.9	315.4	5108.5	6298.6
Li	P	Mg	Mn	Mo	Na	Ni	Pb	Ti	V	Zn
2.2	25641.3	5526.4	1153.0	5.0	1161.8	30.8	32.3	111.2	2.0	596.0

M: moisture content; A: ash content; V: volatile matter content; FC: fixed carbon.
[a] Dry basis;
[b] Ash free basis;
[c] Calculated by difference, FC (%) = 100 – A – V, O (%) = 100 – C – H – N;
[d] Higher heating value, calculated using the equation (Vallios et al., 2009) HHV (MJ/kg) = 34.1 C + 123.9 H – 9.85 O + 6.3 N + 19.1 S;
[e] Net heating value, calculated using the equation (Vallios et al., 2009) NHV (MJ/kg) = (HHV – 21.92 H) (1 – MCWB/100) – 0.02452 MCWB, where MCWB is the moisture content on a wet basis of biomass.

A commercial zeolite, namely ZSM-5 (Si/Al = 30, surface area = 405 m^2/g), in the ammonium form purchased from Zeolyst International (Conshohocken, PA) was used as the catalyst for the fMAP process in the present study. Prior to use, the catalyst was calcined at 500 ºC in air for 5 h to its active hydrogen form HZSM-5.

4.2.2 Apparatus

The fast microwave-assisted catalytic pyrolysis of microalgae and their three major components, co-pyrolysis of microalgae and scum, and catalytic pyrolysis of sewage sludge were carried out using the system as described in Section 3.3. The two-step process of microalgae pyrolysis and downstream catalytic reforming was conducted using the microwave-based system coupled with a downstream catalytic fixed bed placed in the outlet quartz connector as the secondary reformer.

The procedure for fMAP of microalgae was described in Section 3.3. For catalytic co-pyrolysis of microalgae and scum, the sample for each experiment was prepared by physically mixing 15 g microalgae and scum mixture with a prescribed amount of catalyst. For fMAP of microalgae and their three major components, the sample for each experiment was prepared by physically mixing 15 g microalgae or each model compound with a prescribed amount of catalyst. For the two-step process of microalgae pyrolysis

and downstream catalytic reforming, 15 g microalgae was used for each experiment, with 0.75 g catalyst filled in the outlet connecter as the secondary reformer. For the comparative one-step microalgae catalytic pyrolysis, the sample for each experiment was prepared by physically mixing 15 g microalgae with a prescribed amount of catalyst. For catalytic pyrolysis of sewage sludge, the sample for each experiment was prepared by physically mixing 15 g sewage sludge with a prescribed amount of catalyst.

4.2.3 Bio-oil analysis

The composition of bio-oil was determined using an Agilent 7890–5975C gas chromatography/mass spectrometer (GC/MS) with a HP-5 MS capillary column. Helium was used as the carrier gas at a flow rate of 1.2 mL/min. The injection size was 1 μL with a split ratio of 1:10. The oven temperature was 40 °C initially held for 3 min and then increased to 290 °C at a rate of 5 °C/min, and held at 290 °C for 5 min. The temperatures of injector and detector were maintained at 250 °C and 230 °C, respectively. The compounds were identified by comparing their mass spectra with those from the National Institute of Standards and Technology (NIST) mass spectral data library. Calibration was not carried out due to the large number of compounds in the pyrolysis bio-oil. A semi-quantitative method was used to determine the relative proportion of each compound in the bio-oil by calculating the area percentage of corresponding chromatographic peak.

4.2.4 Biochar analysis

For the characterization of biochar, elemental analysis was conducted to determine the contents of C, H, N and O, using an Exeter Analytical Inc. (EAI) CE-440 elemental analyzer. In addition, inductively coupled plasma-optical emission spectrometry (ICP-

OES) multi-element determination was carried out on an Applied Research Laboratories (ARL) 3560 optical emission spectrometer to determine the contents of other mineral elements including K, Ca, Mg, Fe, etc.

4.2.5 Catalyst characterization

The X-ray powder diffraction (XRD) patterns, obtained on a Bruker-AXS (Siemens) D5005 X-ray diffractometer instrument with a Cu–K_α radiation at 45 kV and 40 mA, were used to identify the major crystalline phases present in the catalysts. Data collected from the instrument were analyzed using software MDI Jade 8.0.

4.3 Catalytic co-pyrolysis of microalgae and scum

4.3.1 Effect of pyrolysis temperature on bio-oil production

The effects of co-pyrolysis temperature on the yield and composition of the bio-oil were investigated at temperatures ranging from 450 to 650 ºC, with the microalgae to scum ratio being 1:1 and catalyst to feed ratio being 2:1.

As shown in Fig. 4.1(a), temperature had great influence on product distribution from the co-pyrolysis of microalgae and scum. A continuous decrease in char yield and a continuous increase in gas yield with increasing temperature were observed. The bio-oil yield first increased with pyrolysis temperature and then decreased. A maximum bio-oil yield of 22.0 wt% was obtained at the temperature of 550 ºC. The decomposition and devolatilization of solids was promoted by higher temperature since more energy was available to break the strong organic bonds. This was the main reason for the initial decrease in char yield and increase in bio-oil and gas yields with temperature. However,

the endothermic secondary reactions would become dominant when the temperature was higher than 550 ºC, which broke long-chain compounds into smaller molecules. The secondary thermal cracking of oil vapors into incondensable gases was the main cause for the decrease in bio-oil yield and significant increase in gas yield when the temperature reached above 550 ºC.

The chemical composition of the bio-oil was also influenced by temperature. As can be seen in Fig. 4.1(b), the proportion of aromatic hydrocarbons in the bio-oil increased with temperature and reached the maximum at 500 ºC. However, from the perspective of aromatics production, the optimal temperature was 550 ºC taking into account both the bio-oil yield and the proportion of aromatics in the bio-oil. It is also noticed that the proportion of polycyclic aromatic hydrocarbons (PAHs) significantly increased, but the proportions of aliphatic hydrocarbons, oxygen- and nitrogen-containing compounds decreased with increasing temperature. It can be inferred that higher temperature favored the deoxygenation and denitrogenation reactions, as well as the conversion of aliphatic and aromatic hydrocarbons to PAHs. Since PAHs are identified as carcinogenic and mutagenic, bio-oils produced at 500–550 ºC had relatively better quality due to the higher proportions of aliphatic and aromatic hydrocarbons and lower proportions of PAHs, oxygen- and nitrogen-containing compounds in the pyrolysis bio-oil, making it more suitable to be used as a fuel or feedstock for the production of valuable chemical products. Overall, the optimal temperature for bio-oil production from microwave-assisted catalytic co-pyrolysis of microalgae and scum was 550 ºC considering both the bio-oil yield and composition.

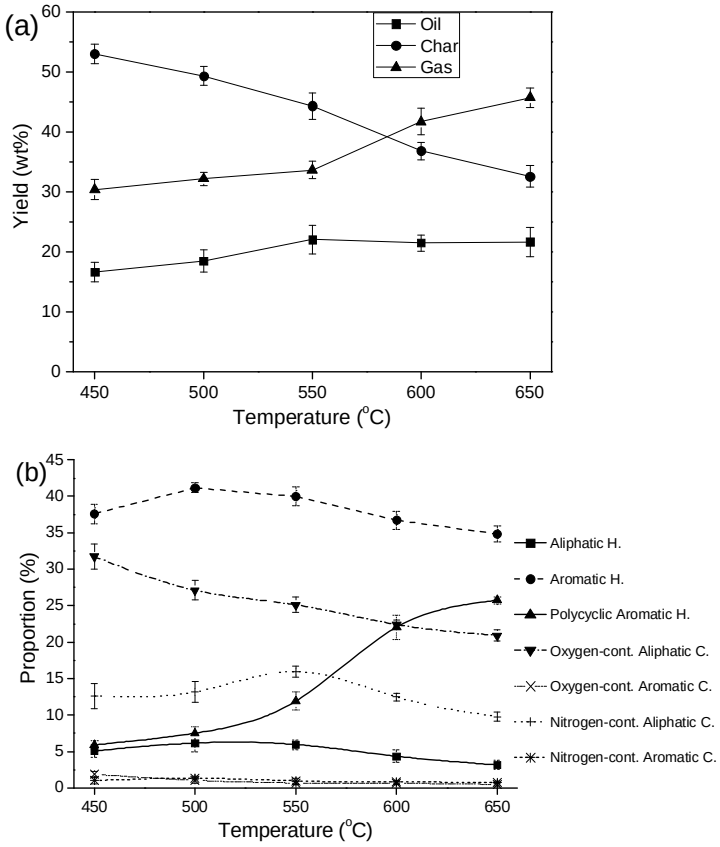

Fig. 4.1 Effect of temperature on fast microwave-assisted catalytic co-pyrolysis of microalgae and scum. (a) Product distribution. (b) Bio-oil composition.

4.3.2 Effect of catalyst to feed ratio on bio-oil production

The effects of catalyst to feed ratio on bio-oil yield and composition were investigated at the pyrolysis temperature of 550 ºC, with the microalgae to scum ratio being 1:1.

As shown in Fig. 4.2(a), the bio-oil yield decreased, while the char and gas yields increased when catalyst was used. The decrease in bio-oil yield was probably due to an increase in the catalytic thermal cracking reactions, which resulted in increased conversion of oil vapors to gases. Another possible reason was that the catalyst utilization

improved the formation of carbonaceous material through repolymerization of oil vapors, which led to the increase in char yield. However, an increase in bio-oil yield and a significant decrease in gas yield were observed when the catalyst to feed ratio increased from 1:1 to 2:1. It is likely that more catalysts resulted in increased recombination of short-chain gas molecules into aromatic compounds and PAHs through a series of aromatization, alkylation, and isomerization reactions, and thus the bio-oil yield increased. In addition, the carbonization reaction was further promoted by more catalysts, causing a remarkable increase in char yield.

The effect of catalyst to feed ratio on bio-oil composition is presented in Fig. 4.2(b). It can be noticed that the proportions of aromatic hydrocarbons and PAHs in the bio-oil from catalytic pyrolysis were significantly increased compared with non-catalytic pyrolysis, at the expense of aliphatic hydrocarbons, oxygen- and nitrogen-containing compounds. Similar results were obtained for catalytic pyrolysis of lignocellulosic biomass over the HZSM-5 catalyst (Mihalcik et al., 2011; Mullen and Boateng, 2010). The HZSM-5 catalyst has a 3-dimensional pore system containing straight 10-member-ring channels connected by sinusoidal channels (Aho et al., 2008), and more importantly, the pore diameter of HZSM-5 is similar to the dynamics diameters of some aromatics such as benzene, toluene, and xylene. The peculiar pore structure of the HZSM-5 catalyst determines its high shape-selectivity to the aromatic hydrocarbons (Zhang et al., 2014). In addition, some oxygen-containing compounds such as acids, ketones, and alcohols, could be deoxygenated and cracked into C2–C6 olefins and alkanes on the HZSM-5 catalyst. The short-chain olefins and alkanes would be transformed to benzene through a series of aromatization reactions, followed by the conversion to other aromatics through

alkylation and isomerization reactions (Carlson et al., 2010; Williams and Horne, 1994). It can be also noted in Fig. 4.2(b) that the proportions of aromatic hydrocarbons and PAHs in the bio-oil significantly increased as the catalyst to feed ratio increased from 1:1 to 2:1. This was probably because a ratio of 1:1 could not provide enough surface contact between the pyrolysis vapors and catalyst particles.

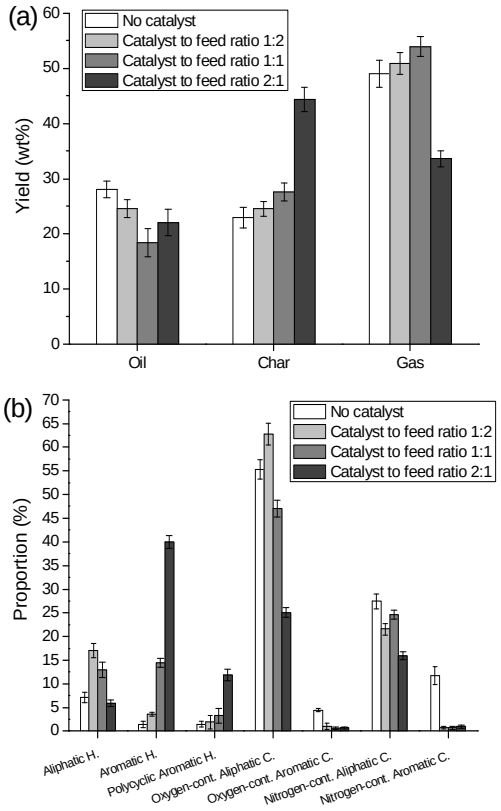

Fig. 4.2 Effect of catalyst to feed ratio on fast microwave-assisted catalytic co-pyrolysis of microalgae and scum. (a) Product distribution. (b) Bio-oil composition.

4.3.3 Effect of microalgae to scum ratio on bio-oil production

The effects of microalgae to scum ratio on bio-oil yield and composition were investigated at the pyrolysis temperature of 550 ºC, with the weight of microalgae and scum mixture being constant of 15 g and catalyst to feed ratio being 2:1. A negative

correlation was observed between the EHI value of feedstock and microalgae to scum ratio, as shown in Fig. 4.3.

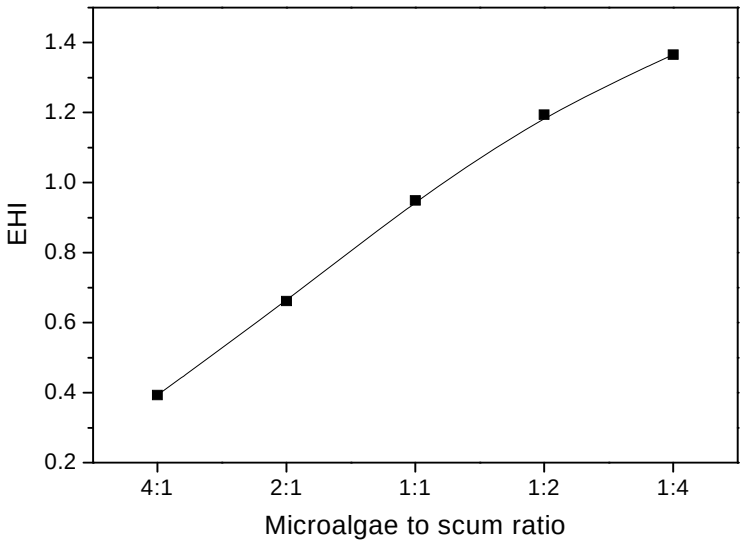

Fig. 4.3 EHI values of feedstock under different microalgae to scum ratios.

The effect of microalgae to scum ratio on bio-oil yield is shown in Fig. 4.4(a). Obviously, the bio-oil and gas yields increased, while the char yield decreased with the decreasing microalgae to scum ratio. It indicates that the co-feeding of scum improved the bio-oil and gas production at the expense of biochar. The main reason is that scum is primarily composed of volatile matters such as vegetable oil, animal fat, and waxes, with very low ash content. In addition, the oxygen-containing compounds in the microalgae pyrolysis vapors could promote the chain scission and cracking of triglycerides in scum (Zhang et al., 2013), further increasing the bio-oil and gas yields.

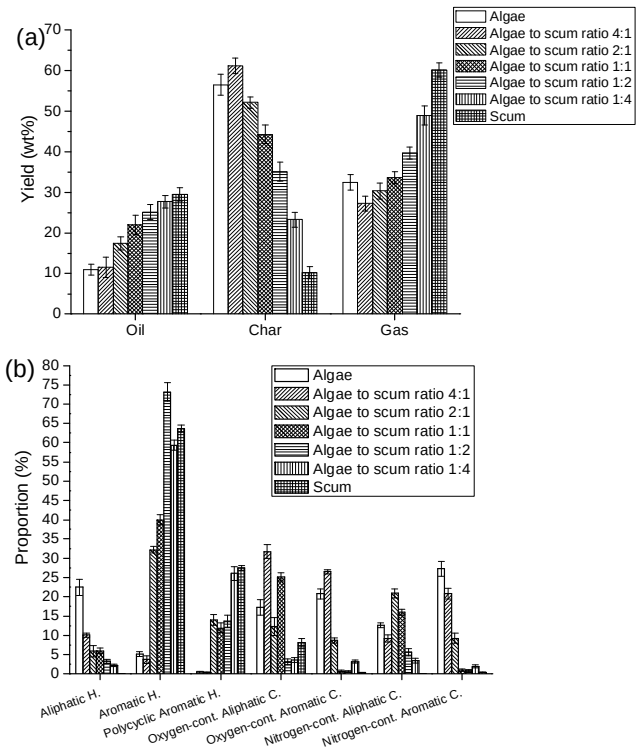

Fig. 4.4 Effect of microalgae to scum ratio on fast microwave-assisted catalytic co-pyrolysis of microalgae and scum. (a) Product distribution. (b) Bio-oil composition.

The bio-oil composition was also greatly influenced by microalgae to scum ratio. As shown in Fig. 4.4(b), an increase in the proportions of aromatic hydrocarbons and PAHs and a decrease in the proportions of aliphatic hydrocarbons, oxygen- and nitrogen-containing compounds in the bio-oil were obtained with an increasing proportion of scum in the feedstock mixture. The main cause also lies in the composition of scum. The vegetable oil, animal fat, waxes, and other volatiles in the scum could be easily pyrolyzed into short-chain olefins and alkanes, which would be transformed to benzene and other aromatics on the HZSM-5 catalyst. More importantly, scum provided hydrogen atoms and increased the EHI value of feedstock, which would significantly improve the production of aromatic hydrocarbons. In addition, the cracking of triglycerides in scum to

hydrocarbons was enhanced by the oxygenated compounds in the microalgae pyrolysis vapors, further promoting the aromatics production. It should be noted that the highest proportion of aromatics in the bio-oil was obtained when microalgae to scum ratio was 1:2, and much more PAHs were produced when microalgae to scum ratio was lower than 1:2. From the perspective of aromatics production, the optimal microalgae to scum ratio was 1:2, with the EHI value of feedstock being approximately 1.2.

The theoretical value (V_T) of bio-oil yield or proportion of aromatics in the bio-oil from fast microwave-assisted catalytic co-pyrolysis of microalgae and scum under different microalgae to scum ratios can be calculated using the following equation,

$$V_T = P_{microalgae} \times V_{microalgae} + P_{scum} \times V_{scum} \quad (4.1)$$

where $P_{microalgae}$ and P_{scum} are the weight proportions of microalgae and scum in the feedstock, respectively; $V_{microalgae}$ and V_{scum} are the actual values of bio-oil yield or proportion of aromatics in the bio-oil from fast microwave-assisted catalytic pyrolysis of microalgae and scum, respectively. A comparison between the theoretical values and the actual values (V_A) of bio-oil yield and proportion of aromatics in the bio-oil under different microalgae to scum ratios is shown in Table 4.4. It can be seen that the actual values are larger than the theoretical values for both bio-oil yield and proportion of aromatics in the bio-oil when microalgae to scum ratio is lower than 2:1, indicating a synergistic effect between microalgae and scum during the co-pyrolysis process. As mentioned above, scum acted as a hydrogen supplier and increased the overall EHI value of feedstock, promoting the production of aromatic hydrocarbons. Meanwhile, the oxygen-containing compounds in the microalgae pyrolysis vapors enhanced the scum

cracking, which further increased the bio-oil yield and improved the production of aromatic hydrocarbons. Note that the synergistic effect became significant only when microalgae to scum ratio was lower than 2:1, or the EHI value of feedstock was larger than about 0.7. Zhang et al. (2015) conducted catalytic co-pyrolysis of corn stalk and high density polyethylene on HZSM-5 catalyst and found that the EHI value of feedstock had an important impact on the relative content of aromatic hydrocarbons only when it exceeded a certain value of approximate 1.0. Similar results were obtained in other studies (Wang et al., 2013; Wang et al., 2014).

Table 4.4 Comparison between the theoretical values and the actual values of bio-oil yield and proportion of aromatics in the bio-oil under different microalgae to scum ratios.

		Microalgae to scum ratio						
		Microalgae	4:1	2:1	1:1	1:2	1:4	Scum
Bio-oil yield (wt%)	V_T	10.9	14.7	17.1	20.3	23.4	25.8	29.6
	V_A	10.9	11.6	17.5	22.0	25.2	27.7	29.6
Proportion of aromatics (%)	V_T	5.1	16.8	24.6	34.4	44.1	51.9	63.6
	V_A	5.1	3.7	32.2	40.0	73.2	59.3	63.6

4.4 Pyrolysis pathways for fMAP of microalgae

4.4.1 FMAP of microalgae and model compounds

FMAP of microalgae and the three model compounds was conducted at the pyrolysis temperature of 550 ºC. The relative proportions of main compounds in the bio-oils are shown in Table 4.5. It can be seen that the composition of algal bio-oil is very different from that of lignocellulosic materials derived pyrolysis bio-oil which is mainly composed of oxygenates (Huber et al., 2006). The main cause lies in the much difference between the components of feedstocks, which are basically carbohydrates, proteins, and

lipids for microalgae while cellulose, hemicellulose, and lignin for lignocellulosic biomass.

Table 4.5 Contents of main compounds in the bio-oils produced from fMAP of microalgae and model compounds at 550 ºC (GC/MS peak area percentage, %).

Compounds	Microalgae	Cellulose	Egg whites	Canola oil
1H-Indole, 4-methyl-	0.28	–	10.59	–
1-Decene	–	–	–	2.41
1-Octene	–	–	–	2.70
2-Aminopyridine	2.89	–	2.10	–
2-Furancarboxaldehyde, 5-methyl-	–	11.78	–	–
2-Pyridinecarbonitrile	4.33	–	1.26	–
2-Pyrrolidinone	2.76	–	1.27	–
5-Isopropyl-2,4-imidazolidinedione	–	–	8.69	–
6-Octadecenoic acid, (Z)-	–	–	–	3.57
Acetamide	0.45	–	4.61	–
Benzenepropanenitrile	2.13	–	0.58	–
Benzyl nitrile	1.45	–	0.92	–
Butanamide, 3-methyl-	3.70	–	9.50	–
Ethylbenzene	–	–	–	2.18
Furfural	–	41.59	–	–
Heptadecane	1.95	–	–	0.53
Indole	3.01	–	8.62	–
n-Decanoic acid	–	–	–	4.99
Nonane	–	–	–	3.64
Pentanamide, 4-methyl-	3.34	–	3.70	–
Phenol	2.39	1.41	5.18	–
Phenol, 4-methyl-	0.31	–	0.36	–
Propanamide	1.20	–	2.45	–
Pyridine	6.49	–	3.88	–
Styrene	–	–	–	4.83
Toluene	1.28	1.18	2.13	3.11
Xylene	–	–	–	3.70

The symbol "–" means that the corresponding compound was not detected.

According to the pyrolytic products of model compounds, furfural and 5-methyl-2-furancarboxaldehyde resulted from the decomposition of carbohydrates such as cellulose and starch. Zhao et al. (2007) proposed a possible pathway for conversion of sugars to 5-

hydroxymethylfurfural (5-HMF). As shown in Fig. 4.5, β-D-glucopyranose was transformed to β-D-fructofuranose through isomerization reaction, followed by dehydration to produce 5-HMF which could be easily converted to furfurals. However, furfurals were not detected in the bio-oil from microalgae pyrolysis. It is possible that furfurals were converted to other compounds such as phenols and short chain hydrocarbons during the fMAP process.

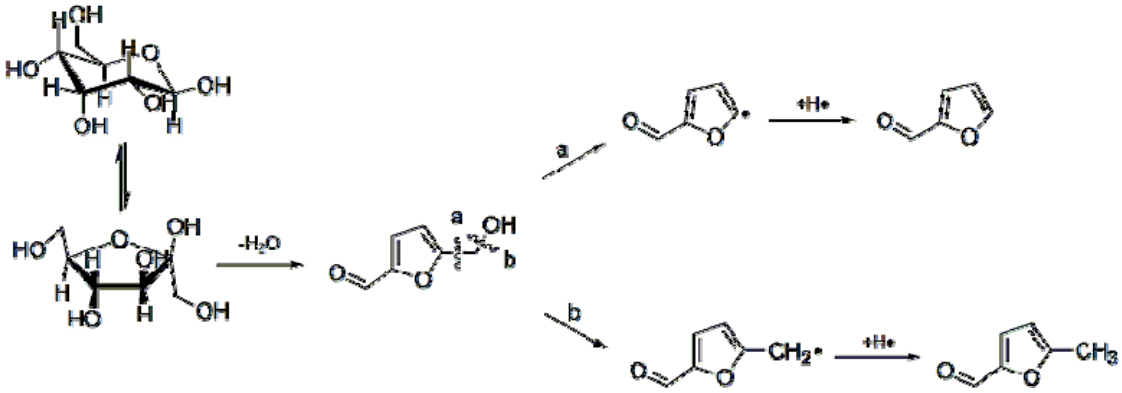

Fig. 4.5 Postulated pathways for fMAP of carbohydrates.

Nitrogenated compounds, including amides, nitriles, pyridine and indole, were found in the bio-oils from fMAP of microalgae and egg whites, indicating that nitrogenated compounds were formed from proteins. As shown in Fig. 4.6, acetamide, propanamide, and 3-methyl-butanamide were produced from asparagine, glutamine, and valine, respectively. The postulated mechanism of the formation of indole and benzyl nitrile from tryptophan and phenylalanine respectively was also illustrated in Fig. 4.6. Since microalgae contain no lignin, lignin derivatives, such as guaiacols and syringols, were not detected. However, phenol and cresol were observed in the pyrolysis bio-oils of microalgae and egg whites, which revealed that phenols were mainly formed from

proteins. In addition, aromatic hydrocarbons such as toluene could be also derived from the protein fraction in microalgae.

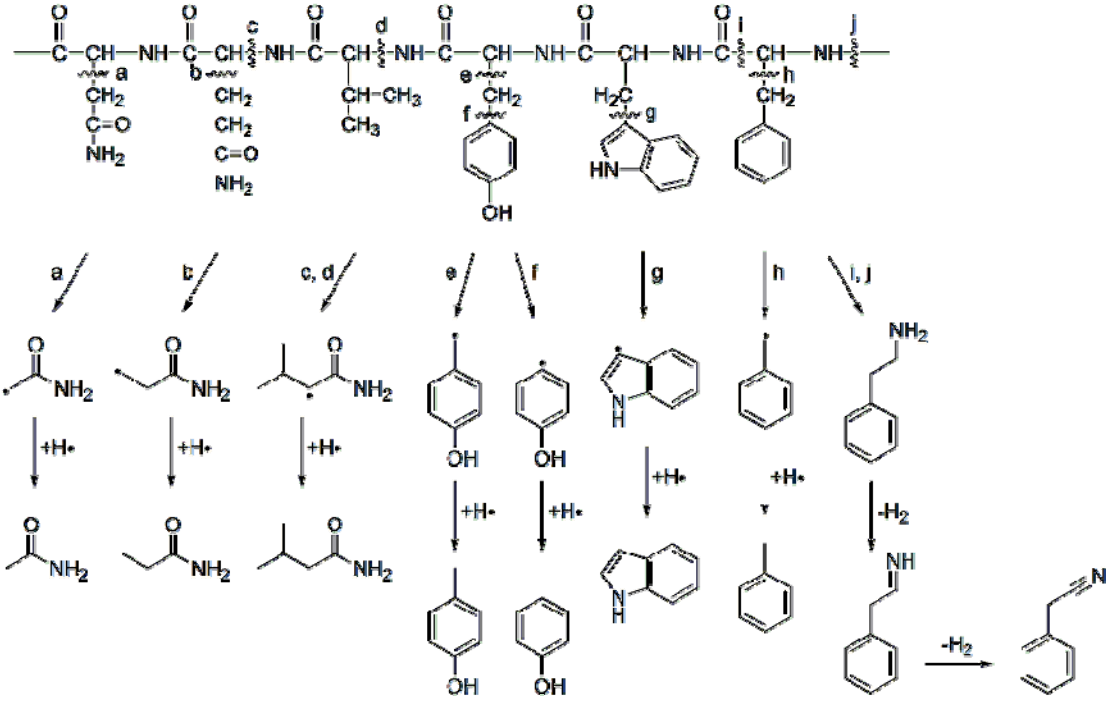

Fig. 4.6 Postulated pathways for fMAP of proteins.

The postulated pathways for fMAP of lipids were shown in Fig. 4.7. Although thermal cracking of triglycerides produced short chain hydrocarbons (Maher and Bressler, 2007), long chain fatty acids also existed (Scheme 1, Fig. 4.7) because of the short residence time in fast microwave-assisted pyrolysis. In addition, as shown in Scheme 2 of Fig. 4.7, aromatic hydrocarbons were also produced from canola oil pyrolysis, indicating that cyclization and aromatization reactions occurred during the fMAP process.

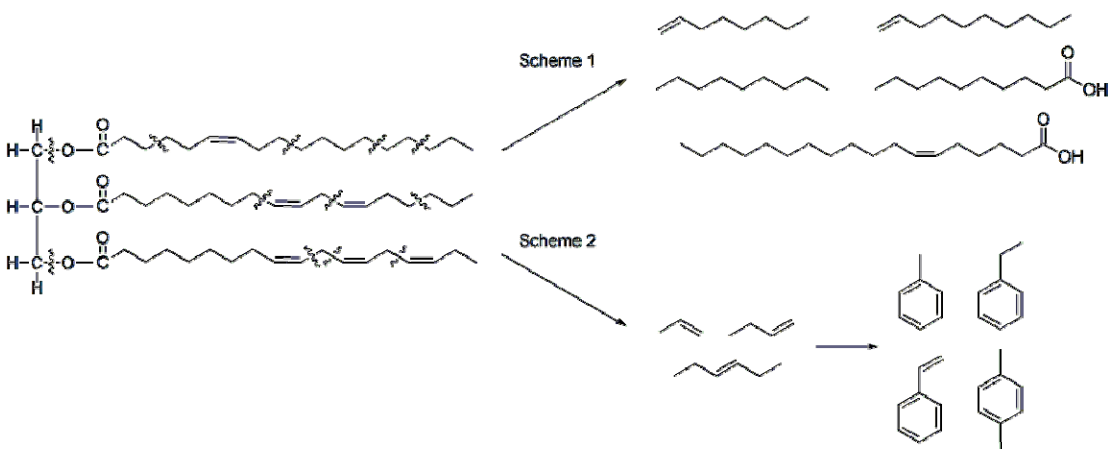

Fig. 4.7 Postulated pathways for fMAP of lipids.

4.4.2 Catalytic pyrolysis of microalgae and model compounds

The bio-oils from fMAP of microalgae and the three model compounds were very complex and the proportions of aromatic hydrocarbons in the bio-oils were very low. Thus, HZSM-5 was employed as the catalyst in the fMAP process to improve the bio-oil quality. As shown in Table 4.6, significantly more aromatic hydrocarbons were produced from catalytic pyrolysis than non-catalytic pyrolysis for all materials studied. This is consistent with many other studies that reported lignocellulosic derived organics could be deoxygenated and cracked to produce aromatics over HZSM-5 (Mihalcik et al., 2011; Mullen and Boateng, 2010). The EHI values for cellulose, egg whites, and canola oil are 0, 0.22, and 1.47, respectively. However, egg whites rather than cellulose, among the three model compounds, produced the least amount of aromatic hydrocarbons. This could be because that nitrogen-containing heterocyclic compounds, such as indole and pyridine, were more stable than oxygenates, which made denitrogenation much more difficult than deoxygenation (Joo and Guin, 1996; Odebunmi and Ollis, 1983). The highest aromatic proportion in the bio-oil was obtained from catalytic pyrolysis of canola oil probably due

to the low oxygen content and relatively simpler chemical structure of canola oil for catalytic cracking. Aside from aromatic hydrocarbons, the relative proportions of most other compounds, such as pyridine an indole derivatives, decreased when catalyst was used for all materials studied. However, more phenols were formed from catalytic pyrolysis than non-catalytic pyrolysis, mainly because phenols were hard for conversion and tightly bound to the acidic active sites of HZSM-5 (Graca et al., 2009).

Table 4.6 Contents of main compounds in the bio-oils produced from fast microwave-assisted catalytic pyrolysis of microalgae and model compounds at 550 ºC (GC/MS peak area percentage, %).

Compounds	Microalgae	Cellulose	Egg whites	Canola oil
1H-Indole, 4-methyl-	4.32	–	1.16	–
Benzene	–	–	–	4.41
Benzene, alkyl-	21.74	2.19	1.79	65.35
Hydrocarbons	4.33	7.45	20.22	0.13
Indene	2.53	–	–	0.20
Indole	3.25	–	6.68	–
Naphthalene	8.22	–	–	5.20
Naphthalene, alkyl-	13.05	–	–	17.44
Nitriles	8.80	–	7.48	–
Phenols	3.70	13.20	24.82	–
Pyridine	1.53	–	2.47	–

The symbol "–" means that the corresponding compound was not detected.

Many studies have been carried out on the catalytic pyrolysis of carbohydrates and lignocellulosic biomass on HZSM-5 (Carlson et al., 2010; Williams et al., 1994), and the reaction pathways of deoxygenation have been proposed based on the transformation of key model components in bio-oil. Light organics, including alcohols, aldehydes, acids, and ketones, derived from carbohydrates in biomass were deoxygenated and cracked into C2–C6 olefins. Then these olefins underwent a series of aromatization reactions to produce benzene followed by alkylation and isomerization reactions to produce other

aromatics as shown in Scheme 1 of Fig. 4.8 (Adjaye and Bakhshi, 1995; Gayubo et al., 2004a; Gayubo et al., 2004b).

The catalytic pyrolysis of triglycerides on HZSM-5 has also been extensively studied (Idem et al., 1996; Katikaneni et al., 1996). Based on these studies, canola oil was proposed to be thermally decomposed to heavy oxygenated hydrocarbons, such as long chain fatty acids, ketones, esters, etc., which were then converted to heavy hydrocarbons by deoxygenation. These heavy hydrocarbons were cracked down to olefins, which subsequently underwent a series of oligomerization, cyclization, and aromatization reactions to give aromatics (Scheme 2, Fig. 4.8).

On the other hand, very limited numbers of reports are available for the catalytic pyrolysis of proteins on HZSM-5. Amines were proposed to be converted to alkenes through deamination reactions catalyzed by HZSM-5 (Lequitte et al., 1992). The C–C bond in nitriles could be broken by HZSM-5 zeolite to form HCN. In addition, some oxygenates, such as ketones and aldehydes, could also undergo the same pathways as those derived from cellulose to produce aromatics. However, as discussed above, phenols were relatively stable on HZSM-5, and thus they were not considered as the major source of aromatics. Based on the literature and our results, the postulated mechanism of catalytic pyrolysis of proteins is shown as Scheme 3 of Fig. 4.8. Further studies are still required to elucidate the exact reaction pathways for each individual compound.

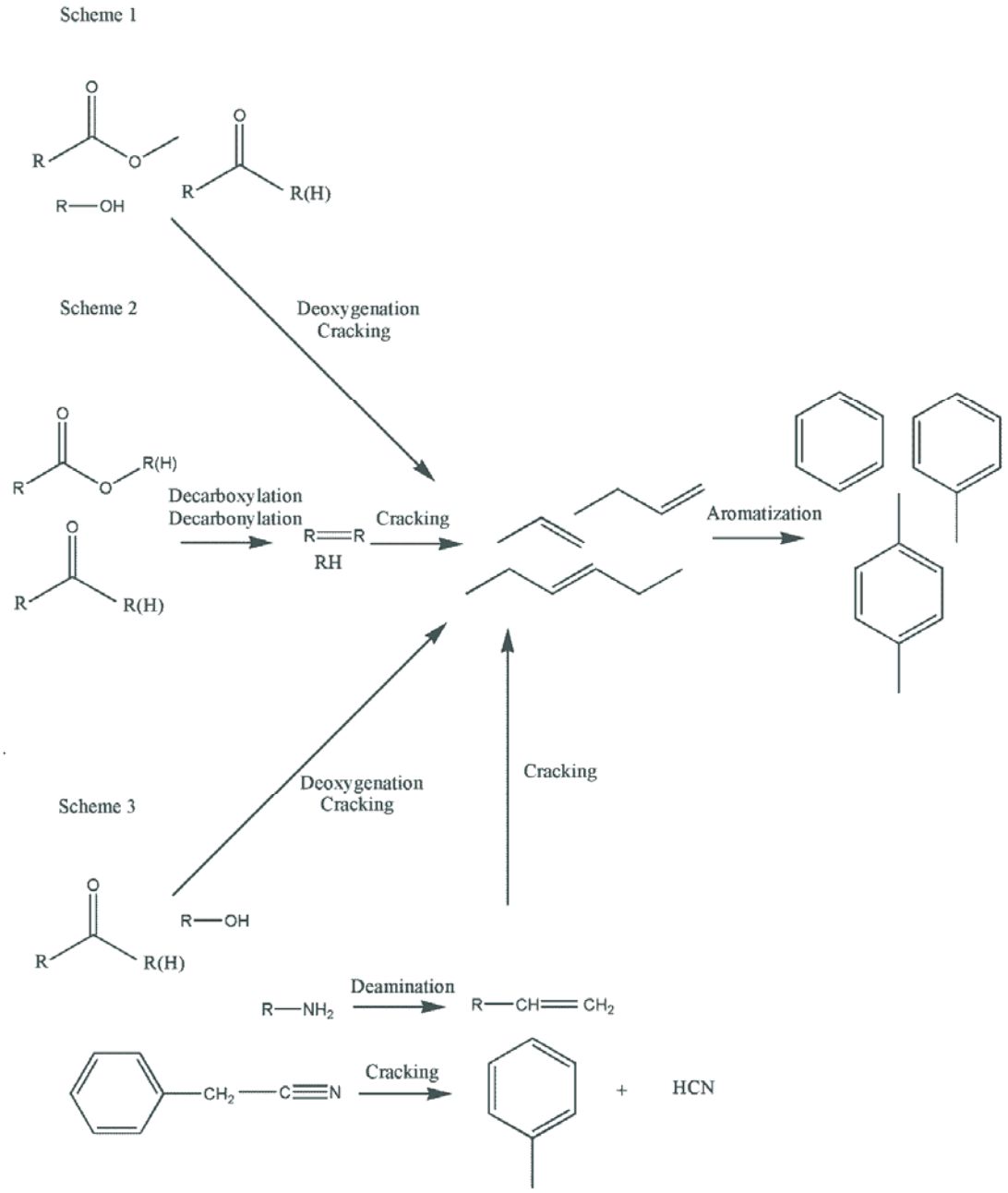

Fig. 4.8 Postulated pathways for fast microwave-assisted catalytic pyrolysis of carbohydrates (Scheme 1), lipids (Scheme 2), and proteins (Scheme 3).

4.5 Two-step process of microalgae pyrolysis and downstream catalytic reforming

The two-step process of microalgae pyrolysis and downstream catalytic reforming was conducted and compared with the one-step process at the temperature of 550 ºC. As

shown in Fig. 4.9(a), less bio-oil and more gas were obtained from the two-step process than the one-step process at the catalyst to feed ratio of 1:20. It can be seen from Fig. 4.9(b) that higher proportions of aliphatic and aromatic hydrocarbons and lower proportions of oxygen-containing and nitrogen-containing compounds in the bio-oil were achieved from the two-step process than the one-step process at the same catalyst to feed ratio. In addition, the results including product distribution and bio-oil composition for the two-step process at the catalyst to feed ratio of 1:20 were similar to those for the one-step process at the catalyst to feed ratio of 1:4.

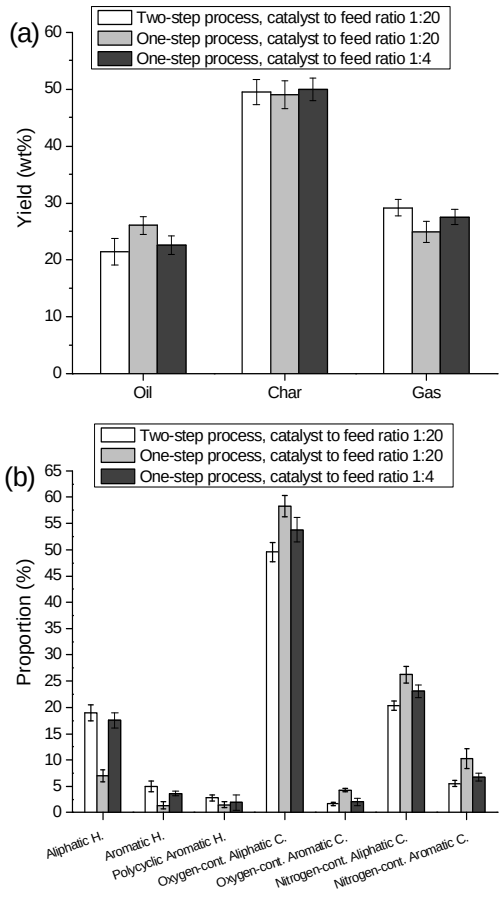

Fig. 4.9 Comparison between two-step and one-step processes of fast microwave-assisted catalytic pyrolysis of microalgae. (a) Product distribution. (b) Bio-oil composition.

During the catalytic pyrolysis, the cracking of microalgae resulted in the production of primary pyrolysis vapors which were mostly composed of oxygen-containing and nitrogen-containing compounds. When the vapors diffused into the internal pores of the HZSM-5 catalyst, some oxygen-containing compounds could be deoxygenated and cracked into olefins and alkanes, which subsequently underwent a series of alkylation, isomerization and aromatization reactions to produce aliphatic and aromatic hydrocarbons (Carlson et al., 2010; Williams and Horne, 1994). During the deoxygenation process, oxygen was removed and transferred to form CO, CO_2 and H_2O. Therefore, these catalytic transformation and upgrading reactions led to an increase in gas yield at the expense of bio-oil. For the two-step process, all the primary pyrolysis vapors would pass through the catalyst layer, resulting in an adequate surface contact between the oil vapors and catalyst particles. However, for the one-step process, the pyrolysis vapors did not have such a good contact with the catalyst as the two-step process, especially when the catalyst to feed ratio was low. In addition, the contact of HZSM-5 catalyst with solid biomass and biochar could cause catalyst deactivation during the one-step process (Güngör et al., 2012). Thus, the two-step process was more effective than the one-step process for the catalytic pyrolysis, which contributed to a lower bio-oil yield and higher bio-oil quality for the two-step process at the same catalyst to feed ratio. Consequently, the two-step process can significantly reduce the use of catalyst in the practical application. Another advantage of the two-step process over the one-step process is that the catalyst can be easily recycled and reused.

4.6 Catalytic pyrolysis of sewage sludge

4.6.1 Effect of pyrolysis temperature on bio-oil production

The effect of pyrolysis temperature on the yield and composition of the bio-oil was investigated at temperatures ranging from 450 to 600 ^{o}C, with the catalyst to feed ratio being 2:1. As shown in Fig. 4.10, temperature has great influence on product distribution from the sewage sludge pyrolysis. The oil yield increased with the pyrolysis temperature and reached a maximum yield of 20.9 wt% at the temperature of 550 ^{o}C. A decrease in oil yield was observed when the temperature increased above 550 ^{o}C. For the yield of biochar, a continuous decrease was found when the temperature increased from 450 to 600 ^{o}C. The formation of bio-oil was mostly due to the devolatilization of organic matter in the sewage sludge, which was promoted by higher temperature as there was more energy available to break the strong organic bonds. This is the main reason for the initial increase in bio-oil yield with increasing temperature. The decrease in oil yield above the optimal temperature was probably because of the secondary reactions such as thermal cracking of the volatile compounds. Thermal cracking is an endothermic reaction and was reported to become significant at temperatures higher than approximately 500 or 550 ^{o}C (Encinar et al., 2000). This can also explain the increase in gas yield when the temperature reached above 550 ^{o}C. In addition, the occurrence of carbonization of volatiles for charcoal is another possible reason for the decrease in oil yield. Since the ash content of sewage sludge is always high, the bio-oil yield is usually expressed on ash free basis, which is 24.4 wt% at 550 ^{o}C in this study. Similar results were obtained through

sewage sludge pyrolysis in a fluidized bed reactor (Fonts et al., 2008) and in a fixed bed reactor under both CO_2 and N_2 atmospheres (Jindarom et al., 2007).

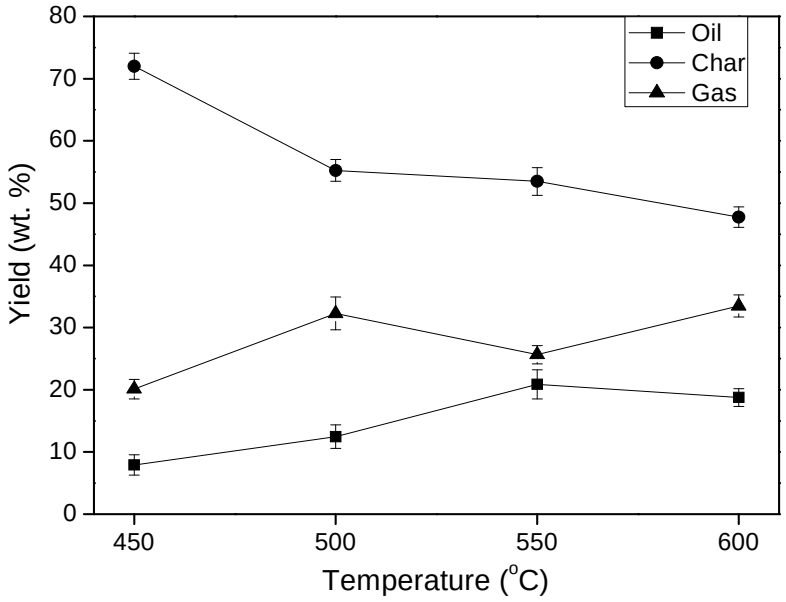

Fig. 4.10 Effect of temperature on product distribution from microwave-assisted pyrolysis of sewage sludge. Catalyst: HZSM-5, catalyst to feed ratio: 2:1.

The chemical composition of bio-oil is also influenced by temperature. As shown in Fig. 4.11, the trends for the effect of temperature were different on the different chemical families present in the oil. The proportions of aliphatic hydrocarbons, aromatic hydrocarbons and polycyclic aromatic hydrocarbons (PAHs) increased with temperature and reached the maximum at 550 ^{o}C. In contrary, the proportions of oxygen-containing aliphatic compounds, nitrogen-containing aliphatic compounds and nitrogen-containing aromatic compounds decreased with increasing temperature and reached the minimum at 550 ^{o}C. For oxygen-containing aromatic compounds, the proportion decreased with temperature initially and reached the minimum at 500 ^{o}C, and then increased when the temperature continued to rise. From the perspective of bio-oil composition, the optimal

temperature for microwave-assisted catalytic pyrolysis of sewage sludge was 550 ^{o}C since under this temperature, the highest proportions of aliphatic and aromatic hydrocarbons and the lowest proportions of oxygen- and nitrogen-containing compounds were obtained in the pyrolysis bio-oil, making it more suitable to be used as a fuel or feedstock for the production of valuable chemical products. The most dominant compounds in the bio-oil included naphthalene (9.5%), *p*-xylene (8.8%), 1,3,5-trimethyl-benzene (8.0%), 1-methyl-naphthalene (7.1%), 1-ethenyl-3-methylene-cyclopentene (6.6%) and indene (5.6%), which all belong to important chemical intermediates or precursors to other chemicals, or can be used as a solvent for chemical reactions. The same conclusion that the maximum proportion of aliphatic hydrocarbons in the pyrolysis oil was obtained at 550 ^{o}C was reached by Fonts et al. (2009) and Jindarom et al. (2007) in a fluidized bed reactor and a fixed bed reactor, respectively. However, the trends of proportion for other chemical families were different than previous studies (Fonts et al., 2009; Jindarom et al., 2007; Park et al., 2008; Sánchez et al., 2009).

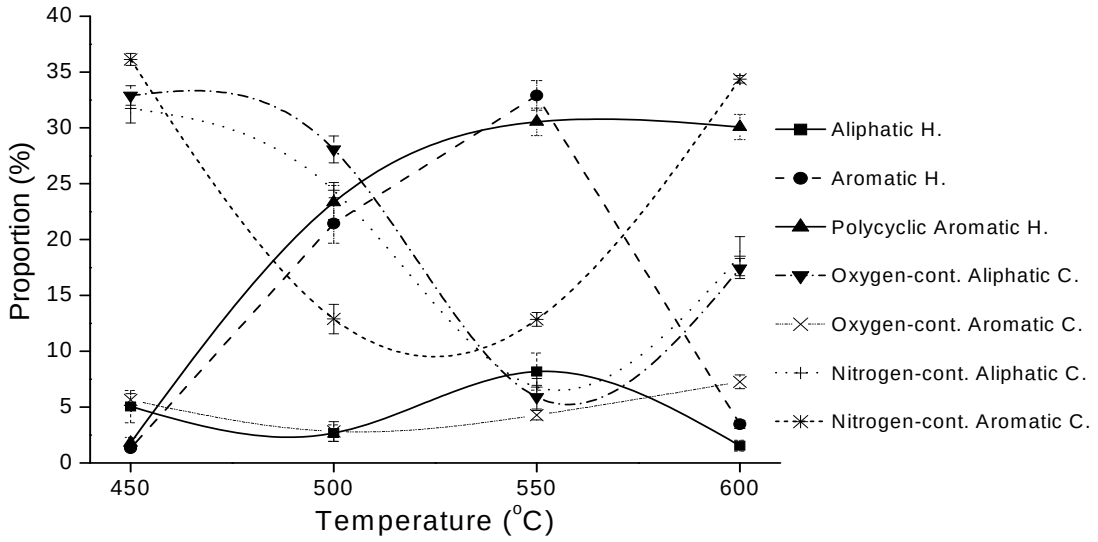

Fig. 4.11 Effect of temperature on bio-oil composition from microwave-assisted pyrolysis of sewage sludge. Catalyst: HZSM-5, catalyst to feed ratio: 2:1.

4.6.2 Effect of catalyst to feed ratio on bio-oil production

Previous research in catalytic pyrolysis of sewage sludge was very limited (Beckers et al., 1999; Fonts et al., 2012; Kim and Parker, 2008). The use of catalyst in sewage sludge pyrolysis and the effects of catalyst to feed ratio on bio-oil yield and composition were investigated in this study. As shown in Fig. 4.12, the use of catalyst in the pyrolysis resulted in a slight decrease in oil yield. This is probably because the pyrolysis vapors had to pass through the catalyst particles, increasing the gas residence time. Consequently, the thermal cracking and carbonization reactions of volatiles occurred with higher probability, which would reduce the bio-oil yield. This explanation can be confirmed by the increase in the char yield when catalyst was used in the sewage sludge pyrolysis process. However, the oil yield increased and the gas yield decreased as the catalyst to feed ratio increased from 1:1 to 2:1. A possible reason was that the short-chain gas molecules from thermal cracking of volatiles recombined on the catalyst and underwent a series of aromatization, alkylation and isomerization reactions to produce aliphatic and aromatic compounds, increasing the bio-oil yield. From the perspective of product distribution, catalyst does not improve the bio-oil yield. The study of sewage sludge pyrolysis in a laboratory-scale horizontal batch reactor conducted by Kim and Parker (2008) demonstrated a decrease in liquid yield when the catalyst to feed ratio increased over 1.5. The authors attributed such a decrease to an increase in the catalytic cracking reactions, which resulted in increased conversion of volatiles to gas.

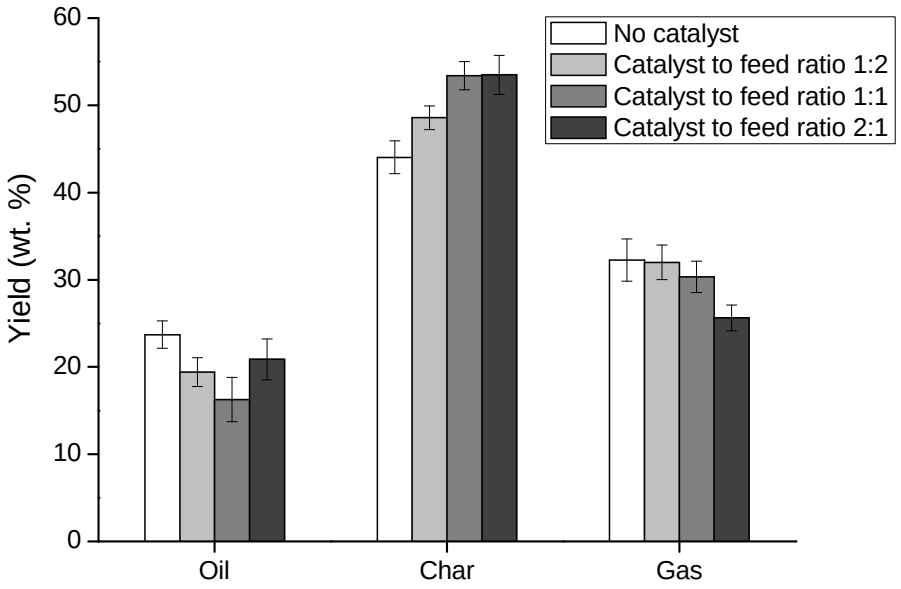

Fig. 4.12 Effect of catalyst to feed ratio on product distribution from microwave-assisted pyrolysis of sewage sludge. Catalyst: HZSM-5, pyrolysis temperature: 550 ºC.

Fig. 4.13 presents the effect of catalyst to feed ratio on bio-oil composition from microwave-assisted pyrolysis of sewage sludge at 550 ^{o}C. It can be seen that although the proportion of aliphatic hydrocarbons in the bio-oil did not change too much with catalyst, significant increase in proportion of aromatic hydrocarbons was observed from catalytic pyrolysis compared with non-catalytic pyrolysis. This is consistent with previous studies on lignocellulosic biomass showing that the organics derived in the pyrolysis process could be deoxygenated and cracked to produce aromatics over the HZSM-5 catalyst (Mihalcik et al., 2011; Mullen and Boateng, 2010). The reaction mechanism and pathways can be illustrated using those postulated for the catalytic pyrolysis of carbohydrates and lignocellulosic biomass on HZSM-5 (Carlson et al., 2010; Williams and Horne, 1994). Carbohydrate derived organics, including alcohols, ketones, aldehydes and acids, were deoxygenated and cracked into C2–C6 olefins, which were transformed

to benzene through a series of aromatization reactions. Benzene could be converted to other aromatics through alkylation and isomerization reactions. This was consistent with the decrease in the proportion of oxygen-containing aliphatic compounds in the bio-oil. In addition, the proportions of nitrogen-containing aliphatic and aromatic compounds were also decreased with catalyst, which was not mentioned in previous studies and needs further investigation. The proportions of oxygen- and nitrogen-containing compounds decreased significantly when the catalyst to feed ratio increased from 1:1 to 2:1. This was probably because the surface contact between the pyrolysis vapors and catalyst particles was not adequate when the catalyst to feed ratio was 1:1.

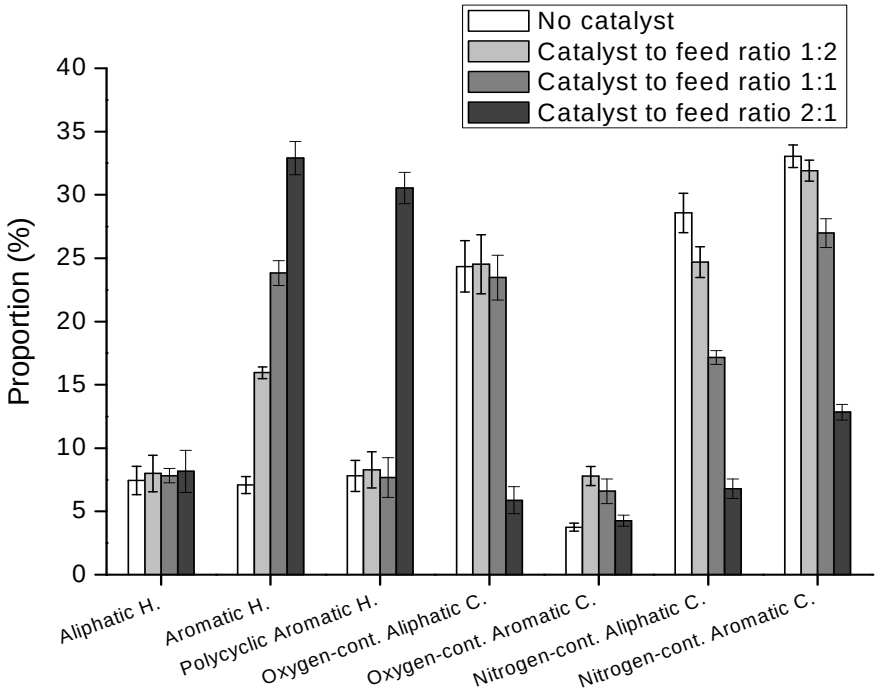

Fig. 4.13 Effect of catalyst to feed ratio on bio-oil composition from microwave-assisted pyrolysis of sewage sludge. Catalyst: HZSM-5, pyrolysis temperature: 550 ºC.

4.6.3 Analysis of biochar

The elemental analysis and ICP-OES multi-element determination were carried out for the biochar from microwave-assisted pyrolysis of sewage sludge at 550 ^{o}C. The contents of C, H and N in the biochar were 46.6%, 3.1% and 5.3%, respectively. The carbon content of biochar from sewage sludge pyrolysis was lower than that from lignocellulosic biomass pyrolysis (Borges et al., 2014), which was probably due to the high ash content of sewage sludge.

Table 4.7 shows the contents of mineral elements in the biochar. It can be seen that the contents of P, Ca, K and Mg which belong to essential elements to plants were very high, whereas the hazardous heavy metals including Cd, As, Ti and Pb were in very low proportions. Comparing the results in Table 4.3 and Table 4.7, it can be concluded that the essential elements were concentrated in the biochar after the pyrolysis process. Therefore, in addition to the use for adsorbent and fuel production, biochar could be used as a soil amendment to achieve mineral recovery and increase soil fertility. Biochar addition to soil could improve crop yield through reducing nutrient leaching and soil acidity, as well as enhancing the crop uptake of the essential nutrients. In addition, returning biochar into soil would reduce the need for fertilizers, thereby reducing the agricultural cost and environmental pollution caused by the fertilizer production and application.

Table 4.7 Contents of mineral elements in biochar from microwave-assisted pyrolysis of sewage sludge at 550 ^{o}C.

Mineral elements (mg/L)										
Al	As	B	Be	Ca	Cd	Co	Cr	Cu	Fe	K
9522.7	4.8	40.8	0.35	44401.5	2.6	8.2	114.4	623.5	7710.2	11364.0

Li	P	Mg	Mn	Mo	Na	Ni	Pb	Ti	V	Zn
3.7	53362.0	11842.0	2528.1	12.2	2542.0	79.0	72.0	49.7	5.2	1305.0

4.6.4 Catalyst characterization

The HZSM-5 catalysts before and after pyrolysis reactions under different temperatures were characterized and compared using X-ray diffraction (XRD) technique to determine the effect of microwave-assisted pyrolysis process on the catalyst structure. The results showed that the primary diffraction peaks of the HZSM-5 catalyst occurred at the diffraction angles of 23.2°, 23.9° and 24.5°. The main crystalline phase existing in the catalyst was silicon-aluminum compound $Al_2O_3 \cdot 54SiO_2$ which was obtained through data analysis using the Jade 8.0. Comparing the XRD patterns of catalysts before and after pyrolysis reactions, little change of phase composition and crystalline structure on catalyst was observed for all the temperatures studied. It demonstrated that the HZSM-5 catalyst had good stability during the microwave-assisted pyrolysis process towards deactivation caused by coking or sintering.

The peak areas and crystalline sizes at the characteristic angels (23.2°, 23.9° and 24.5°) of HZSM-5 XRD patterns before and after pyrolysis reactions are shown and compared in Table 4.8. It can be seen that there is no obvious difference between peak areas of fresh catalyst and catalysts after reaction under different temperatures except at 500 ^{o}C. For the crystalline size estimated by the Scherrer equation, no significant increase was found for catalysts after reactions, even at 600 ^{o}C. It means that the HZSM-5 catalyst standed high temperatures with negligible deactivation by coking and sintering, which was probably due to the short time on stream for the fast microwave-assisted pyrolysis

process. Therefore, it can be concluded that HZSM-5 has good stability and is a suitable catalyst for the microwave-assisted catalytic pyrolysis of sewage sludge.

Table 4.8 Comparison of peak areas and crystallite sizes at characteristic diffraction angles of HZSM-5 XRD patterns before and after pyrolysis reactions under different temperatures.

Catalyst	Area (a.u.)			Crystallite size (Å)		
	23.2°	23.9°	24.5°	23.2°	23.9°	24.5°
Fresh catalyst	6679	3563	1100	224	181	373
450 ^{o}C	6043	3365	958	224	185	374
500 ^{o}C	7183	4002	1678	244	184	279
550 ^{o}C	6825	3274	1240	247	216	351
600 ^{o}C	5651	3436	1232	239	164	293

4.7 Conclusions

In this chapter, fast microwave-assisted catalytic co-pyrolysis of microalgae and scum for bio-oil production was studied. Scum proved to be a good hydrogen supplier to increase the overall EHI value of feedstock. In order to maximize the production of bio-oil and aromatic hydrocarbons, the optimal co-pyrolysis temperature, catalyst to feed ratio, and microalgae to scum ratio were 550 ºC, 2:1, and 1:2, respectively. A significant synergistic effect between microalgae and scum was achieved only when the EHI value of feedstock was larger than about 0.7. In addition, several pyrolysis pathways for non-catalytic and catalytic fMAP of microalgae were postulated by analysis and identification of pyrolysis products from the model algal biomass compounds. Furthermore, comparison between two-step and one-step processes of fast microwave-assisted catalytic pyrolysis of microalgae demonstrated the priority of the two-step process, especially in catalyst saving and reuse. Moreover, the study of microwave-assisted catalytic pyrolysis of sewage sludge shows that microwave heating is effective for sewage sludge pyrolysis.

The optimal temperature and catalyst to feed ratio for bio-oil production were 550 ^{o}C and 2:1, respectively. The lowest proportions of oxygen- and nitrogen-containing compounds in the bio-oil were achieved under the optimal conditions. The biochar after pyrolysis contained considerable amounts of mineral elements and could be used to improve soil fertility. Catalyst characterization indicated good stability of HZSM-5 catalyst against deactivation during the pyrolysis process.

CHAPTER 4 FAST MICROWAVE-ASSISTED CATALYTIC BIOMASS GASIFICATION FOR SYNGAS PRODUCTION

Abstract

In the present chapter, a microwave-assisted biomass gasification system was developed for syngas production. Three catalysts including Fe, Co and Ni with Al_2O_3 support were examined and compared for their effects on syngas production and tar removal. Experimental results show that microwave is an effective heating method for biomass gasification. Ni/Al_2O_3 was found to be the most effective catalyst for syngas production and tar removal. The gas yield reached above 80% and the composition of tar was the simplest when Ni/Al_2O_3 catalyst was used. The optimal catalyst to biomass ratio was determined to be 1:5–1:3. The addition of steam was found to be able to improve the gas production and syngas quality. Results of XRD analyses demonstrate that Ni/Al_2O_3 catalyst had good stability during gasification process. Finally, a new concept of microwave-assisted dual fluidized bed gasifier was put forward for the first time in all studies in the literature.

5.1 Introduction

Currently, increasing researches have been conducted on sustainable energy sources, as an alternative to traditional fossil fuels. Since biomass is a carbon-neutral energy source (McKendry, 2002b), the efficient uses of biomass are considered very promising in the future energy portfolio (Richardson et al., 2012). Among all the utilization technologies, the production of syngas from biomass gasification is considered as an

attractive route to produce chemicals, biofuels, hydrogen and electricity (Damartzis and Zabaniotou, 2011; Kirkels and Verbong, 2011; Lin and Huber, 2009). It has been estimated that syngas production from biomass accounts for at least half, and in many cases more than 75% of the cost of biofuel production (Hamelinck and Faaij, 2002; Spath and Dayton, 2003). Therefore, the successful development of cost-effective processes for high-quality syngas production will greatly promote biomass utilization.

Traditional types of biomass gasification reactors include fixed bed and fluidized bed (Dong et al., 2010; Van der Meijden et al., 2008; Xie et al., 2012). Microwave irradiation is an alternative heating method and has already been successfully applied to biomass pyrolysis (Bu et al., 2012; Du et al., 2011; Wang et al., 2012). Compared with conventional heating processes where heat is transferred from the surface to the core of the material through conduction driven by temperature gradients, microwaves induce heat at the molecular level by direct conversion of the electromagnetic energy into heat (Sobhy and Chaouki, 2010), and therefore, they can provide uniform internal heating for material particles. In addition, the instantaneous response of microwave makes it easier for a rapid start-up and shut-down. Furthermore, the process operation involves a simple set-up and can be easily adapted to currently available large-scale industrial technologies. Microwave heating is a mature technology and development of microwave heating system is of low cost. Although many advantages of microwave heating over traditional heating methods and some progress made in biomass pyrolysis, no research has been conducted in biomass gasification using microwave technology.

In this chapter, fast microwave-assisted gasification of corn stover was carried out under different conditions. Catalysts including Fe, Co and Ni with Al_2O_3 support were

selected and compared for their effects on syngas production and tar removal. The effect of steam on syngas yield and quality was also investigated. In addition, X-ray Diffraction (XRD) analyses of catalysts before and after reactions were conducted to study their stability during gasification process.

5.2 Materials and methods

5.2.1 Materials

The corn stover chosen as the biomass material for the gasification process was obtained from a farm field located in Saint Paul Campus, University of Minnesota (Twin Cities). The basic physico-chemical characteristics of the corn stover including proximate analysis and element analysis are shown in Table 3.2. Prior to its use, the corn stover samples were ground using a rotary cutting mill and then screened to limit the particle size smaller than 0.5 mm. Afterwards, these ground samples were dried at 80±1 ºC for more than 24 h.

The catalysts used in the experiments included Fe/Al_2O_3, Co/Al_2O_3, and Ni/Al_2O_3 prepared by impregnating porous alumina (60 mesh, surface area 150 m^2/g) in nitrate solution. Alumina was used as the catalyst support. Catalyst loading of 15% was used for all the three catalysts. After impregnation for 12 h, the catalysts were dried at 105 ºC, and then ground and screened to achieve a particle size smaller than 3 mm. After being calcined at 500 ºC in a muffle furnace for 4 h, Fe-, Co- and Ni-based catalysts were reduced at 500 ºC, 350 ºC and 450 ºC, respectively, using a gas mixture of H_2/He (200 sccm) with a molar ratio of 1:1 for 12 h prior to application.

5.2.2 Apparatus

The fast microwave-assisted catalytic gasification of corn stover was carried out using the system as described in Section 3.3. Briefly, the experiments were performed in a microwave oven (MAX, CEM Corporation), with the power of 750 W at a frequency of 2,450 MHz. The microwave-based system is composed of a biomass feeder, a microwave oven, a quartz reactor with a layer of microwave absorbent bed inside, thermocouples (K-type) to measure the temperatures of oven cavity and bed particles, condensers and liquid fraction collectors, a gas collector, and some quartz connectors. For safety purpose, a microwave detector (MD-2000, Digital Readout) was used to monitor microwave leakage. The two-step process of corn stover gasification and downstream catalytic reforming was conducted using the microwave-based system coupled with a downstream catalytic fixed bed as the secondary reformer.

The procedure for fMAG of corn stover was described in Section 3.3. The sample for each experiment was prepared by physically mixing 15 g corn stover with 5 g catalyst. The temperature of the SiC bed was set to be 900 ºC.

5.2.3 Gas and tar analyses

Offline gas analysis was performed using a Varian CP4900 Micro-gas chromatograph (GC) with a thermal conductivity detector (TCD). The two columns used were PoraPlot Q and 5Å molecular sieve with helium as carrier gas. The temperatures of both injector and detector were set at 110 °C. The temperatures of PoraPlot Q and 5Å molecular sieve columns were kept at 80 °C and 150 °C, respectively.

The components of liquid product were specified using an Agilent 7890–5975C gas chromatography/ mass spectrometer (GC/MS) with a HP-5 MS capillary column. Helium was employed as the carrier gas at a flow rate of 1.2 mL/min. The injection size was 1 μL with a split ratio of 1:10. The initial oven temperature was 40 °C held for 3 min and then increased to 290 °C at a rate of 5 °C/min, and held at 290 °C for 5 min, while the injector and detector were maintained at constant temperature of 250 °C and 230 °C, respectively. The compounds were identified by comparing their mass spectra with those from the National Institute of Standards and Technology (NIST) mass spectral data library.

5.2.4 Catalyst characterization

The X-ray powder diffraction (XRD) patterns, obtained on a Siemens D5005 X-ray diffractometer instrument with a Cu–K_α radiation at 45 kV and 40 mA, were used to identify the major phases present in the catalysts.

5.3 Results and discussion

5.3.1 Effects of different catalysts on syngas production

The experiments of microwave-assisted biomass gasification were conducted with and without catalyst, and different catalysts were compared to examine their effects on syngas yield and quality. As shown in Fig. 5.1, it can be seen that microwave is an effective heating method for biomass gasification and the gas yield reached more than 65 wt% for all the experiments. Catalyst was found to be necessary to further improve gas yield and reduce tar production. Tars could be converted into valuable gaseous compounds on catalysts at gasification temperature. Elements from group VIII (Fe, Co

and Ni) are known for their good catalytic activity for tar destruction and thermal stability under gasification conditions. The most active catalytic phase for the three catalysts is the metallic phase, i.e., Fe^0, Co^0 and Ni^0 (Nordgreen et al., 2006; Torres et al., 2007). It can be also found that the catalytic effect of Ni/Al_2O_3 is better than the other two catalysts. The gas yield reached above 80 wt% while tar content was as low as 7 wt% when using Ni-based catalyst. The results were even much better compared with some traditional methods (Xie et al., 2012). Due to their low price, nickel-based catalysts often exhibit a good cost/activity compromise (Rostrup-Nielsen et al., 2002; Sehested, 2006).

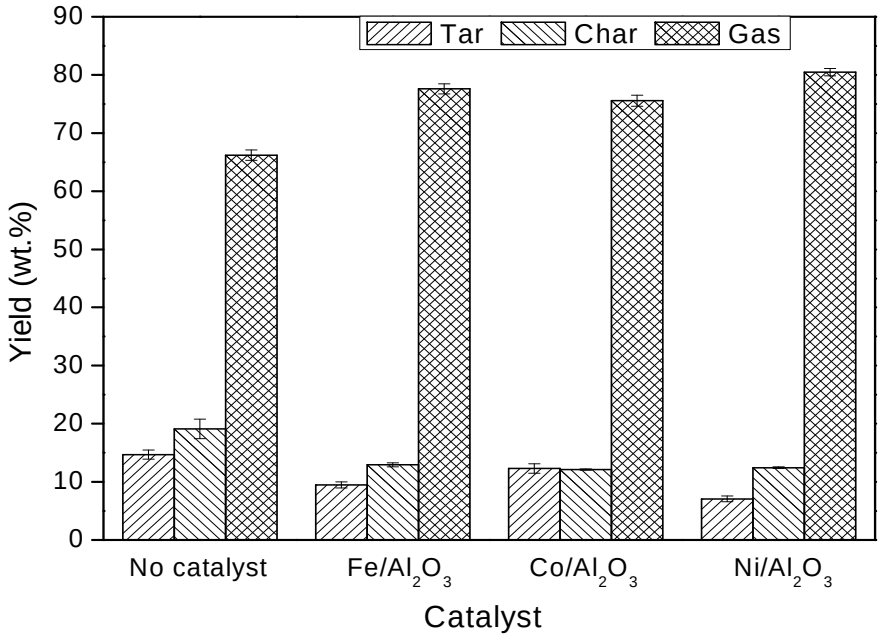

Fig. 5.1 Effect of catalyst on product distribution in microwave-assisted gasification of corn storver. Gasification temperature: 900 ºC.

The contents of major gases (H_2, CO, CH_4 and CO_2) as shown in Fig. 5.2 were also affected by catalyst. The concentrations of both H_2 and CO increased when catalyst was used. Catalyzed by Ni/Al_2O_3, the maximum syngas (H_2+CO) yield was obtained from

microwave-assisted biomass gasification, which also demonstrated that Ni-based catalyst exhibits the best catalytic effect for tar conversion and syngas production.

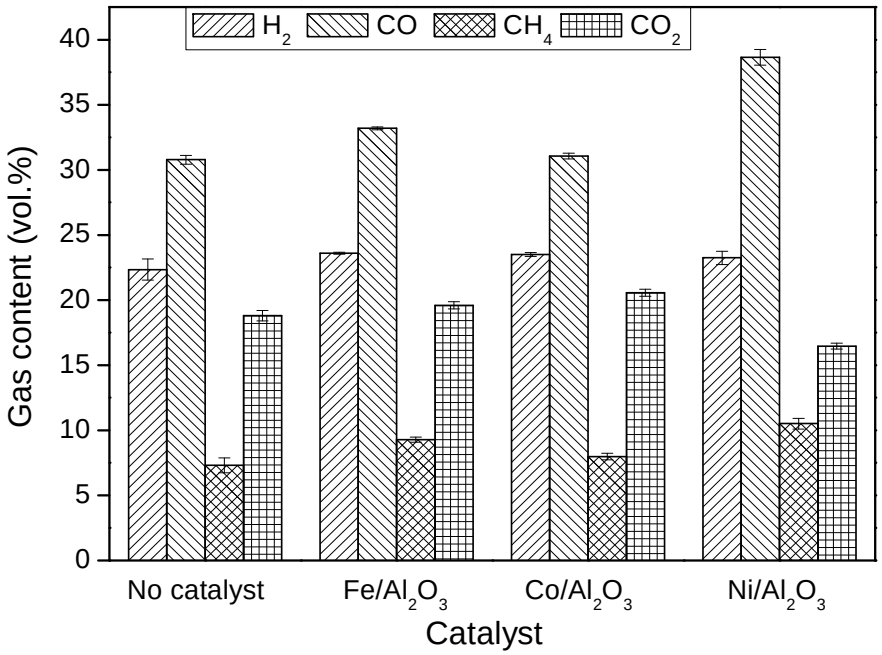

Fig. 5.2 Effect of catalyst on major gases contents in microwave-assisted gasification of corn storver. Gasification temperature: 900 ºC.

The lower heating value of the produced gas was calculated by the following equation (Lv et al., 2004; Yang et al., 2006).

$$LHV = (30[CO] + 25.7[H_2] + 85.4[CH_4] + 151.3[C_mH_n]) \times 4.2/1000 \text{ MJ/m}^3 \quad (5.1)$$

while the higher heating value was calculated using the following correlation (Li et al., 2004).

$$HHV = (12.63[CO] + 12.75[H_2] + 39.82[CH_4] + 63.43[C_mH_n])/100 \text{ MJ/m}^3 \quad (5.2)$$

where $[H_2]$, $[CO]$, $[CH_4]$ and $[C_mH_n]$ are the molar fractions of H_2, CO, CH_4 and C_mH_n in the produced gas. As shown in Table 5.1, the LHV and HHV of produced gases from

microwave-assisted catalytic gasification at 900 ºC varied from 9.31 to 11.15 MJ/m^3 and from 10.10 to 12.03 MJ/m^3, respectively. It can be also seen from Table 5.1 that the ratio of H_2 to CO was relatively low and hence appropriate conditioning strategies such as steam reforming are required to improve the syngas quality. Moreover, additional gas purification stage is needed to eliminate CO_2 which was formed probably as a consequence of O_2 presence inside the reactor.

Table 5.1 Comparison of effects of different catalysts in microwave-assisted biomass gasification for syngas production.

Catalyst	Gas yield (wt%)	Syngas (% v/v)	H_2/CO	LHV (MJ/m^3)	HHV (MJ/m^3)
No catalyst	66.19	53.12	0.73	8.91	9.65
Fe/Al_2O_3	77.60	56.79	0.71	10.05	10.89
Co/Al_2O_3	75.57	54.55	0.76	9.31	10.10
Ni/Al_2O_3	80.47	61.88	0.60	11.15	12.03

5.3.2 Effects of different catalysts on tar conversion

Tars accompanying the syngas were condensed and collected in this study, and then analyzed using GC/MS. Table 5.2 shows that tar is a complex mixture of many organic compounds including acids and aromatic compounds, making it difficult to deal with. The number of compounds in tars was reduced by catalyst and only 34 compounds were detected when Ni/Al_2O_3 was used. In addition, the content of simple organic solvents including acids, alcohols and acetones increased while that of aromatic organic compounds decreased in the tar. It demonstrated that the main compounds of tar became simpler and therefore easier to deal with when catalyst was used in the gasification process. The destruction and conversion of tars were achieved through cracking and reforming reactions promoted by catalysts. The cracking and reforming reactions of tars

that can occur during gasification process are represented by Eqs. (5.3)–(5.5), using toluene as an example of tars.

Cracking:

$$C_7H_8 \rightarrow 7C + 4H_2 \quad (5.3)$$

Dry reforming reactions:

$$C_7H_8 + 7CO_2 \rightarrow 14CO + 4H_2 \quad (5.4)$$

$$C_7H_8 + 11CO_2 \rightarrow 18CO + 4H_2O \quad (5.5)$$

Table 5.2 Main compounds in tars obtained over different catalysts.

Catalyst	Number of compounds detected by GC/MS	Compounds	GC/MS peak area percentage/%
No catalyst	80	Acetic acid	24.68
		2-Propanone, 1-hydroxy-	10.86
		Phenol	5.32
		Propanoic acid	3.37
		Furfural	3.16
		Benzofuran, 2,3-dihydro-	3.08
Fe/Al_2O_3	51	Acetic acid	17.70
		2-Propanone, 1-hydroxy-	5.97
		Furfural	5.47
		Phenol	4.40
		1-Hydroxy-2-butanone	4.03
		Propanoic acid	3.99
Co/Al_2O_3	49	Acetic acid	32.18
		2-Propanone, 1-hydroxy-	12.06
		Phenol	8.15
		Propanoic acid	4.92
		Phenol, 4-methyl-	2.50
		Phenol, 4-ethyl-	2.46
Ni/Al_2O_3	34	Acetic acid	36.60
		2-Propanone, 1-hydroxy-	13.61
		Phenol	10.64

		Propanoic acid	6.00
		1,2-Ethanediol	3.18
		Phenol, 4-methyl-	2.66

Therefore, the conversion of tars on catalysts contributed to purify the syngas and improve syngas yield and quality.

5.3.3 Effect of catalyst to biomass ratio on gasification process

The effect of catalyst to biomass ratio on syngas production and tar removal was investigated to determine the optimal catalyst amount. The increase in gas yield and decrease in tar production can be observed from Fig. 5.3(a) as the ratio of Ni/Al_2O_3 to corn stover increased from 1:10 to 1:5. However, no significant change was found when larger amount of catalysts were used. A possible reason is that insufficient catalysts led to inadequate contact with biomass particles and tar molecules, causing incomplete tar destruction and conversion. Complete catalysis was achieved when the catalyst to biomass ratio reached between 1:5 and 1:3. Similar conclusions can be reached from Fig. 5.3(b) which shows the contents of major gases produced from different catalyst to biomass ratios. The content of H_2 increased while that of CO decreased when the ratio increased from 1:10 to 1:5, indicating that syngas of higher quality was obtained. Although higher content of H_2 and lower content of CO were achieved when the catalyst to biomass ratio was 1:1, much higher content of CO_2 will make subsequent syngas purification and conditioning processes more expensive. Considering the practical application and high cost of catalyst, the optimal catalyst to biomass ratio can be determined as 1:5–1:3.

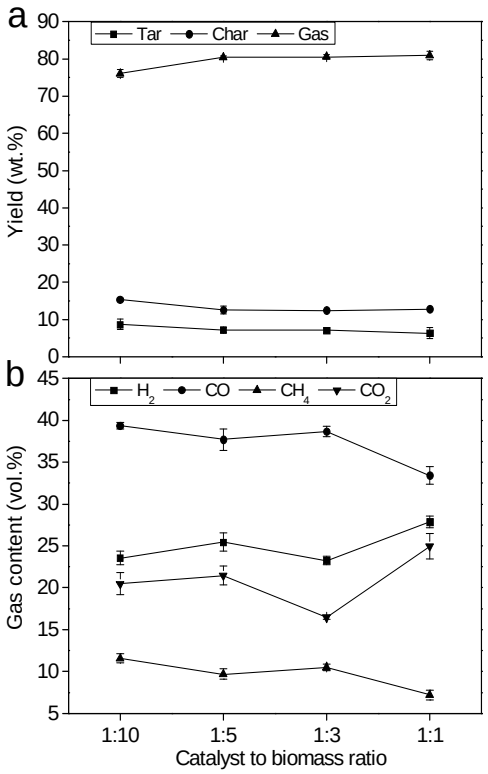

Fig. 5.3 Effect of catalyst to biomass ratio on (a) product distribution, and (b) major gases contents. Catalyst: Ni/Al_2O_3, gasification temperature: 900 ºC.

5.3.4 Effect of steam on syngas production and tar removal

Steam is reported to be effective in tar reforming and syngas conditioning (Karmakar and Datta, 2011; Xiao et al., 2011; Xie et al., 2012). In this study, steam at a flow rate of 10 ml/min was introduced into the gasifier to investigate its effect on syngas production and tar removal, using Ni/Al_2O_3 as the catalyst. The results showed that the addition of steam improved the gas production and syngas quality. The gas yield was increased to 83.91 wt% and the tar content was reduced to 5.11 wt%. The ratio of H_2 to CO reached 1.49 which was much higher than that without steam. In addition, CH_4 in gas product was completely removed and converted to H_2 and CO by steam reforming. The

main reactions related to steam are represented by Eqs. (5.6)–(5.10), using toluene as an example of tars.

Tar steam reforming reactions:

$$C_7H_8 + 7H_2O \rightarrow 7CO + 11H_2 \quad (5.6)$$

$$C_7H_8 + 14H_2O \rightarrow 7CO + 18H_2 \quad (5.7)$$

Methane steam reforming reaction:

$$CH_4 + H_2O \rightarrow CO + 3H_2 \quad (5.8)$$

Water-gas shift reactions:

$$C + H_2O \rightarrow CO + H_2 \quad (5.9)$$

$$CO + H_2O \rightarrow H_2 + CO_2 \quad (5.10)$$

The water gas shift (WGS) reaction (Eq. (5.10)) increased the concentration of H_2 at the expense of CO, but produced more CO_2 as well. Therefore, the higher heating value (HHV) of the gas product was a little lower than that without steam.

5.3.5 Catalyst characterization

Ni/Al_2O_3 catalyst was analyzed using X-ray diffraction (XRD) to compare the catalyst structures before and after gasification process. The main phases detected on Ni/Al_2O_3 catalyst include metallic nickel (Ni^0) (2θ=44.3° and 51.7°), nickel oxide (NiO) (2θ=43.2°), alumina (Al_2O_3) (2θ=35.0°, 52.4°, 57.3°, 66.4° and 68.0°), and some nickel aluminum oxides (Fig. 5.4). Little change in catalyst structure was observed before and after gasification reactions with or without steam. In addition, little change in catalyst

structure was found even after the Ni/Al_2O_3 catalyst had been separated and reused three times. It demonstrated that the nickel based catalyst has good stability with regard to deactivation caused by coking or sintering.

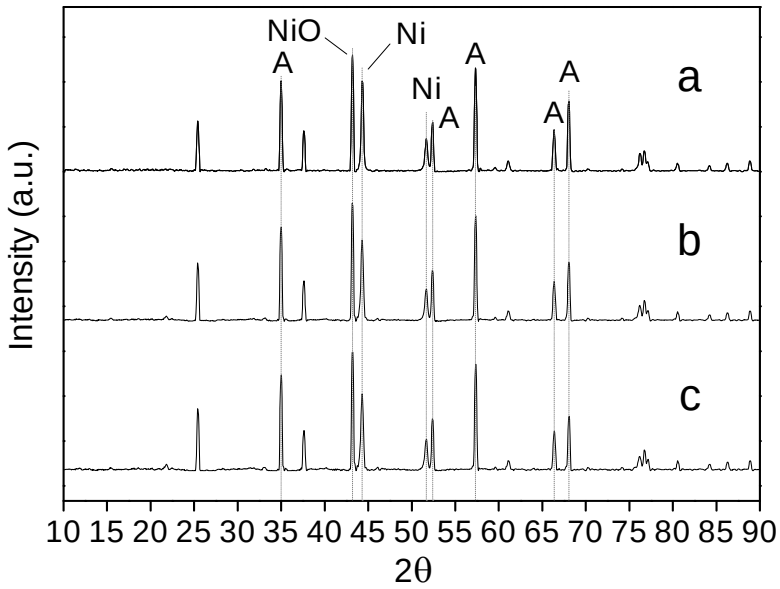

Fig. 5.4 XRD patterns for Ni/Al_2O_3 catalyst (a) before reaction, (b) after reaction without steam, and (c) after reaction with steam, with phases labeled as: Ni (cubic Ni^0), NiO (NiO), and A (Al_2O_3).

The area and crystallite size of Ni^0 and NiO phases on catalysts before and after reaction were shown and compared in Table 5.3. It can be seen that the area of NiO phase increased while that of Ni^0 phase decreased after reaction, which indicated an increasing amount of nickel oxide and a decreasing amount of metallic nickel on the catalyst after gasification. The metallic nickel is known to be the most active catalytic phase for Ni/Al_2O_3 catalyst, and therefore the decreased metallic nickel might decrease the catalyst activity. However, we can still conclude that nickel based catalyst has relatively good stability during gasification process as little reduction of Ni^0 was found. In addition, a small difference between Ni^0 crystallite sizes before and after reaction was observed,

indicating that little sintering occurred on the catalyst during microwave-assisted gasification process.

Table 5.3 Comparison of NiO and Ni^0 phases on catalysts before and after reaction.

Catalyst	Area (a.u.)			Crystallite size (Å)		
	NiO (43.2°)	Ni^0 (44.3°)	Ni^0 (51.7°)	NiO (43.2°)	Ni^0 (44.3°)	Ni^0 (51.7°)
Fresh catalyst	2659	2358	1158	403	334	247
After reaction (without steam)	2682	2321	1044	410	316	255
After reaction (with steam)	2700	2291	953	400	291	259

5.3.6 A new concept of microwave-assisted dual fluidized bed gasifier

Extremely high temperature (>1200 ºC) can be easily obtained using microwave heating method combined with some microwave absorbents, making the gas product much cleaner than in lower temperature and the energy consumption much lower than that of traditional fluidized bed gasifier. In addition, microwave heating is a mature technology and development of microwave heating system for biomass gasification is of low cost.

Based on many advantages of microwave heating technology and the results obtained above, a new gasifier concept which is a combination of microwave heating and dual fluidized bed gasifier (DFBG) was put forward for the first time in all studies in the literature. DFBG is a technically proven technology that has already been implemented at demonstration scale and has been identified as a promising biomass gasification technology, especially for the production of high-quality syngas (Göransson et al., 2011). The basic idea of the new gasifier concept is to divide the fluidized bed into two zones, i.e., a gasification zone and a heating zone. A circulation loop of bed material is created

between these two zones. The circulating bed material acts as heat carrier from the heating to the gasification zone. A schematic of the new gasifier concept is represented in Fig. 5.5.

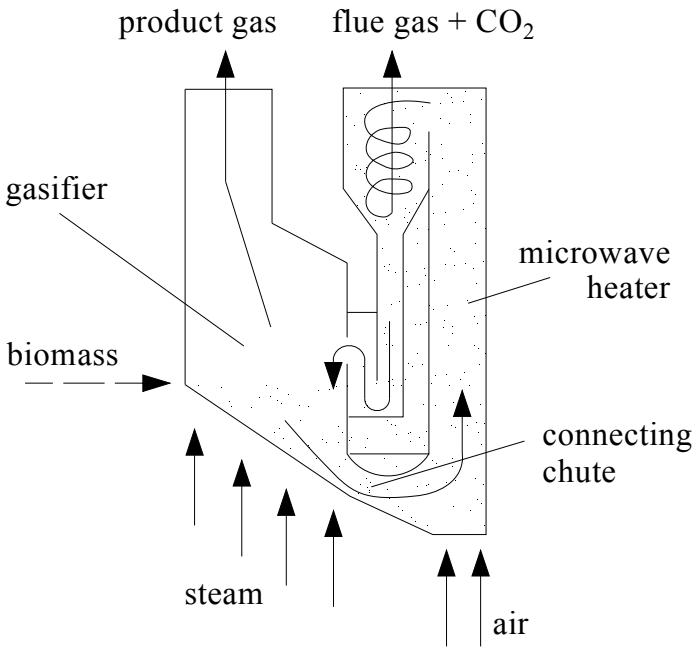

Fig. 5.5 Schematic of the microwave-assisted dual fluidized bed gasifier.

As shown in Fig. 5.5, the biomass material is fed into the gasification zone and gasified with steam. SiC is selected as the bed material for its large heat capacity and good ability to absorb microwave. The bed material, together with the catalyst, circulates to the heating zone. This zone is fluidized with air and SiC absorbs the microwave and is heated to about 900 ºC. After gas-solid separation, the bed material is transported back to the gasification zone. The flue gas will be removed without coming in contact with the product gas. The hot bed material provides the energy for the endothermic gasification with steam. In addition, limestone (CaO) can be incorporated into the gasifier and mixed with the bed material for in-situ CO_2 absorption. With this concept it is possible to obtain

a H_2-rich gas, with a low tar content, usable for cogeneration systems, F-T synthesis or to feed fuel cells.

As far as the catalyst is concerned, Ni/Al_2O_3 has good activity for tar conversion and reforming reactions. However, the biggest problem of Ni/Al_2O_3 lies in catalyst attrition in the fluidized bed. Due to its hardness, olivine offers the advantage of being attrition resistant, making it a suitable material for fluidization (Devi et al., 2005; Świerczyński et al., 2006). Therefore, Ni/olivine catalyst can be used in the new microwave-assisted dual fluidized bed gasifier.

5.4 Conclusions

In this chapter, the microwave-assisted system was used for catalytic gasification of corn stover for syngas production and tar removal. The results show that microwave heating is effective for biomass gasification and Ni/Al_2O_3 had the best catalytic effect on syngas production and tar conversion. More than 80 wt% of gas was obtained in the product and only 34 compounds were detected in the tar when Ni/Al_2O_3 was used as the catalyst. Catalyst characterization indicated good stability of Ni/Al_2O_3 against deactivation during gasification process. A new concept of microwave-assisted dual fluidized bed gasifier was put forward for large-scale applications.

CHAPTER 5 SINGLE-STEP SYNTHESIS OF DME FROM SYNGAS

Abstract

In this chapter, single-step synthesis of DME from syngas on bifunctional catalysts containing Cu-ZnO-Al_2O_3 and seven different zeolites was investigated. Various characterization techniques were used to determine the structure, reducibility, and surface acidity of the catalysts. Experimental results show that the zeolite type had great influence on the activity, selectivity and stability of the bifunctional catalyst during the syngas-to-DME process. Zeolite properties including density of weak and strong acid sites, pore structure, and Si/Al distribution were found to affect the CO conversion and DME selectivity of the bifunctional catalyst. In addition, the deactivation of the bifunctional catalyst could be attributed to the sintering of metallic Cu and a loss of the zeolite dehydration activity.

6.1 Introduction

Dimethyl ether (DME) attracts increasing interest since it can be used as an alternative to diesel fuel, an important feedstock in the production of chemicals or hydrogen, a residential fuel replacing liquefied petroleum gas (LPG) or propane, or a low-temperature solvent and extraction agent (Arcoumanis et al., 2008; Hu et al., 2005; Semelsberger et al., 2006).

DME is conventionally produced using a two-step process comprising synthesis of methanol from syngas on a Cu-ZnO-based catalyst and methanol dehydration to DME on a solid acid catalyst (Spivey, 1991). A new single-step synthesis of DME directly from

syngas has gained much attention due to its thermodynamic and economic advantages (García-Trenco and Martínez, 2012; Hayer et al., 2011; Li et al., 2011). A bifunctional catalyst that is able to simultaneously catalyze both the methanol synthesis and the methanol dehydration reactions is required for the single-step of synthesis of DME from syngas. The bifunctional catalyst typically consists of a Cu-ZnO-based component for the conversion of syngas to methanol and a solid acid component for the methanol dehydration to DME.

Extensive studies have been conducted on methanol synthesis reaction. Cu-ZnO-based catalyst is reported to be the best for methanol production from syngas. However, the methanol dehydration process has received comparatively less attention. From previous studies, γ-Al_2O_3 (Mao et al., 2006; Moradi et al., 2007; Yaripour et al., 2005a) and zeolites (Ereña et al., 2005; Mao et al., 2005; Vishwanathan et al., 2004; Wang et al., 2006) are the most common used catalysts as the solid acid component for the DME synthesis. It is widely accepted that γ-Al_2O_3 undergoes a rapid and irreversible deactivation (Yaripour et al., 2005b), while zeolites exhibit much higher activity and stability during the methanol dehydration reaction (Takeguchi et al., 2000; Xu et al., 1997). In addition, the acidic properties and reaction activity of the solid acid component could be affected when it is mixed with the Cu-ZnO-based catalyst. Therefore, it is important and essential to examine the influence of different zeolites on the activity of the bifunctional catalysts and thus the efficiency of the single-step synthesis of DME from syngas.

In this chapter, seven different zeolites mixed with Cu-ZnO-Al_2O_3 (CZA) were used as the bifunctional catalysts for the single-step synthesis of DME from syngas. Various

catalyst characterization techniques including X-ray diffraction (XRD), temperature-programmed reduction (TPR), and temperature-programmed desorption of ammonia (NH_3-TPD) were employed to examine the properties of the bifunctional catalysts. The influence of zeolite type on the overall activity, selectivity, and stability of the bifunctional catalyst during the syngas-to-DME process was investigated.

6.2 Materials and methods

6.2.1 Catalyst preparation

The CuO-ZnO-Al_2O_3 functioning as the precursor for the methanol synthesis catalyst was prepared using coprecipitation method described by Baltes et al (2008). A solution of metal nitrates [$Cu(NO_3)_2$ (0.6 mol/L), $Zn(NO_3)_2$ (0.3 mol/L), and $Al(NO_3)_3$ (0.1 mol/L)] and a solution of Na_2CO_3 (1 mol/L) were simultaneously pumped at a constant flow rate of 5 ml/min into a stirred and heated glass reactor with a starting volume of 200 ml of deionized water. During the precipitation process, the reactor was kept at a constant temperature of 70±1 ºC and a constant pH of 7.0±0.1. After the addition of the metal nitrates solution, the suspension was aged for 1h at the same temperature. The pH was also kept constant at 7.0 during the aging process through the controlled addition of the metal nitrates or sodium carbonate solutions. Subsequently, the precipitate was filtered and exhaustively washed with deionized water, and then dried at 105 ºC for 12 h. After grinding to the size of smaller than 1 mm, the dried hydroxyl carbonate precursor was calcined at 300 ºC under air for 3 h, yielding the oxide catalyst precursor.

Four types of commercial zeolites namely, H-ZSM-5, H-Y, H-Beta, and H-Ferrierite purchased from Zeolyst International (Conshohocken, PA) were used as the solid acid component in the preparation of bifunctional catalysts. ZSM-5, Beta and Ferrierite zeolites were provided in their ammonium form and they were calcined at 550 ºC in air for 5 h to their active hydrogen form prior to use.

The bifunctional catalysts were prepared by physically mixing the Cu-ZnO-Al_2O_3 and zeolite components, with CZA/zeolite mass ratio kept at 2:1.

6.2.2 Catalyst characterization

The Brunauer-Emmett-Teller (BET) surface areas of the zeolites were estimated from nitrogen adsorption isotherm data obtained on a Micromeritics ASAP 2000 physisorption analyzer.

The powder X-ray diffraction (XRD) patterns, obtained on a Bruker-AXS (Siemens) D5005 X-ray diffractometer instrument with a Cu–K_α radiation at 45 kV and 40 mA, were used to identify the major crystalline phases present in the CZA-Zeolite bifunctional catalysts and their crystallinity. Data collected from the instrument were analyzed using software MDI Jade 8.0.

The reduction behavior of the CZA oxide precursor was investigated through the temperature-programmed reduction (TPR) experiments carried out with a ChemBET Pulsar TPR/TPD automated chemisorption flow analyzer (Quantachrome Instruments). About 30 mg of sample was initially flushed with He at 350 ºC for 2 h to remove the adsorbed water and other contaminants followed by being cooled to 50 ºC. The gas was then switched to the reductive mixture of 5 vol% H_2 in Ar at a flow rate of 30 ml/min and

the temperature was linearly increased up to 600 ºC at a heating rate of 10 ºC/min and kept at 600 ºC for 30 min. The effluent gas flowed through a molecular sieve trap with the generated water removed, and was then analyzed by GC equipped with a thermal conductivity detector (TCD).

The acid properties of the bifunctional catalysts were determined by the temperature-programmed desorption of ammonia (NH_3-TPD) profiles obtained in a ChemBET Pulsar TPR/TPD automated chemisorption flow analyzer (Quantachrome Instruments). Prior to ammonia adsorption, ca. 100 mg of sample was degassed under a He flow at 250 ºC for 2 h. After being cooled to 100 ºC, the sample was saturated with anhydrous NH_3 for about 20 min. The sample was then purged with He to remove excess NH_3 from the sample surface. Finally, the TPD measurement was performed by heating the sample from 100 to 650 ºC at a heating rate of 10 ºC/min under a He flow.

6.2.3 Catalytic synthesis experiments

The single-step synthesis of DME from syngas was conducted in a 316 stainless-steel fixed-bed reactor with a diameter of 12.7 mm charged with 6.0 g of bifunctional catalyst. Prior to reaction, the CuO in the CZA oxide precursor needs to be reduced to its active metallic Cu state by catalyst exposure to a diluted H_2 flow (5 vol% H_2 in N_2) at 245 ºC for 10 h. The gaseous feed stream with H_2/CO volumetric ratio at 2:1 was introduced into the reactor, using two mass flow controllers to precisely control their flow rates separately. The DME synthesis reaction was carried out at temperature of 260 ºC, pressure of 50 bar, and space velocity of 1500 $mL_{syngas}/(g_{cat}\ h)$. The pressure of the system was controlled using a back pressure regulator set at the end of the reactor. The

effluent products were analyzed by a Varian CP-4900 micro gas chromatograph equipped with a 5Å molecular sieve column for the analysis of H_2 and CO, and simultaneously with a PoraPlot Q column for the analysis of CO_2, methanol and DME. The columns were connected to a thermal conductivity detector (TCD) and helium was used as the carrier gas. The CO conversion and products selectivity were calculated based on the total carbon mass balance. The data shown in this study are the averaged values in the range of 15–25 h on stream, with the results representing stable CO conversion and products selectivity.

6.3 Results and discussion

6.3.1 Characterization of catalysts

The physicochemical properties of the zeolites used in this study are summarized in Table 6.1. It is noticed that the zeolites of H-Y type have larger surface area and pore size than those of other zeolite types. It is reported that the structure plays an important role in maintaining the catalyst stability (Jin et al., 2007). The bifunctional catalysts were denoted as CZA/Z(Si:Al), where Z and Si:Al are the type and Si/Al ratio of the zeolites, respectively. For instance, the bifunctional catalyst denoted as CZA/ZSM-5(280) refers to the catalyst prepared by mixing the Cu-ZnO-Al_2O_3 and CBV28014 zeolite.

Table 6.1 Physicochemical properties of the zeolites.

Product name	Type	Framework type	Si/Al ratio	Pore size (Å)	BET surface area (m^2/g)
CBV28014	H-ZSM-5	MFI	280	5.6×5.3, 5.5×5.1	400
CBV8014	H-ZSM-5	MFI	80	5.6×5.3, 5.5×5.1	425
CBV3024E	H-ZSM-5	MFI	30	5.6×5.3,	405

CBV400	H-Y	FAU	5.1	5.5×5.1 7.4×7.4	730
CBV780	H-Y	FAU	80	7.4×7.4	780
CP811C-300	H-Beta	BEA	300	7.6×6.4, 5.6×5.6	620
CP914C	H-Ferrierite	FER	20	4.2×5.4, 3.5×4.8	400

The H_2-TPR profiles for the seven bifunctional catalysts are shown in Fig. 6.1. A single reduction feature peak can be observed for the TPR profiles of all the bifunctional catalysts. The temperature of peak maximum (T_{max}) for the bifunctional catalysts CZA/ZSM-5(280), CZA/ZSM-5(80), CZA/ZSM-5(30), CZA/Y(5.1), CZA/Y(80), CZA/Beta(300), and CZA/Ferrierite(20) appears at 373 ºC, 372 ºC, 382 ºC, 351 ºC, 392 ºC, 372 ºC, and 414 ºC, respectively. Therefore, the nature of zeolite has great influence on the overall reducibility of the bifunctional catalysts. However, it is reported that the reduction of copper species occurs at about 205 ºC (García-Trenco and Martínez, 2012), and thus, the H_2-reduction treatment at 245 ºC performed in situ prior to reaction is adequate to convert Cu^{2+} to the active metallic Cu.

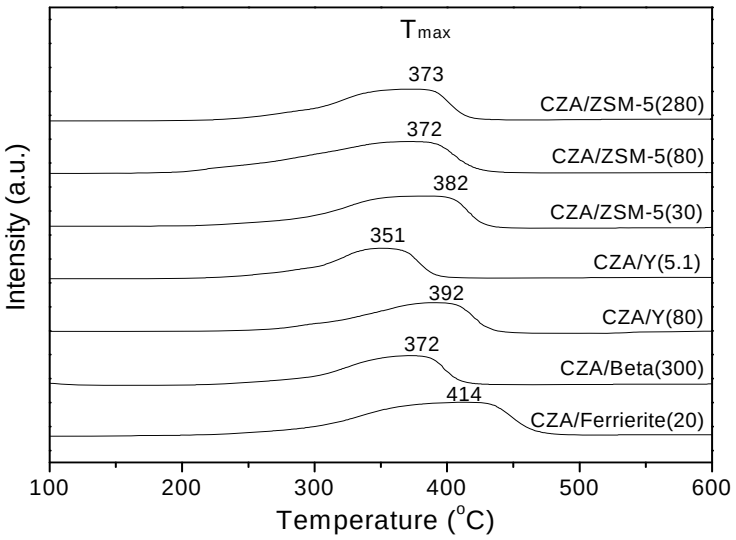

Fig. 6.1 TPR profiles for the bifunctional catalysts.

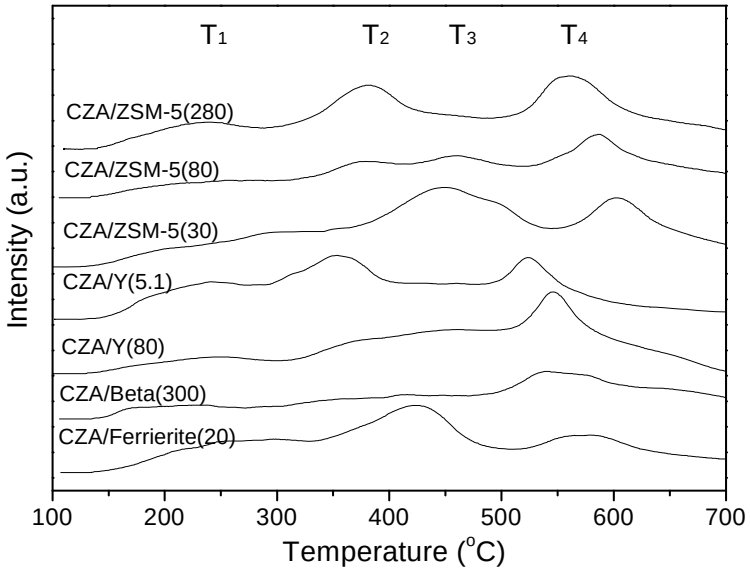

Fig. 6.2 NH_3-TPD profiles for the bifunctional catalysts.

The NH_3-TPD profiles for the seven bifunctional catalysts are displayed in Fig. 6.2. Three or four desorption peaks, which appear in the temperature regions of 230–270 ºC (T_1), 350–430 ºC (T_2), 450–490 ºC (T_3), and 520–610 ºC (T_4), respectively, were observed for the catalysts. The desorption peak at lower temperature (T_1) is attributed to the acidity in the zeolite matrix alone and hence it represents weak acid sites, while the peaks at higher temperatures (T_2, T_3 and T_4) are contributed by the acidity on the surface of the zeolite and thus they are assigned to relatively strong acid sites (Prasad et al., 2008). The density of acid sites for each peak was calculated by comparing the area under the peak with those of the calibration peaks obtained by injecting known amount of ammonia. As shown in Table 6.2, the amounts of weak, strong and total acid sites on CZA/ZSM-5(30), CZA/Y(5.1), and CZA/Ferrierite(20) are larger than the other bifunctional catalysts. The weak acid sites play an important role for the methanol dehydration

activity of the catalyst, however, high density of strong acid sites could facilitate the water-gas shift (WGS) reaction for CO_2 production (Prasad et al., 2008).

Table 6.2 Surface acidity of the bifunctional catalysts as determined by NH_3-TPD.

Catalyst	Density of acid sites (μmol NH_3/g)					Density of acid sites (μmol NH_3/g)		
	T_1	T_2	T_3	T_4	Total	Weak	Strong	Total
CZA/ZSM-5(280)	465.8	266.4	–	242.6	974.8	465.8	509.0	974.8
CZA/ZSM-5(80)	345.5	128.2	284.8	225.1	983.6	345.5	638.1	983.6
CZA/ZSM-5(30)	955.6	–	961.4	518.9	2435.9	955.6	1480.3	2435.9
CZA/Y(5.1)	722.2	547.4	–	434.7	1704.3	722.2	982.1	1704.3
CZA/Y(80)	432.8	205.6	221.0	338.7	1198.1	432.8	765.3	1198.1
CZA/Beta(300)	337.3	383.0	–	364.4	1084.7	337.3	747.4	1084.7
CZA/Ferrierite(20)	720.0	679.8	–	344.3	1744.1	720.0	1024.1	1744.1

6.3.2 Catalytic synthesis experiments

The results of single-step synthesis of DME from syngas using different zeolites as the solid acid component for the bifunctional catalysts are summarized in Table 6.3. Higher CO conversion and DME yield were obtained when ZSM-5(30), or Y(5.1), or Ferrierite(20) was used than when the other zeolites were used. Careful examination of product selectivity reveals a low CH_3OH content and high DME/CH_3OH selectivity ratio in the product for these three zeolites. The distinct activity and selectivity behavior of the seven bifunctional catalysts can be determined by multiple parameters, such as reducibility, surface acidity, elemental composition, and pore structure of the catalyst.

Table 6.3 The influence of different zeolites on single-step synthesis of DME from syngas.

Catalyst	CO conversion (%)	Selectivity (%)			DME yield ($g \cdot kg_{cat}^{-1} \cdot h^{-1}$)
		DME	CH_3OH	CO_2	
CZA/ZSM-5(280)	44.6	70.4	24.5	5.2	161.0
CZA/ZSM-5(80)	65.5	62.9	24.9	12.3	211.2
CZA/ZSM-5(30)	87.8	65.9	3.4	30.7	297.0
CZA/Y(5.1)	91.9	63.9	3.0	33.1	301.7

CZA/Y(80)	50.6	23.3	64.5	12.2	60.6
CZA/Beta(300)	30.0	25.9	64.1	9.9	40.0
CZA/Ferrierite(20)	93.0	61.4	2.8	35.8	293.4

The reducibility of the Cu species is reported to have great influence on the CO hydrogenation activity (Prasad et al., 2008). However, no obvious correlation was found between CO conversion and the peak temperature (T_{max}) of the TPR profiles for the bifunctional catalysts. It means that, in this study, the syngas-to-DME process is not controlled by the reduction behavior of the catalyst which probably due to the complete conversion of Cu^{2+} to Cu^0 under the H_2-reduction pretreatment.

The methanol dehydration activity of the bifunctional catalyst is mainly determined by the surface acidity especially the density of weak acid sites on the catalyst. Larger amounts of weak acid sites mean higher activity of the catalyst for methanol dehydration to DME, resulting in higher selectivity to DME and lower selectivity to methanol. This is the most important reason for the high DME selectivity on CZA/ZSM-5(30), CZA/Y(5.1), and CZA/Ferrierite(20). However, the high DME selectivity on CZA/ZSM-5(280) and CZA/ZSM-5(80) is probably due to other factors which will be discussed later. When the overall syngas-to-DME reaction is controlled by the methanol dehydration step, a higher methanol dehydration activity of the bifunctional catalyst, which would facilitate the CO/CO_2 hydrogenation by shifting the chemical equilibrium of reactions (2.2) and (2.3) to the right-hand side, leads to a higher CO conversion (García-Trenco and Martínez, 2012; Mao et al., 2006). In addition, a high density of strong acid sites on the catalyst could favor the CO_2 formation from CO through the WGS reaction, which further increases the CO conversion. Therefore, the high surface acidity is responsible for the

high CO conversion and CO_2 selectivity observed for CZA/ZSM-5(30), CZA/Y(5.1), and CZA/Ferrierite(20) during the syngas-to-DME process.

Pore structure is another important factor that affects catalyst activity and selectivity. The structures of different types of zeolites are given in Table 6.4 (Aho et al., 2008). It is likely that the peculiar channel structure of H-Ferrierite facilitates the diffusion and transfer of reaction products. Therefore, the chemical equilibrium of reactions (2.2)–(2.4) can be further shifted to the right-hand side, allowing high CO conversion and DME selectivity over CZA/Ferrierite(20) to be attained. In contrary, the peculiar channel structure of H-Beta probably blocks and restricts the transportation of CH_3OH and DME, making the syngas to methanol process easily reach the thermodynamic equilibrium which would result in low CO conversion and DME selectivity.

Table 6.4 Pore structures of different types of zeolites.

Zeoilte type	Pore structure
H-ZSM-5	3-Dimensional pore system; straight 10-member-ring channels connected by sinusoidal channels
H-Y	3-Dimensional pore structure; circular 12-member-ring windows connected by spherical cavities
H-Beta	3-Dimensional pore system; 12-ring channel in c direction plus two 12-ring channels in a direction perpendicular to c direction
H-Ferrierite	Orthorhombic pore structure; 10-member-ring channels perpendicularly intersected with 8-member-ring channels

Si/Al distribution is considered as the most important crystalchemical feature of the zeolite framework, affecting particularly its catalytic properties (Alberti et al., 2002). Comparing the three H-ZSM-5 zeolites with different Si/Al ratio, it can be found that the lowest CO conversion but highest DME selectivity was obtained when ZSM-5(280) with the highest Si/Al ratio was used. Higher Si/Al ratio would be expected to lead to higher

reaction rate due to more catalytically active sites and lower activation barrier (Celik et al., 2010). Thus the reaction activity for methanol dehydration is high over the zeolite with high Si/Al ratio, resulting in high DME selectivity. The low CO conversion for the zeolite with high Si/Al ratio is probably because of the diffusion barrier within the pore channels of zeolite. In addition, it is reported that the catalytic activity does not depend on the Si/Al ratio for H-Y zeolite (Xu et al., 2007). Therefore, the CO conversion and DME selectivity on such type of zeolite are mainly determined by the copper activity and surface acidity.

The stability of the bifunctional catalyst is also influenced by the zeolite type. The CO conversion as a function of time on stream (TOS) in syngas-to-DME experiments over the seven bifunctional catalysts is presented in Fig. 6.3. The results obtained for catalyst stability are basically the same as those for CO conversion on the seven catalysts. Higher stability is observed for CZA/Y(5.1), CZA/Ferrierite(20), and CZA/ZSM-5(30) with lower deactivation rate compared with that for the other bifunctional catalysts. The most obvious deactivation is observed for CZA/Y(80).

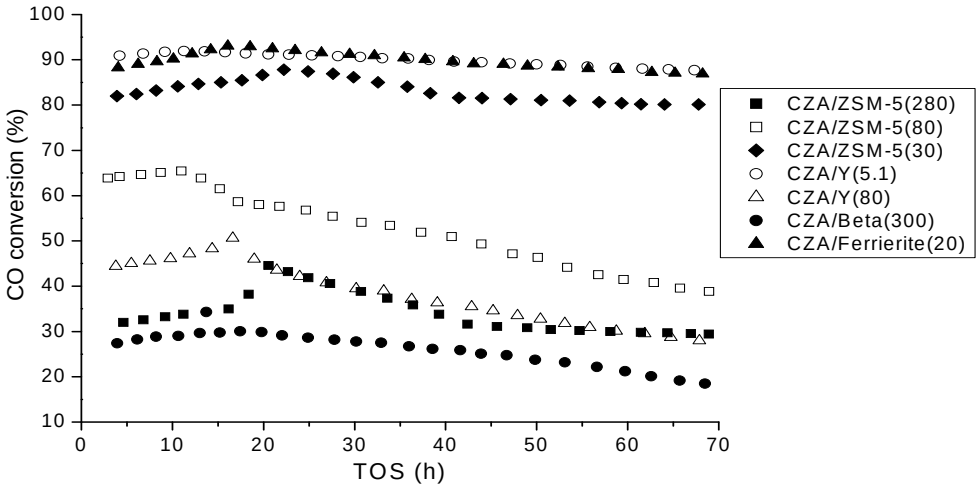

Fig. 6.3 CO conversion as a function of time on stream (TOS) in syngas-to-DME experiments using different bifunctional catalysts.

The bifunctional catalysts after the 70 h run were characterized and compared using X-ray diffraction (XRD) technique to examine the structure change of the catalysts. As shown in Fig. 6.4, the characteristic peaks of corresponding zeolite can be observed for each type of bifunctional catalyst, meaning that the zeolite structures were retained during the syngas-to-DME process. However, distinct diffraction peaks occur at the diffraction angles of 43.5° which corresponds to metallic Cu. The intensity of the diffraction peak varies for different bifunctional catalysts after reaction. The crystalline sizes of metallic Cu for the seven catalysts, as estimated by the Scherrer equation, were as follows: CZA/ZSM-5(280) (15.8 nm), CZA/ZSM-5(80) (13.4 nm), CZA/ZSM-5(30) (12.3 nm), CZA/Y(5.1) (12.6 nm), CZA/Y(80) (12.7 nm), CZA/Beta(300) (14.5 nm), and CZA/Ferrierite(20) (12.6 nm). Smaller particle sizes were found for CZA/ZSM-5(30), CZA/Y(5.1), and CZA/Ferrierite(20) than the other bifunctional catalysts, indicating a low deactivation rate of metallic Cu. It could explain the high stability of CO conversion on these three catalysts during the syngas-to-DME experiments. However, the small crystalline size of metallic Cu does not mean high stability of CO conversion for the catalyst CZA/Y(80). The deactivation of this catalyst is perhaps attributed to other causes.

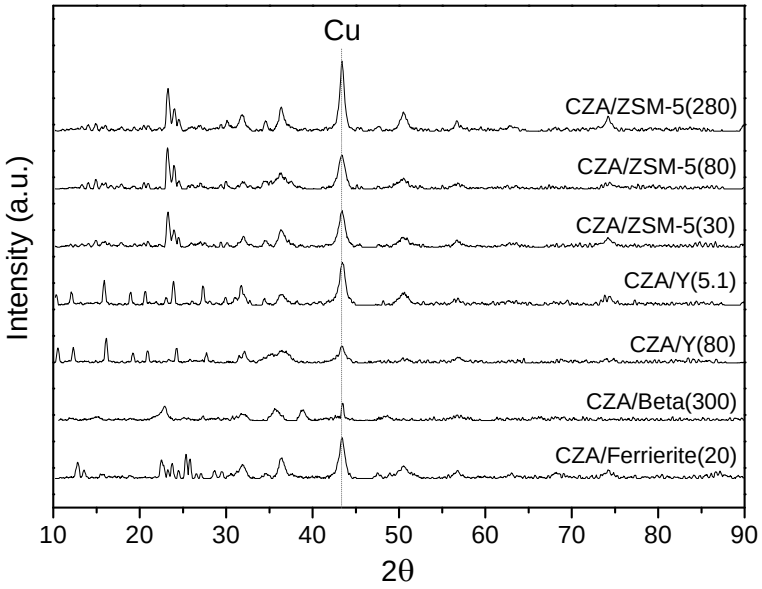

Fig. 6.4 XRD patterns of bifunctional catalysts after reaction.

The selectivity to the main reaction products as a function of TOS in syngas-to-DME experiments on bifunctional catalysts CZA/Y(5.1) and CZA/Y(80) is displayed in Fig. 6.5. As shown in Fig 6.5(a), the selectivity values remained almost constant during the 70 h run for CZA/Y(5.1) although the CO conversion slightly decreased with TOS (Fig. 6.3). It suggests that for CZA/Y(5.1) the main cause for the decease of CO conversion with TOS is the deactivation of the Cu-based methanol synthesis component (Barbosa et al., 2008; Luan et al., 2007). However, a different selectivity behavior with TOS can be observed for CZA/Y(80), as depicted in Fig. 6.5(b). The selectivity to DME gradually decreased with TOS but that to CH_3OH increased. It can be inferred from the decrease in the DME/CH_3OH selectivity ratio that for CZA/Y(80), in addition to the deactivation of the Cu-based catalyst, the decrease in CO conversion with TOS is largely due to a loss of the zeolite dehydration activity. Therefore, the influence of zeolite type on the stability of the bifunctional catalyst is rendered mainly through the stability of the

surface acidity. It can be concluded that the zeolite acidity has a great impact on the activity, selectivity, and stability of the bifunctional catalyst during the single-step synthesis of DME from syngas.

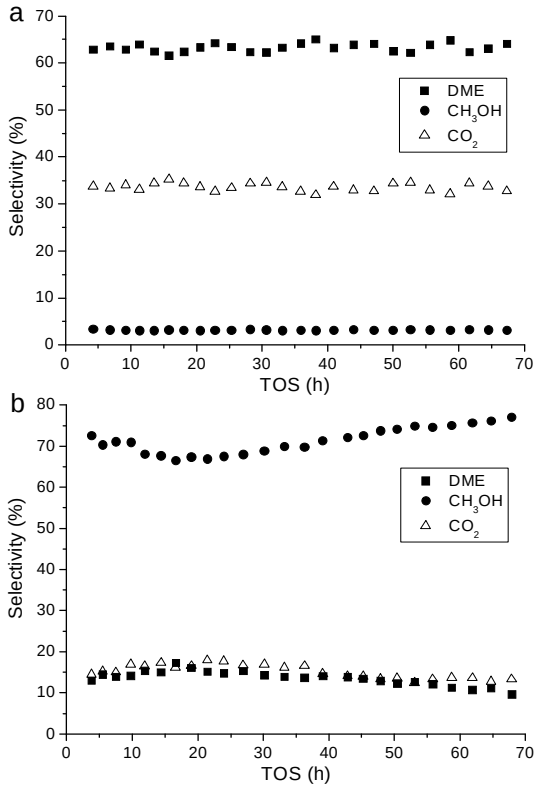

Fig. 6.5 Selectivity to the main reaction products as a function of TOS in syngas-to-DME experiments on bifunctional catalysts (a) CZA/Y(5.1) and (b) CZA/Y(80).

6.4 Conclusions

In this chapter, the influence of the type of zeolite in the CuZnAl/zeolite bifunctional catalysts on the single-step synthesis of DME from syngas was investigated. Seven different zeolites were used to prepare the bifunctional catalysts, which were characterized using XRD, H_2-TPR, and NH_3-TPD techniques. The activity, selectivity and stability behavior of the bifunctional catalyst during the syngas-to-DME process was

found to be affected by the zeolite properties, including surface acidity, pore structure, and Si/Al ratio of zeolite.

CHAPTER 6 SUMMARY AND FUTURE WORK

7.1 Summary

The research work presented in this dissertation offers preliminary insight into fast microwave-assisted thermochemical conversion of biomass for biofuel production. The microwave heating characteristics of various biomass feedstocks and microwave absorbents were determined and compared. Microwave absorbents absorbed microwave more effectively than biomass and the addition of these microwave absorbents to biomass feedstock significantly improved the microwave heating characteristics. Silicon carbide was found to have the highest microwave absorbing ability and hence used as the microwave absorbent in this study. A microwave based system was then developed for biomass pyrolysis and gasification. As to biomass pyrolysis, fast microwave-assisted catalytic co-pyrolysis of microalgae and scum for bio-oil production was studied. Scum proved to be a good hydrogen supplier to increase the overall EHI value of feedstock. In order to maximize the production of bio-oil and aromatic hydrocarbons, the optimal co-pyrolysis temperature, catalyst to feed ratio, and microalgae to scum ratio were 550 ºC, 2:1, and 1:2, respectively. A significant synergistic effect between microalgae and scum was achieved only when the EHI value of feedstock was larger than about 0.7. In addition, several pyrolysis pathways for non-catalytic and catalytic fMAP of microalgae were postulated by analysis and identification of pyrolysis products from the model algal biomass compounds. Furthermore, comparison between two-step and one-step processes of fast microwave-assisted catalytic pyrolysis of microalgae demonstrated the priority of the two-step process, especially in catalyst saving and reuse. Moreover, the study of

microwave-assisted catalytic pyrolysis of sewage sludge shows that microwave heating is effective for sewage sludge pyrolysis. The optimal temperature and catalyst to feed ratio for bio-oil production were 550 ^{o}C and 2:1, respectively. The lowest proportions of oxygen- and nitrogen-containing compounds in the bio-oil were achieved under the optimal conditions. The biochar after pyrolysis contained considerable amounts of mineral elements and could be used to improve soil fertility. Catalyst characterization indicated good stability of HZSM-5 catalyst against deactivation during the pyrolysis process. The microwave-assisted system was also used in catalytic gasification of corn stover for syngas production and tar removal. The results show that microwave heating is effective for biomass gasification and Ni/Al_2O_3 had the best catalytic effect on syngas production and tar conversion. More than 80 wt% of gas was obtained in the product and only 34 compounds were detected in the tar when Ni/Al_2O_3 was used as the catalyst. Catalyst characterization indicated good stability of Ni/Al_2O_3 against deactivation during gasification process. A new concept of microwave-assisted dual fluidized bed gasifier was put forward for large-scale applications. To further utilize the syngas produced from biomass gasification, single-step synthesis of DME from syngas on various CuZnAl/zeolite bifunctional catalysts was investigated. The influence of the type of zeolite in the bifunctional catalysts on DME synthesis was examined. Seven different zeolites were used to prepare the bifunctional catalysts, which were characterized using XRD, H_2-TPR, and NH_3-TPD techniques. The activity, selectivity and stability behavior of the bifunctional catalyst during the syngas-to-DME process was found to be affected by the zeolite properties, including surface acidity, pore structure, and Si/Al ratio of zeolite.

7.2 Future work

7.2.1 Development of a continuous microwave-based biomass conversion system for biofuel production

The experiments in this dissertation were conducted based on a batch reactor. In order to realize the industrialization of the microwave-assisted pyrolysis and gasification technology, a continuous system needs to be developed and investigated for biofuel production. The key features of the continuous system could include a motor-driven mixer, multiple-point temperature detection, automatic temperature control, mechanisms for easy input of feedstock and discharge of solid materials and reassembling, etc. Microwave ovens with capability to vary power input and with different frequencies are desirable. Based on the results from a bench-scale continuous microwave-based system, a demonstration system could be designed and developed in future.

7.2.2 FMAP of microalgae cultivated in different metabolic pathways

The metabolic pathways, growth modes and cell organization of some species of microalgae can be controlled and changed by simple manipulation of the chemical properties of the culture medium (Behrens and Kyle, 1996). Microalgae can be photoautotrophically or heterotrophically grown under different culture conditions, and heterotrophic growth usually results in higher biomass production and lipid content in cells (Miao and Wu, 2004). Miao and Wu (2004) performed fast pyrolysis of *Chlorella protothecoides* in different metabolic pathways and the yield of bio-oil obtained from heterotrophic cells (57.2%) was about 3.4 times higher than that from autotrophic cells (16.6%). In addition, the bio-oils produced from heterotrophic cells had better quality

than those from autotrophic cells and wood in terms of bio-oil density, viscosity and heating value. Therefore, microalgae could be cultivated in different metabolic pathways, and used and compared as the feedstock for bio-oil production from fast microwave-assisted catalytic pyrolysis.

7.2.3 Fast microwave-assisted co-gasification for syngas production

There are some issues with biomass gasification, including low H_2 content in the syngas, high contents of impurity gases such as NO_x, low heating value of gas product, etc. As mentioned in Chapter 3, co-pyrolysis of biomass with an additional feedstock with a high EHI value could improve the bio-oil yield and quality. Similarly, co-feeding of biomass with an additional feedstock with high carbon and hydrogen contents in the fast microwave-assisted gasification process could improve the syngas yield and quality. Based on the results from previous studies (Brown et al., 2000; Kumabe et al., 2007; Nemanova et al., 2014), coal and petroleum coke can be co-fed with biomass for the production of high-quality syngas from the fMAG process.

7.2.4 Modification of zeolite for single-step DME synthesis from syngas

As concluded in Chapter 5, the zeolite acidity has a great impact on the activity, selectivity, and stability of the bifunctional catalyst during the single-step synthesis of DME from syngas. Therefore, zeolite can be modified to adjust the surface acidity and hence improve the activity, selectivity, and stability of the catalyst. Chemicals such as Fe, Zr, MgO, and rare earth metals were used in previous studies to modify the zeolite in single-step DME synthesis from syngas (Jin et al., 2007; Kang et al., 2008; Mao et al.,

2005; Xia et al., 2004). Other chemicals should be tested in zeolite modification to further promote the catalyst performance.

BIBLIOGRAPHY

[1] U.S. Department of Energy and Department of Agriculture. 2002. Biomass Research and Development Technical Advisory Committee, "Vision for Bioenergy & Biobased Products in the United States" www.climatevision.gov/sectors/electricpower/pdfs/bioenergy_vision.pdf.
[2] Adjaye, J.D., Bakhshi, N.N., 1995. Production of hydrocarbons by catalytic upgrading of a fast pyrolysis bio-oil. Part Ⅱ: Comparative catalyst performance and reaction pathways. Fuel Process. Technol. 45, 185–202.
[3] Ahmed, I., Gupta, A.K., 2009. Evolution of syngas from cardboard gasification. Appl. Energy 86, 1732–1740.
[4] Aho, A., Kumar, N., Eränen, K., Salmi, T., Hupa, M., Murzin, D.Yu., 2008. Catalytic pyrolysis of woody biomass in a fluidized bed reactor: Influence of the zeolite structure. Fuel 87, 2493–2501.
[5] Alberti, A., Cruciani, G., Galli, E., Merlino, S., Millini, R., Quartieri, S., Vezzalini, G., Zanardi, S., 2002. Crystal structure of tetragonal and monoclinic polytypes of tschernichite, the natural counterpart of synthetic zeolite beta. J. Phys. Chem. B 106, 10277–10284.
[6] Anis, S., Zainal, Z.A., 2011. Tar reduction in biomass producer gas via mechanical, catalytic and thermal methods: A review. Renew. Sustain. Energy Rev. 15, 2355–2377.
[7] Arcoumanis, C., Bae, C., Crookes, R., Kinoshita, E., 2008. The potential of di-methyl ether (DME) as an alternative fuel for compression-ignition engines: A review. Fuel 87, 1014–1030.
[8] Ateş, F., Pütün, E., Pütün, A.E., 2004. Fast pyrolysis of sesame stalk: yields and structural analysis of bio-oil. J. Anal. Appl. Pyrolysis 71, 779–790.
[9] Babich, I.V., Van der Hulst, M., Lefferts, L., Moulijn, J.A., O'Connor, P., Seshan, K., 2011. Catalytic pyrolysis of microalgae to high-quality liquid bio-fuels. Biomass Bioenergy 35, 3199–3207.
[10] Balat, M., 2008a. Mechanisms of thermochemical biomass conversion processes. Part 1: reactions of pyrolysis. Energy Sources, Part A 30, 620–635.
[11] Baltes, C., Vukojević, S., Schüth, F., 2008. Correlations between synthesis, precursor, and catalyst structure and activity of a large set of $CuO/ZnO/Al_2O_3$ catalysts for methanol synthesis. J. Catal. A 258, 334–344.
[12] Barbosa, F.S.R., Ruiz, V.S.O., Monteiro, J.L.F., De Avillez, R.R., Borges, L.E.P., Appel, L.G., 2008. The deactivation modes of $Cu/ZnO/Al_2O_3$ and HZSM-5 physical mixture in the one-step DME synthesis. Catal. Lett. 126, 173–178.
[13] Beckers, W., Schuller, D., Vaizert, O., 1999. Thermolytical treatment of dried sewage sludge and other biogenic materials – including upgrading of pyrolysis vapours by a cracking catalyst and examination of heavy metals by X-ray fluorescence. J. Anal. Appl. Pyrolysis 50, 17–30.
[14] Behrens, P.W., Kyle, D.J., 1996. Microalgae as a source of fatty acids. J. Food Lipid 3, 259–272.

[15] Bi, C., Min, M., Nie, Y., Xie, Q., Lu, Q., Deng, X., Anderson, E., Li, D., Chen, P., Ruan, R., 2015. Process development for scum to biodiesel conversion. Bioresour. Technol. 185, 185–193.
[16] Bjorgen, M., Olsbye, U., Kolboe, S., 2003. Coke precursor formation and zeolite deactivation: mechanistic insights from hexamethylbenezene conversion. J. Catal. 215, 30–44.
[17] Bjorgen, M., Svelle, S., Joensen, F., Nerlov, J., Kolboe, S., Francesca, B., Palumbo, L., Bordiga, S., Olsbye, U., 2007. Conversion of methanol to hydrocarbons over zeolite H-ZSM-5: On the origin of the olefinic species. J. Catal. 249, 195–207.
[18] Borges, F.C., Du, Z., Xie, Q., Trierweiler, J.O., Cheng, Y., Wan, Y., Liu, Y., Zhu, R., Lin, X., Chen, P., Ruan, R., 2014. Fast microwave assisted pyrolysis of biomass using microwave absorbent. Bioresour. Technol. 156, 267–274.
[19] Borges, F.C., Xie, Q., Min, M., Muniz, L.A.R., Farenzena, M., Trierweiler, J.O., Chen, P., Ruan, R., 2014. Fast microwave-assisted pyrolysis of microalgae using microwave absorbent and HZSM-5 catalyst. Bioresour. Technol. 166, 518–526.
[20] Bridgwater, A.V., Peacocke, G.V.C., 2000. Fast pyrolysis processes for biomass. Renew. Sust. Energy Rev. 4, 1–73.
[21] Bridle, T.R., Pritchard, D., 2004. Energy and nutrient recovery from sewage sludge via pyrolysis. Water Sci. Technol. 50, 169–175.
[22] Brown, R.C., Liu, Q., Norton, G., 2000. Catalytic effects observed during the co-gasification of coal and swithgrass. Biomass Bioenergy 18, 499–506.
[23] Bu, Q., Lei, H., Ren, S., Wang, L., Zhang, Q., Tang, J., Ruan, R., 2012. Production of phenols and biofuels by catalytic microwave pyrolysis of lignocellulosic biomass. Bioresour. Technol. 108, 274–279.
[24] Budarin, V.L., Clark, J.H., Lanigan, B.A., Shuttleworth, P., Breeden, S.W., Wilson, A.J., Macquarrie, D.J., Milkowski, K., Jones, J., Bridgeman, T., Ross, A., 2009. The preparation of high-grade bio-oils through the controlled, low temperature microwave activation of wheat straw. Bioresour. Technol. 100, 6064–6068.
[25] Carlson, T.R., Jae, J., Lin, Y.C., Tompsett, G.A., Huber, G.W., 2010. Catalytic fast pyrolysis of glucose with HZSM-5: the combined homogeneous and heterogeneous reactions. J. Catal. 270, 110–124.
[26] Celik, F.E., Kim, T.J., Bell, A.T., 2010. Effect of zeolite framework type and Si/Al ratio on dimethoxymethane carbonylation. J. Catal. 270, 185–195.
[27] Chen, N.Y., Degnan, T.F., Koenig, L.R., 1986. Liquid fuel from carbohydrates. Chemtech 16, 506–511.
[28] Chen, P., Min, M., Chen, Y., Wang, L., Li, Y., Chen, Q., Wang, C., Wan, Y., Wang, X., Cheng, Y., Deng, S., Hennesy, K., Lin, X., Liu, Y., Wang, Y., Martinez, B., Ruan, R., 2009. Review of the biological and engineering aspects of algae to fuels approach. Int. J. Agric. Biol. Eng. 2, 1–30.
[29] Chisti, Y., 2008. Biodiesel from microalgae beats bioethanol. Trends Biotechnol. 26, 126–131.
[30] Damartzis, T., Zabaniotou, A., 2011. Thermochemical conversion of biomass to second generation biofuels through integrated process design-A review. Renew. Sustain. Energy Rev. 15, 366–378.

[31] Demirbas, A., 2001. Biomass resource facilities and biomass conversion processing for fuels and chemicals. Energy Convers. Manage. 42, 1357–1378.
[32] Devi, L., Craje, M., Thüne, P., Ptasinski, K.J., Janssen, F.J.J.G., 2005. Olivine as tar removal catalyst for biomass gasifiers: Catalyst characterization. Appl. Catal., A 294, 68–79.
[33] Devi, L., Ptasinski, K.J., Janssen, F.J.J.G., 2003. A review of the primary measures for tar elimination in biomass gasification processes. Biomass Bioenergy 24, 125–140.
[34] Devi, L., Ptasinski, K.J., Janssen, F.J.J.G., Van Paasen, S.V.B., Bergman, P.C.A., Kiel, J.H.A., 2005. Catalytic decomposition of biomass tars: use of dolomite and untreated olivine. Renew. Energy 30, 565–587.
[35] Domínguez, A., Menéndez, J.A., Inguanzo, M., Bernad, P.L., Pis J.J., 2003. Gas chromatographic–mass spectrometric study of the oil fractions produced by microwave-assisted pyrolysis of different sewage sludges. J. Chromatogr. A 1012, 193–206.
[36] Domínguez, A., Menéndez, J.A., Inguanzo, M., Pis J.J., 2006. Production of bio-fuels by high temperature pyrolysis of sewage sludge using conventional and microwave heating. Bioresour. Technol. 97, 1185–1193.
[37] Dong, L., Xu, G., Suda, T., Murakami, T., 2010. Potential approaches to improve gasification of high water content biomass rich in cellulose in dual fluidized bed. Fuel Process. Technol. 91, 882–888.
[38] Du, Z., Hu, B., Ma, X., Cheng, Y., Liu, Y., Lin, X., Wan, Y., Lei, H., Chen, P., Ruan, R., 2013. Catalytic pyrolysis of microalgae and their three major components: carbohydrates, proteins, and lipids. Bioresour. Technol. 130, 777–782.
[39] Du, Z., Li, Y., Wang, X., Wan, Y., Chen, Q., Wang, C., Lin, X., Liu, Y., Chen, P., Ruan, R., 2011. Microwave-assisted pyrolysis of microalgae for biofuel production. Bioresour. Technol. 102, 4890–4896.
[40] Du, Z., Ma, X., Li, Y., Chen, P., Liu, Y., Lin, X., Lei, H., Ruan, R., 2013. Production of aromatic hydrocarbons by catalytic pyrolysis of microalgae with zeolites: Catalyst screening in a pyroprobe. Bioresour. Technol. 139, 397–401.
[41] Du, Z., Mohr, M., Ma, X., Cheng, Y., Lin, X., Liu, Y., Zhou, W., Chen, P., Ruan, R., 2012. Hydrothermal pretreatment of microalgae for production of pyrolytic bio-oil with a low nitrogen content. Bioresour. Technol. 120, 13–18.
[42] Duman, G., Okutucu, C., Ucar, S., Stahl, R., Yanik, J., 2011. The slow and fast pyrolysis of cherry seed. Bioresour. Technol. 102, 1869–1878.
[43] Ehimen, E.A., Sun, Z.F., Carrington, C.G., 2010. Variables affecting the in situ transesterification of microalgae lipids. Fuel 89, 677–684.
[44] Encinar, J.M., Gonzalez, J.F., Gonzalez, J., 2000. Fixed-bed pyrolysis of *Cynara cardunculus* L. Product yields and compositions. Fuel Process. Technol. 68, 209–222.
[45] Ereña, J., Garoña, R., Arandes, J.M., Aguayo, A.T., Bilbao, J., 2005. Effect of operating conditions on the synthesis of dimethyl ether over a CuO-ZnO-Al_2O_3/NaHZSM-5 bifunctional catalyst. Catal. Today 107–108, 467–473.
[46] Fargione, J., Hill, J., Tilman, D., Polasky, S., Hawthorne, P., 2008. Land clearing and the biofuel carbon debt. Science 319, 1235–1238.
[47] Fernández, Y., Menéndez, J.A., 2011. Influence of feed characteristics on the microwave-assisted pyrolysis used to produce syngas from biomass wastes. J. Anal. Appl. Pyrolysis 91, 316–322.

[48] Fonts, I., Azuara, M., Lázaro, L., Gea, G., Murillo, M.B., 2009. Gas chromatography study of sewage sludge pyrolysis liquids obtained at different operational conditions in a fluidized bed. Ind. Eng. Chem. Res. 48, 5907–5915.
[49] Fonts, I., Gea, G., Azuara, M., Ábrego, J., Arauzo, J., 2012. Sewage sludge pyrolysis for liquid production: A review. Renew. Sustain. Energy Rev. 16, 2781–2805.
[50] Fonts, I., Juan, A., Gea, G., Murillo, M.B., Sánchez, J.L., 2008. Sewage sludge pyrolysis in fluidized bed, 1: Influence of operational conditions on the product distribution. Ind. Eng. Chem. Res. 47, 5376–5385.
[51] Fytili, D., Zabaniotou, A., 2008. Utilization of sewage sludge in EU application of old and new methods–A review. Renew. Sustain. Energy Rev. 12, 116–140.
[52] Gao, N., Li, A., Quan, C., 2009. A novel reforming method for hydrogen production from biomass steam gasification. Bioresour. Technol. 100, 4271–4277.
[53] García-Trenco, A.; Martínez, A., 2012. Direct synthesis of DME from syngas on hybrid CuZnAl/ZSM-5 catalysts: New insights into the role of zeolite acidity. Appl. Catal., A 411–412, 170–179.
[54] Gayubo, A.G., Aguayo, A.T., Atutxa, A., Aguado, R., Bilbao, J., 2004a. Transformation of oxygenate components of biomass pyrolysis oil on a HZSM-5 zeolite. I. Alcohols and phenols. Ind. Eng. Chem. Res. 43, 2610–2618.
[55] Gayubo, A.G., Aguayo, A.T., Atutxa, A., Aguado, R., Olazar, M., Bilbao, J., 2004b. Transformation of oxygenate components of biomass pyrolysis oil on a HZSM-5 zeolite. Ⅱ. Aldehydes, ketones, and acids. Ind. Eng. Chem. Res. 43, 2619–2626.
[56] Gercel, H.F., 2011. Bio-oil production from *Onopordum acanthium L.* by slow pyrolysis. J. Anal. Appl. Pyrolysis 92, 233–238.
[57] Göransson, K., Söderlind, U., He, J., Zhang, W., 2011. Review of syngas production via biomass DFBGs. Renew. Sustain. Energy Rev. 15, 482–492.
[58] Gouveia, L., Oliveira, A.C., 2009. Microalgae as a raw material for biofuels production. J. Ind. Microbiol. Biotechnol. 36, 269–274.
[59] Goyal, H., Seal, D., Saxena, R., 2008. Bio-fuels from thermochemical conversion of renewable resources: a review. Renew. Sustain. Energy Rev. 12, 504–517.
[60] Graca, I., Comparot, J.D., Laforge, S., Magnoux, P., Lopes, J.M., Ribeiro, M.F., Ribeiro, F.R., 2009. Influence of phenol addition on the H-ZSM-5 zeolite catalytic properties during methylcyclohexane transformation. Energy Fuels 23, 4224–4230.
[61] Grierson, S., Strezov, V., Shah, P., 2011. Properties of oil and char derived from slow pyrolysis of *Tetraselmis chui*. Bioresour. Technol. 102, 8232–8240.
[62] Güngör, A., Önenç, S., Uçar, S., Yanik, J., 2012. Comparison between the “one-step” and “two-step” catalytic pyrolysis of pine bark. J. Anal. Appl. Pyrolysis 97, 39–48.
[63] Hamelinck, C.N., Faaij, A.P.C., 2002. Future prospects for production of methanol and hydrogen from biomass. J. Power Sources 111, 1–22.
[64] Han, J., Kim, H., 2008. The reduction and control technology of tar during biomass gasification/pyrolysis: An overview. Renew. Sustain. Energy Rev. 12, 397–416.
[65] Haw, J.F., Song, W., Marcus, D.M., Nicholas, J.B., 2003. The mechanism of methanol to hydrocarbon catalysis. Acc. Chem. Res. 36, 317–326.
[66] Hayer, F.; Bakhtiary-Davijany, H.; Myrstad, R.; Holmen, A.; Pfeifer, P.; Venvik, H., 2011. Synthesis of dimethyl ether from syngas in a microchannel reactor–Simulation and experimental study. Chem. Eng. J. 167, 610–615.

[67] Houillon, G., Jolliet, O., 2005. Life cycle assessment of processes for the treatment of wastewater urban sludge: energy and global warming analysis. J. Cleaner. Prod. 13, 287–299.
[68] Hu, J.; Wang, Y.; Cao, C.; Elliott, D.C.; Stevens, D.J.; White, J.F., 2005. Conversion of biomass syngas to DME using a microchannel reactor. Ind. Eng. Chem. Res. 44, 1722–1727.
[69] Huang, Y.F., Kuan, W.H., Lo, S.L., Lin, C.F., 2010. Hydrogen-rich fuel gas from rice straw via microwave-induced pyrolysis. Bioresour. Technol. 101, 1968–1973.
[70] Huber, G.W., Iborra, S., Corma, A., 2006. Synthesis of transportation fuels from biomass: chemistry, catalysts, and engineering. Chem. Rev. 106, 4044–4098.
[71] Idem, R.O., Katikaneni, S.P.R., Bakhshi, N.N., 1996. Thermal cracking of canola oil: reaction products in the presence and absence of steam. Energy Fuels 10, 1150–1162.
[72] Inguanzo, M., Domínguez, A., Menéndez, J.A., Blanco C.G., Pis J.J., 2002. On the pyrolysis of sewage sludge: the influence of pyrolysis conditions on solid, liquid and gas fractions. J. Anal. Appl. Pyrolysis 63, 209–222.
[73] Jena, U., Das, K.C., 2011. Comparative evaluation of thermochemical liquefaction and pyrolysis for bio-oil production from microalgae. Energy Fuels 25, 5472–5482.
[74] Jin, D., Zhu, B., Hou, Z., Fei, J., Lou, H., Zheng, X., 2007. Dimethyl ether synthesis via methanol and syngas over rare earth metals modified zeolite Y and dual Cu–Mn–Zn catalysts. Fuel 86, 2707–2713.
[75] Jindarom, C., Meeyoo, V., Rirksomboon, T., Rangsunvigit, P., 2007. Thermochemical decomposition of sewage sludge in CO_2 and N_2 atmosphere. Chemosphere 67, 1477–1484.
[76] Joo, H.S., Guin, J.A., 1996. Activity of noble metal-promoted hydroprocessing catalysts for pyridine HDN and naphthalene hydrogenation. Fuel Process. Technol. 49, 137–155.
[77] Kang, S.H., Bae, J.W., Jun, K.W., Potdar, H.S., 2008. Dimethyl ether synthesis from syngas over the composite catalysts of Cu–ZnO–Al_2O_3/Zr-modified zeolites. Catal. Commun. 9, 2035–2039.
[78] Karaosmanoglu, F., Tetik, E., Gollu, E., 1999. Biofuel production using slow pyrolysis of the straw and stalk of the rapeseed plant. Fuel Process. Technol. 59, 1–12.
[79] Karmakar, M.K., Datta, A.B., 2011. Generation of hydrogen rich gas through fluidized bed gasification of biomass. Bioresour. Technol. 102, 1907–1913.
[80] Katikaneni, S.P.R., Adjaye, J.D., Idem, R.O., Bakhshi, N.N., 1996. Catalytic conversion of canola oil over potassium-impregnated HZSM-5 catalysts: C2–C4 olefin production and model reaction studies. Ind. Eng. Chem. Res. 35, 3332–3346.
[81] Kim, Y., Parker, W., 2008. A technical and economic evaluation of the pyrolysis of sewage sludge for the production of bio-oil. Bioresour. Technol. 99, 1409–1416.
[82] Kirkels, A.F., Verbong, G.P.J., 2011. Biomass gasification: Still promising? A 30-year global overview. Renew. Sustain. Energy Rev. 15, 471–481.
[83] Koubaa, A., Perré, P., Hutcheon, R.M., Lessard, J., 2008. Complex dielectric properties of the sapwood of aspen, white birch, yellow birch, and sugar maple. Drying Technol. 26, 568–578.
[84] Kumabe, K., Hanaoka, T., Fujimoto, S., Minowa, T., Sakanishi, K., 2007. Co-gasification of woody biomass and coal with air and steam. Fuel 86, 684–689.

[85] Lam, S.S., Chase, H.A., 2012. A review on waste to energy processes using microwave pyrolysis. Energies 5, 4209–4232.
[86] Lasri, J., Ramesh, P.D., Schächter, L., 2000. Energy conversion during microwave sintering of a multiphase ceramic surrounded by a susceptor. J. Am. Ceram. Soc. 83, 1465–1468.
[87] Laturnus, F., Von Arnold, K., Gron, C., 2007. Organic contaminants from sewage sludge applied to agricultural soils–False alarm regarding possible problems for food safety? Environ. Sci. Pollut. Res. Int. 14, 53–60.
[88] Lee, K.H., Kang, B.S., Park, Y.K., Kim, J.S., 2005. Influence of reaction temperature, pretreatment, and a char removal system on the production of bio-oil from rice straw by fast pyrolysis, using a fluidized bed. Energy Fuels 19, 2179–2184.
[89] Lequitte, M., Figueras, F., Moreau, C., Hub, S., 1992. Deamination of sec-butylamine over acidic zeolites. Appl. Catal., A 84, 155–168.
[90] Li, C., Suzuki, K., 2009. Tar property, analysis, reforming mechanism and model for biomass gasification-An overview. Renew. Sustain. Energy Rev. 13, 594–604.
[91] Li, D., Chen, L., Chen, S., Zhang, X., Chen, F., Ye, N., 2012. Comparative evaluation of the pyrolytic and kinetic characteristics of a macroalga (*Sargassum thunbergii*) and a freshwater plant (*Potamogeton crispus*). Fuel 96, 185–191.
[92] Li, X., Grace, R., Lim, C.J., Watkinson, A.P., Chen, H., Kim, J.R., 2004. Biomass gasification in a circulating fluidized bed. Biomass Bioenergy 26, 171–193.
[93] Li, Y., Wang, T., Yin, X., Wu, C., Ma, L., Li, H., Lv, Y., Sun, L., 2010. 100 t/a-Scale demonstration of direct dimethyl ether synthesis from corncob-derived syngas. Renew. Energy 35, 583–587.
[94] Lin, Y-C., Huber, G.W., 2009. The critical role of heterogeneous catalysis in lignocellulosic biomass conversion. Energy Environ. Sci. 2, 68–80.
[95] Luan, Y., Xu, H., Yu, C., Li, W., Hou, S., 2007. *In-situ* regeneration mechanisms of hybrid catalysts in the one-step synthesis of dimethyl ether from syngas. Catal. Lett. 115, 23–26.
[96] Luque, R., Lovett, J.C., Datta, B., Clancy, J., Campelo, J.M., Romero, A.A., 2010. Biodiesel as feasible petrol fuel replacement: a multidisciplinary overview. Energy Environ. Sci. 3, 1706–1721.
[97] Luque, R., Menéndez, J.A., Arenillas, A., Cot, J., 2012. Microwave-assisted pyrolysis of biomass feedstocks: the way forward? Energy Environ. Sci. 5, 5481–5488.
[98] Lv, P., Xiong, Z., Chang, J., Wu, C., Chen, Y., Zhu, J., 2004. An experimental study on biomass air–steam gasification in a fluidized bed. Bioresour. Technol. 95, 95–101.
[99] Lv, P., Yuan, Z., Wu, C., Ma, L., Chen, Y., Tsubaki, N., 2007. Bio-syngas production from biomass catalytic gasification. Energy Convers. Manage. 48, 1132–1139.
[100] Lv, Y.; Wang, T.; Wu, C.; Ma, L.; Zhou, Y., 2009. Scale study of direct synthesis of dimethyl ether from biomass synthesis gas. Biotechnol. Adv. 27, 551–554.
[101] Maddi, B., Viamajala, S., Varanasi, S., 2011. Comparative study of pyrolysis of algal biomass from natural lake blooms with lignocellulosic biomass. Bioresour. Technol. 102, 11018–11026.
[102] Maher, K.D., Bressler, D.C., 2007. Pyrolysis of triglyceride materials for the production of renewable fuels and chemicals. Bioresour. Technol. 98, 2351–2368.

[103] Mao, D., Yang, W., Xia, J., Zhang, B., Lu, G., 2006. The direct synthesis of dimethyl ether from syngas over hybrid catalysts with sulfate-modified γ-alumina as methanol dehydration components. J. Mol. Catal. A 250, 138–144.
[104] Mao, D., Yang, W., Xia, J., Zhang, B., Song, Q., Chen, Q., 2005. Highly effective hybrid catalyst for the direct synthesis of dimethyl ether from syngas with magnesium oxide-modified HZSM-5 as a dehydration component. J. Catal. 230, 140–149.
[105] McKendry, P., 2002a. Energy production from biomass (part 1): overview of biomass. Bioresour. Technol. 83, 37–46.
[106] McKendry, P., 2002b. Energy production from biomass (part 2): conversion technologies. Bioresour. Technol. 83, 47–54.
[107] Menéndez, J.A., Arenillas, A., Fidalgo, B., Fernández, Y., Zubizarreta, L., Calvo, E.G., Bermúdez, J.M., 2010. Microwave heating processes involving carbon materials. Fuel Process. Technol. 91, 1–8.
[108] Menéndez, J.A., Inguanzo, M., Pis, J.J., 2002. Microwave-induced pyrolysis of sewage sludge. Water Res. 36, 3261–3264.
[109] Miao, X., Wu, Q., 2004. High yield bio-oil production from fast pyrolysis by metabolic controlling of *Chlorella protothecoides*. J. Biotechnol. 110, 85–93.
[110] Miao, X., Wu, Q., Yang, C., 2004. Fast pyrolysis of microalgae to produce renewable fuels. J. Anal. Appl. Pyrolysis 71, 855–863.
[111] Mihalcik, D.J., Mullen, C.A., Boateng, A.A., 2011. Screening acidic zeolites for catalytic fast pyrolysis of biomass and its components. J. Anal. Appl. Pyrolysis 92, 224–232.
[112] Moghtaderi, B., 2007. Effects of controlling parameters on production of hydrogen by catalytic steam gasification of biomass at low temperature. Fuel 86, 2422–2430.
[113] Mohan, D., Pittman, C.U., Steele, P.H., 2006. Pyrolysis of wood/biomass for bio-oil: a critical review. Energy Fuels 20, 848–889.
[114] Moradi, G.R., Nosrati, S., Yaripor, F., 2007. Effect of the hybrid catalysts preparation method upon direct synthesis of dimethyl ether from synthesis gas. Catal. Commun. 8, 598–606.
[115] Mullen, C.A., Boateng, A.A., 2010. Catalytic pyrolysis–GC/MS of lignin from several sources. Fuel Process. Technol. 91, 1446–1458.
[116] Nemanova, V., Abedini, A., Liliedahl, T., Engvall, K., 2014. Co-gasification of petroleum coke and biomass. Fuel 117, 870–875.
[117] Nordgreen, T., Liliedahl, T., Sjöström, K., 2006. Elemental iron as a tar breakdown catalyst in conjunction with atmospheric fluidized bed gasification of biomass: a thermodynamic study. Energy Fuels 20, 890–895.
[118] Oasmaa, A., Solantausta, Y., Arpiainen, V., Kuoppala, E., Sipila, K., 2010. Fast pyrolysis bio-oils from wood and agricultural residues. Energy Fuels 24, 1380–1388.
[119] Odebunmi, E.O., Ollis, D.F., 1983. Catalytic hydrodeoxygenation: III. Interactions between catalytic hydrodeoxygenation of *m*-cresol and hydrodenitrogenation of indole. J. Catal. 80, 76–89.
[120] Paik, M.J., Kim, H., Lee, J., Brand, J., Kim, Y.R., 2009. Separation of triacylglycerols and free fatty acids in microalgal lipids by solid-phase extraction for separate fatty acid profiling analysis by gas chromatography. J. Chromatogr. A 1216, 5917–5923.

[121] Pan, P., Hu, C., Yang, W., Li, Y., Dong, L., Zhu, L., Tong, D., Qing, R., Fan, Y., 2010. The direct pyrolysis and catalytic pyrolysis of *Nannochloropsis* sp. residue for renewable bio-oils. Bioresour. Technol. 101, 4593–4599.
[122] Park, E.S., Kang, B.S., Kim, J.S., 2008. Recovery of oils with high caloric value and low contaminant content by pyrolysis of digested and dried sewage sludge containing polymer flocculants. Energy Fuels 22, 1335–1340.
[123] Park, H.J., Heo, H.S., Park, Y.K., Yim, J.H., Jeon, J.K., Park, J., Ryu, C., Kim, S.S., 2010. Clean bio-oil production from fast pyrolysis of sewage sludge: Effects of reaction conditions and metal oxide catalysts. Bioresour. Technol. 101, S83–S85.
[124] Perry, R.H., 1984. Perry's Chemical Engineers Handbook. McGraw Hill, New York, USA.
[125] Pirt, S.J., 1986. The thermodynamic efficiency (quantum demand) and dynamics of photosynthesis growth. New Phytol. 102, 3–37.
[126] Prasad, P.S.S., Bae, J.W., Kang, S.H., Lee, Y.J., Jun, K.W., 2008. Single-step synthesis of DME from syngas on Cu–ZnO–Al_2O_3/zeolite bifunctional catalysts: The superiority of ferrierite over the other zeolites. Fuel Process. Technol. 89, 1281–1286.
[127] Rao, Q., Labuza, T.P., 2012. Effect of moisture content on selected physicochemical properties of two commercial hen egg white powders. Food Chem. 132, 373–384.
[128] Richards, G.N., Zheng, G.C., 1991. Influence of metal-ions and of salts on products from pyrolysis of wood: applications to thermochemical processing of newsprint and biomass. J. Anal. Appl. Pyrolysis 21, 133–146.
[129] Richardson, Y., Blin, J., Julbe, A., 2012. A short overview on purification and conditioning of syngas produced by biomass gasification: Catalytic strategies, process intensification and new concepts. Prog. Energy Combust. Sci. 38, 765–781.
[130] Rio, S., Le Coq, L., Faur, C., Lecomte, D., Le Cloirec, P., 2006. Preparation of adsorbents from sewage sludge by steam activation for industrial emission treatment. Process Saf. Environ. Prot. 84, 258–264.
[131] Rostrup-Nielsen, J.R., Sehested, J., Nørskov, J.K., 2002. Hydrogen and synthesis gas by steam- and CO_2 reforming. Adv. Catal. 47, 65–139.
[132] Salema, A.A., Ani, F.N., 2011. Microwave induced pyrolysis of oil palm biomass. Bioresour. Technol. 102, 3388–3395.
[133] Sánchez, M.E., Menéndez, J.A., Domínguez, A., Pis, J.J., Martínez, O., Calvo, L.F., Bernad, P.L., 2009. Effect of pyrolysis temperature on the composition of the oils obtained from sewage sludge. Biomass Bioenergy 33, 933–940.
[134] Schenk, P.M., Thomas-Hall, S.R., Stephens, E., Marx, U.C., Mussgnug, J.H., Posten, C., Kruse, O., Hankamer, B., 2008. Second generation biofuels: high-efficiency microalgae for biodiesel production. Bioenergy Res. 1, 20–43.
[135] Sehested, J., 2006. Four challenges for nickel steam-reforming catalysts. Catal. Today 111, 103–110.
[136] Semelsberger, T.A.; Borup, R.L.; Greene, H.L., 2006. Dimethyl ether (DME) as an alternative fuel. J. Power Sources 156, 497–511.
[137] Smith, K.M., Fowler, G.D., Pullket, S., Graham, N.J.D., 2009. Sewage sludge-based adsorbents: a review of their production, properties and use in water treatment applications. Water Res. 43, 2569–2594.

[138] Sobhy, A., Chaouki, J., 2010. Microwave-assisted biorefinery. Chem. Eng. Trans. 19, 25–30.
[139] Spath, P.L., Dayton, D.C., 2003. Preliminary screening – technical and economic assessment of synthesis gas to fuels and chemicals with emphasis on the potential for biomass-derived syngas. Golden, Colorado (US): NREL/TP-510-34929, National Renewable Energy Laboratory.
[140] Spivey, J.J., 1991. Review: dehydration catalysts for the methanol/dimethyl ether reaction. Chem. Eng. Commun. 110, 123–142.
[141] Świerczyński, D., Courson, C., Bedel, L., Kiennemann, A., Vilminot, S., 2006. Oxidation reduction behavior of iron-bearing olivines $(Fe_xMg_{1-x})_2SiO_4$ used as catalysts for biomass gasification. Chem. Mat. 18, 897–905.
[142] Takeguchi, T., Yanagisawa, K., Inui, T., Inoue, M., 2000. Effect of the property of solid acid upon syngas-to-dimethyl ether conversion on the hybrid catalysts composed of Cu-Zn-Ga and solid acids. Appl. Catal., A 192, 201–209.
[143] Thangalazhy-Gopakumar, S., Adhikari, S., Chattanathan, S.A., Gupta, R.B., 2012. Catalytic pyrolysis of green algae for hydrocarbon production using H^+ZSM-5 catalyst. Bioresour. Technol. 118, 150–157.
[144] Thostenson, E.T., Chou, T.W., 1999. Microwave processing: fundamentals and applications. Composites Part A 30, 1055–1071.
[145] Torres, W., Pansare, S.S., Goodwin, J.G., 2007. Hot gas removal of tars, ammonia, and hydrogen sulfide from biomass gasification gas. Catal. Rev. Sci. Eng. 49, 407–456.
[146] Ucar, S., Karagoz, S., 2009. The slow pyrolysis of pomegranate seeds: The effects of temperature on the product yields and bio-oil properties. J. Anal. Appl. Pyrolysis 84, 151–156.
[147] Ueki, Y., Torigoe, T., Ono, H., Yoshiie, R., Kihedu, J.H., Naruse, I., 2011. Gasification characteristics of woody biomass in the packed bed reactor. Proc. Combust. Inst. 33, 1795–1800.
[148] Vallios, I., Tsoutsos, T., Papadakis, G., 2009. Design of biomass district heating systems. Biomass Bioenergy 33, 659–678.
[149] Van der Meijden, C.M., Veringa, H.J., Bergman, P.C.A., Van der Drift, A., Vreugdenhil, B.J., 2009. Scale-up of the Milena biomass gasification technology. 17th European Biomass Conference Exhibition.
[150] Vishwanathan, V., Jun, K.W., Kim, J.W., Roh, H.S., 2004. Vapour phase dehydration of crude methanol to dimethyl ether over Na-modified H-ZSM-5 catalysts. Appl. Catal., A 276, 251–255.
[151] Wan, Y., Chen, P., Zhang, B., Yang, C., Liu, Y., Lin, X., Ruan, R., 2009. Microwave-assisted pyrolysis of biomass: Catalysts to improve product selectivity. J. Anal. Appl. Pyrolysis 86, 161–167.
[152] Wang, K., Brown, R.C., Homsy, S., Martinez, L., Sidhu, S.S., 2013. Fast pyrolysis of microalgae remnants in a fluidized bed reactor for bio-oil and biochar production. Bioresour. Technol. 127, 494–499.
[153] Wang, L., Qi, Y., Wei, Y., Fang, D., Meng, S., Liu, Z., 2006. Research on the acidity of the double-function catalyst for DME synthesis from syngas. Catal. Lett. 106, 61–66.

[154] Wang, S., Cai, Q., Wang, X., Guo, Z., Luo, Z., 2013. Bio-gasoline production from co-cracking of hydroxypropanone and ethanol. Fuel Process. Technol. 111, 86–93.
[155] Wang, S., Cai, Q., Wang, X., Zhang, L., Wang, Y., Luo, Z., 2014. Biogasoline production from the co-cracking of the distilled fraction of bio-oil and ethanol. Energy Fuels 28, 115–122.
[156] Wang, T., Chang, J., Cui, X., Zhang, Q., Fu, Y., 2006. Reforming of raw gas from biomass gasification to syngas over highly stable nickel-magnesium solid solution catalysts. Fuel Process. Technol. 87, 421–428.
[157] Wang, X., Morrison, W., Du, Z., Wan, Y., Lin, X., Chen, P., Ruan, R., 2012. Biomass temperature profile development and its implications under the microwave-assisted pyrolysis condition. Appl. Energy 99, 386–392.
[158] Werther, J., Ogada, T., 1999. Sewage sludge combustion. Prog. Energy Combust. Sci. 25, 55–116.
[159] Williams, P.T., Horne, P.A., 1994. Characterization of oils from the fluidized-bed pyrolysis of biomass with zeolite catalyst upgrading. Biomass Bioenergy 7, 223–236.
[160] Xia, J., Mao, D., Zhang, B., Chen, Q., Tang, Y., 2004. One-step synthesis of dimethyl ether from syngas with Fe-modified zeolite ZSM-5 as dehydration catalyst. Catal. Lett. 98, 235–240.
[161] Xiao, X., Meng, X., Le, D.D., Takarada, T., 2011. Two-stage steam gasification of waste biomass in fluidized bed at low temperature: Parametric investigations and performance optimization. Bioresour. Technol. 102, 1975–1981.
[162] Xie, Q., Kong, S., Liu, Y., Zeng, H., 2012. Syngas production by two-stage method of biomass catalytic pyrolysis and gasification. Bioresour. Technol. 110, 603–609.
[163] Xu, B., Bordiga, S., Prins, R., Van Bokhoven, J.A., 2007. Effect of framework Si/Al ratio and extra-framework aluminum on the catalytic activity of Y zeolite. Appl. Catal., A 333, 245–253.
[164] Xu, M., Lunsford, J.H., Goodman, D.W., Bhattacharyya, A., 1997. Synthesis of dimethyl ether (DME) from methanol over solid-acid catalysts. Appl. Catal., A 149, 289–301.
[165] Yang, H., Yan, R., Chen, H., Lee, D.H., Liang, D.T., Zheng, C., 2006. Pyrolysis of palm oil wastes for enhanced production of hydrogen rich gases. Fuel Process. Technol. 87, 935–942.
[166] Yang, X., Xu, S., Xu, H., Liu, X., Liu, C., 2010. Nickel supported on modified olivine catalysts for steam reforming of biomass gasification tar. Catal. Commun. 11, 383–386.
[167] Yaripour, F., Baghaei, F., Schmidt, I., Perregaard, J., 2005a. Catalytic dehydration of methanol to dimethyl ether (DME) over solid-acid catalysts. Catal. Commun. 6, 147–152.
[168] Yaripour, F., Baghaei, F., Schmidt, I., Perregaard, J., 2005b. Synthesis of dimethyl ether from methanol over aluminium phosphate and silica-titania catalysts. Catal. Commun. 6, 542–549.
[169] Yu, G., Zhang, Y., Schideman, L., Funk, T., Wang, Z., 2011. Distribution of carbon and nitrogen in the products from hydrothermal liquefaction of low-lipid microalgae. Energy Environ. Sci. 4, 4587–4595.

[170] Zhang, B., Yang, C., Moen, J., Le, Z., Hennessy, K., Wan, Y., Liu, Y., Lei, H., Chen, P., Ruan, R., 2010. Catalytic conversion of microwave-assisted pyrolysis vapors. Energy Source. Part A 32, 1756–1762.
[171] Zhang, B., Zhong, Z., Ding, K., Cao, Y., Liu, Z., 2014. Catalytic upgrading of corn stalk fast pyrolysis vapors with fresh and hydrothermally treated HZSM-5 catalysts using Py–GC/MS. Ind. Eng. Chem. Res. 53, 9979–9984.
[172] Zhang, B., Zhong, Z., Ding, K., Song, Z., 2015. Production of aromatic hydrocarbons from catalytic co-pyrolysis of biomass and high density polyethylene: Analytical Py–GC/MS study. Fuel 139, 622–628.
[173] Zhang, H., Carlson, T.R., Xiao, R., Huber, G.W., 2012. Catalytic fast pyrolysis of wood and alcohol mixtures in a fluidized bed reactor. Greem Chem. 14, 98–110.
[174] Zhang, H., Cheng, Y.T., Vispute, T.P., Xiao, R., Huber, G.W., 2011. Catalytic conversion of biomass-derived feedstocks into olefins and aromatics with ZSM-5: the hydrogen to carbon effective ratio. Energy Environ. Sci. 4, 2297–2307.
[175] Zhang, H., Zheng, J., Xiao, R., Shen, D., Jin, B., Xiao, G., Chen, R., 2013. Co-catalytic pyrolysis of biomass and waste triglyceride seed oil in a novel fluidized bed reactor to produce olefins and aromatics integrated with self-heating and catalyst regeneration processes. RSC Adv. 3, 5769–5774.
[176] Zhang, Q., Chang, J., Wang, T., Xu, Y., 2007. Review of biomass pyrolysis oil properties and upgrading research. Energy Convers. Manage. 48, 87–92.
[177] Zhao, H., Holladay, J.E., Brown, H., Zhang, Z.C., 2007. Metal chlorides in ionic liquid solvents convert sugars to 5-hydroxymethylfurfural. Sci. 316, 1597–1600.

APPENDIX A EXPERIMENTAL MATERIALS, EQUIPMENT AND SAMPLES

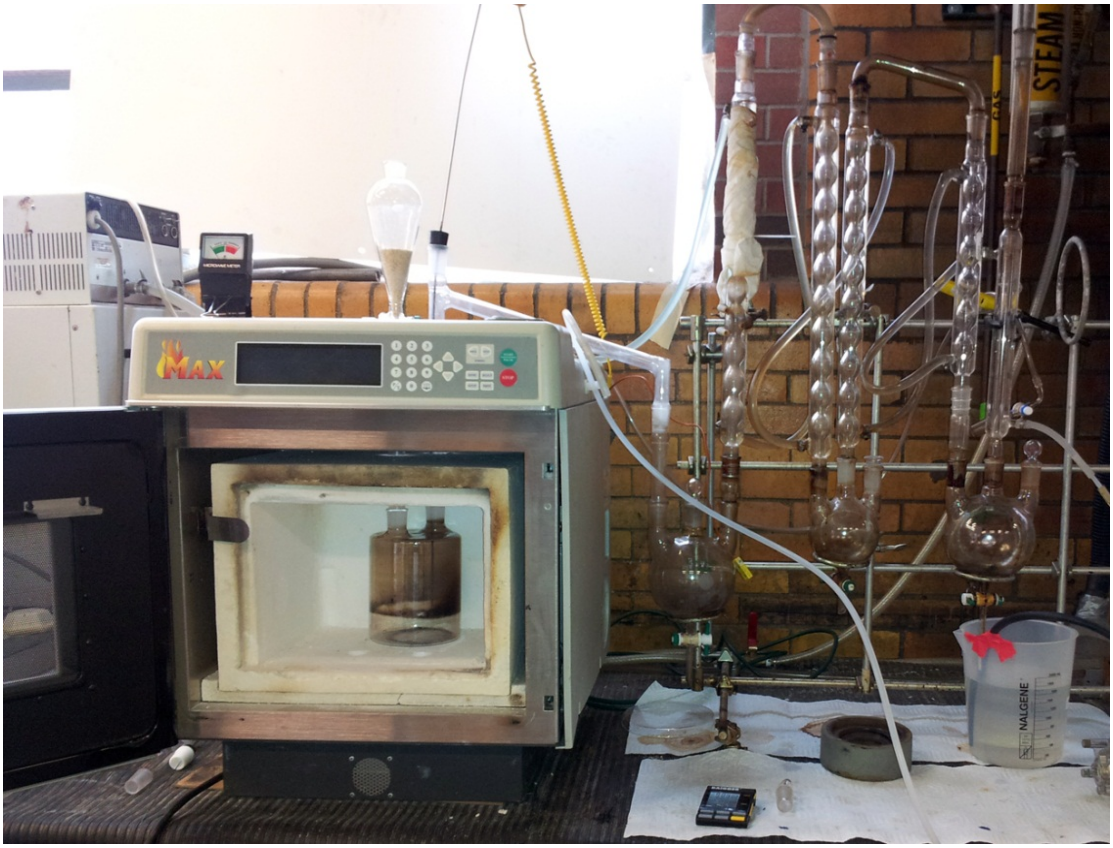

Fig. A.1 Fast microwave-assisted biomass conversion system.

Fig. A.2 *Nannochloropsis* sp. powder used in the fMAP experiments.

Fig. A.3 Scum used in the co-pyrolysis experiments.

Fig. A.4 System for the single-step synthesis of DME from syngas.

Fig. A.5 Catalysts used in the single-step synthesis of DME from syngas.